

Two-loop Yang-Mills diagrams from superstring amplitudes.

Lorenzo Magnea,^a Sam Playle,^a Rodolfo Russo^b and Stefano Sciuto^a

^a*Dipartimento di Fisica, Università di Torino,
and INFN, Sezione di Torino,
Via P. Giuria 1, I-10125 Torino, Italy*

^b*Centre for Research in String Theory,
School of Physics and Astronomy, Queen Mary University of London,
Mile End Road, London, E1 4NS, United Kingdom*

E-mail: lorenzo.magnea@unito.it, playle@to.infn.it,
r.russo@qmul.ac.uk, sciuto@to.infn.it

ABSTRACT: Starting from the superstring amplitude describing interactions among D-branes with a constant world-volume field strength, we present a detailed analysis of how the open string degeneration limits reproduce the corresponding field theory Feynman diagrams. A key ingredient in the string construction is represented by the twisted (Prym) super differentials, as their periods encode the information about the background field. We provide an efficient method to calculate perturbatively the determinant of the twisted period matrix in terms of sets of super-moduli appropriate to the degeneration limits. Using this result we show that there is a precise one-to-one correspondence between the degeneration of different factors in the superstring amplitudes and one-particle irreducible Feynman diagrams capturing the gauge theory effective action at the two-loop level.

KEYWORDS: Superstrings and Heterotic Strings, D-branes

ARXIV EPRINT: [1503.05182](https://arxiv.org/abs/1503.05182)

Contents

1	Introduction	1
2	The string theory setup	5
3	The superstring partition function for the NS sector	8
4	Taking the field theory limit	13
4.1	Expanding in powers of the multipliers	13
4.2	A parametrization for the symmetric degeneration	15
4.3	Mapping moduli to Schwinger parameters	19
4.4	The symmetric degeneration after GSO projection	21
4.5	The incomplete degeneration	23
5	Yang-Mills theory in the background field Gervais-Neveu gauge	28
5.1	The $u(N)$ Lagrangian	29
5.2	Propagators in a constant background field	33
5.3	Selected two-loop vacuum diagrams	35
6	Discussion of results	38
6.1	Comparison between QFT and string theory	38
6.2	Comparison with bosonic string theory	39
A	Super Schottky groups	42
A.1	Super-projective transformations	42
A.2	The super Schottky group	44
A.2.1	Multipliers	46
A.2.2	The super period matrix	46
B	Twisted determinants	47
B.1	The twisted determinant on a Riemann surface	47
B.2	The twisted determinant on a super Riemann surface	52
C	Feynman diagrams	56

1 Introduction

The study of scattering amplitudes has played a central rôle in the development of string theory since its very beginning. In the seventies and the eighties it was instrumental in showing that superstring theories provide perturbative gravitational models that, at loop

level, are free of ultraviolet divergences and anomalies. The analysis of string amplitudes was also crucial in the discovery of D-branes and in the development of the web of dualities among different superstring theories. It is, then, not surprising that this field continues to be under intense study. Recently, there has been renewed interest in several aspects of string perturbation theory in the RNS formalism, with particular focus on contributions beyond one loop: for example, higher-loop diagrams with Ramond external states were discussed in refs. [1, 2]; further, refs. [3–5] focused on the off-shell extension of amplitudes, studying various situations where this is necessary; finally, refs. [6, 7] derived an explicit result for the $D^6\mathcal{R}^4$ term in the type-IIB effective action, checking the predictions following from S-duality and supersymmetry. Another interesting approach to the point-like limit of closed string amplitudes as a ‘tropical’ limit was discussed in [8]. For recent reviews on multiloop string amplitudes, with a more complete list of references, we refer the reader to [9, 10].

Two themes in particular have been at the center of much important progress in our understanding of string interactions: the study of the mathematical properties of the world-sheet formulation of string amplitudes, and their relation to the effective actions describing the light degrees of freedom present in the theory. In this paper, we touch on both these aspects by studying in detail the open string degeneration limits of two-loop amplitudes described by a world-sheet with three borders and no handles. In particular, we expand upon the results of [11]: starting from the Neveu-Schwarz (NS) sector of the open superstring partition function in the background of a constant magnetic field strength, we derive the Euler-Heisenberg effective action for a gauge theory coupled to scalar fields in the ‘Coulomb phase’. The idea of using string theory to investigate effective actions in constant electromagnetic fields has a long history, and was studied at one loop in [12–14], with some results for the bosonic theory at two loops given in [15]. In our analysis we find exact agreement between calculations in field theory and string theory, in the infinite-tension limit, for the two-loop correction to the effective action. Furthermore, we find that the correspondence holds not just for the whole amplitude, but we can precisely identify the string origin of all individual one-particle irreducible (1PI) Feynman diagrams contributing to the effective action. In order to do so, on the string theory side we need to use appropriate world-sheet super-moduli, respecting the symmetry of the Feynman graphs, while on the field theory side we need to use a version of the non-linear gauge condition introduced by Gervais and Neveu in [16], modified by dimensional reduction to involve the scalars also, and given here in eq. (5.10).

On the formal side, it is advantageous to use the formalism of *super* Riemann surfaces [9, 17–21], in which the complex structure is generalized to a super-conformal structure, with local super-conformal coordinates $(z|\theta)$. We follow this approach by constructing the two-loop amplitude in the Schottky parametrization, since there is a close relationship between Schottky super-moduli, in particular the ‘multipliers’, and the sewing parameters of plumbing fixtures. This in turn relates the bosonic world-sheet moduli to the Schwinger parameters associated to the propagators in Feynman graphs, which provides the ideal framework for studying the connection between string integrands and field theory Feynman diagrams. In the bosonic case, it is possible to describe genus h Riemann surfaces

as quotients of the Riemann sphere (with a discrete set of points removed) by a discrete (Schottky) group, freely generated by h Möbius transformations. Heuristically, quotienting the Riemann sphere by a Möbius transformation has the effect of cutting out a pair of circles and gluing them to each other along their boundaries. Schottky groups arose naturally in the early treatment of multi-loop string amplitudes [22–27] and remained useful [18, 28–32] even after alternative methods of analysis were found. In the supersymmetric case, higher genus super Riemann surfaces are similarly generated by quotienting the super manifold $\mathbf{CP}^{1|1}$ (with a discrete set of points removed) by a discrete group, generated by h ‘super-projective’ $\text{OSp}(1|2)$ transformations.

As is well known, the presence of a constant background field strength in the space-time description of the amplitudes translates on the world-sheet side into the presence of non-trivial monodromies along either the a or the b cycles of the Riemann surface. It is thus not surprising that the amplitudes we are interested in involve super 1|1-forms (sections of the Berezinian bundle) with twisted periodicities, also known as Prym differentials. The bosonic counterparts of these objects was discussed, in the Schottky parametrization, in [33], and their periods along the untwisted cycles appear in any string amplitude where the fields have non-trivial monodromies [15, 34–36]. We extend these past results in two directions: first we generalise the twisted period matrix to the supersymmetric case; then we must calculate the supersymmetric version of the twisted determinant to sufficiently high order in the complete degeneration limit, so as to obtain the gauge theory Feynman graphs with multiple gluon propagators. In order to do this, we introduce an alternative formulation of the twisted super-determinant in terms of an integral along a Pochhammer contour, and we show that this simplifies drastically its perturbative evaluation in the Schottky parametrization.

The main result of this paper is to show how the two-loop 1PI Feynman diagrams listed in figure 1 arise from the degeneration limits of the superstring result. The graphical notation for the field propagators is explained in detail in appendix C; here we note in particular that we are using two different types of edges to denote gluons, depending on whether they are polarized parallel or perpendicular to the plane of the background field. We note also that some of the graphs (those in figures 1i–1l) include vertices with an odd number of scalars: these vertices arise because of the non-vanishing scalar vacuum expectation values (to which these graphs are proportional); these diagrams appear automatically in the string calculation, and they appear on the field-theory side as a result of having imposed the gauge condition of Gervais and Neveu [16] *before* dimensional reduction. Our investigation is thus also a contribution to a long-standing program aimed to use string theory to gain insights into field-theory amplitudes, which was started in ref. [37] in the language of dual models, and generalized to the superstring framework in [38]. The practical usefulness of string theory as an organizing principle for tree-level gauge-theory amplitudes was first noticed and applied in [39, 40]. At genus one, several results are available in the literature: they include the derivation of the leading contribution to the Callan-Symanzik β -function of pure Yang-Mills theory in [41], as well as a general analysis of one-loop scattering amplitudes in [42–46]. This was later used to calculate the one-loop five-gluon amplitude in QCD for the first time in [47]. String theory also inspired many developments in the world-line

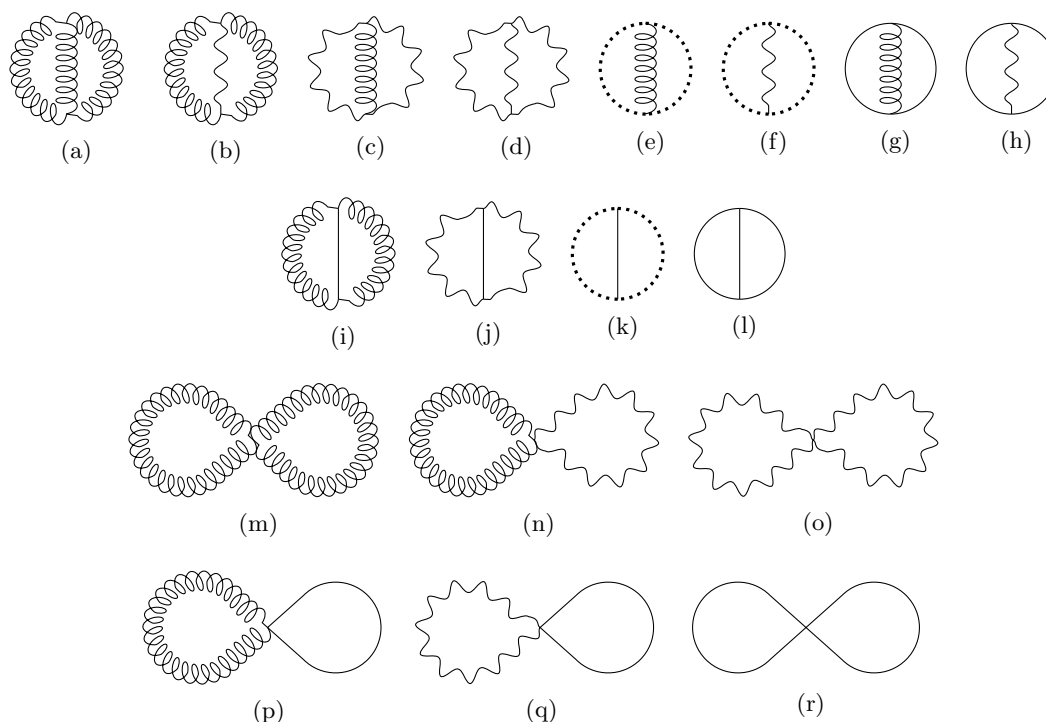


Figure 1. Two-loop 1PI vacuum Feynman graphs in Yang-Mills with adjoint scalars with VEVs. The dotted edges signify Faddeev-Popov ghosts, and the plain edges symbolize scalars, the helical edges denote gluons polarized *parallel* to the plane of the background magnetic field and the wavy edges indicate gluons polarized *perpendicular* to the background magnetic field.

approach to perturbative quantum field theory (QFT), starting with the work of Strassler in [48], with subsequent progress in [49, 50], summarized in [51], and more recently, for example, in [52, 53]. Bosonic strings were also used to compute Yang-Mills renormalization constants at one loop in [54], and one-loop off-shell gluon Green’s functions in [55]. At the two-loop level much less is known: explicit QFT amplitudes with only scalar fields were obtained from bosonic strings in [56] and [57, 58]. Two-loop amplitudes with gluons, however, have proved difficult to study with this technology [59–61]. Our analysis here marks significant progress in this direction, showing that the prescriptions discussed in [11] are indeed sufficient to derive from string theory all the bosonic two-loop 1PI gauge-theory diagrams listed in figure 1.

The structure of the paper is as follows. In section 2 we describe the D-brane setup in which our calculations are carried out. In section 3 we recall the integration measure for the NS sector of open superstrings in the super Schottky parametrization and explain how to modify it in order to accommodate our background. In section 4 we expand the measure in powers the Schottky multipliers, and then we identify the appropriate parametrizations to describe the two degenerations of the Riemann surface which are relevant for our purposes: the *symmetric* degeneration leading to the diagrams with the topology of figures 1a–1l, and the *incomplete* degeneration, leading to diagrams with only two field-theory propaga-

tors and a four-point vertex, depicted in figures 1m–1r. An analysis of the various factors contributing to the string amplitude, arising from different world-sheet conformal field theories, then enables to unambiguously identify each diagram in the field-theory limit. In section 5 we obtain and discuss the Lagrangian for the world-volume QFT in the appropriate non-linear gauge, and we use it to compute example Feynman diagrams. Finally, in section 6.1 we compare our string-theory and QFT calculations, and in section 6.2 we discuss the differences between the present calculation and the analogous calculation using the bosonic string. In appendix A we discuss super-projective transformations and the super Schottky group, in appendix B we give the calculation of the twisted (Prym) super period matrix, and in appendix C we list the values of all of the Feynman graphs in figure 1 with our choice of background fields.

2 The string theory setup

We consider a stack of N parallel d -dimensional D-branes embedded in a \mathcal{D} -dimensional Minkowski space-time, where, as usual, $\mathcal{D} = 10$ for type II theories and $\mathcal{D} = 26$ for bosonic string theory. When $d < \mathcal{D} - 2$, and provided the string coupling g_s is small, so that $g_s N \ll 1$, this configuration can be described in terms of open strings moving in flat space and being supported by the D-branes. We will work generically in the ‘Coulomb phase’ where the D-branes are spatially separated from each other in the directions perpendicular to their world-volumes. Furthermore, on each of the D-branes we switch on a uniform $U(1)$ background field in the $\{x_1, x_2\}$ plane, with a field strength tensor given by

$$F_{\mu\nu}^A = B^A (\eta_{\mu 1} \eta_{2\nu} - \eta_{\mu 2} \eta_{\nu 1}), \tag{2.1}$$

where B^A is a constant ‘magnetic’ field on the A -th brane (thus $A = 1, \dots, N$). The positions of the D-branes in the transverse directions will be labelled by Y_I^A , with $I = d, d + 1, \dots, \mathcal{D} - 1$. Such a D-brane configuration is depicted from various viewpoints in figures 2 and 3. A string stretched between branes A and B will have squared length

$$Y_{AB}^2 = \sum_{I=d}^{\mathcal{D}-1} (Y_I^A - Y_I^B)^2, \tag{2.2}$$

and will receive a classical contribution m_{AB} to its mass from the elastic potential energy associated with the stretching of the string, given by

$$m_{AB} = T Y_{AB} = \frac{Y_{AB}}{2\pi\alpha'}, \tag{2.3}$$

where T is the string tension and α' the related Regge slope. These strings will also be charged under the magnetic fields B^A and B^B , with the sign of the charge depending on their orientation. Open strings that start and end on the same D-brane are uncharged and their mass is independent of Y_I^A . For generic values of Y_I^A , this configuration breaks the symmetry of the world-volume theory from $U(N)$ to $U(1)^N$.

The theory describing open strings supported by this D-brane configuration is free [12, 13]. The constant background magnetic fields on the D-brane world-volumes manifest

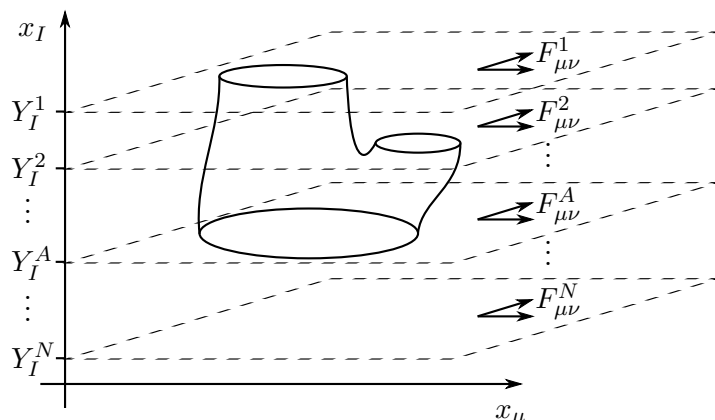


Figure 2. A stack of spatially separated D-branes with constant gauge fields on their world-volumes, connected by open strings ending on three different branes, in a double-annulus configuration.

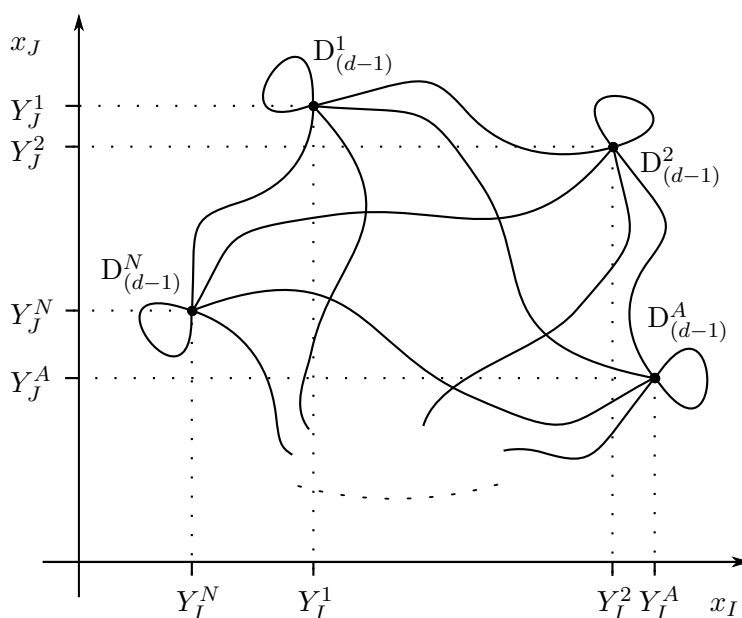


Figure 3. A two-dimensional section of the space transverse to the D-branes, which therefore appear as points, connected by a web of open strings.

themselves in the world-sheet picture by altering the boundary conditions of string coordinates in the magnetized plane. On the double cover of the surface, this gives twisted boundary conditions, or, in other words, non-trivial monodromies, to the zero modes in the two magnetized space directions. To describe this setup, we will use the conventions of section 3 of ref. [11], which we summarize below.

To begin with, let us briefly consider the spectrum of low-lying string excitations. In the bosonic case, the world-sheet theory, in a covariant approach, comprises \mathcal{D} embedding coordinates X^μ and the ghost system (b, c) . The holomorphic components of these fields

admit the mode expansions

$$b(z) = \sum_{n \in \mathbf{Z}} b_n z^{-n-2}, \quad c(z) = \sum_{n \in \mathbf{Z}} c_n z^{-n+1}, \quad \partial_z X^\mu = -i \sqrt{2\alpha'} \sum_{n \in \mathbf{Z}} \alpha_n^\mu z^{-n-1}. \quad (2.4)$$

In the presence of constant abelian background fields, the theory remains free, but string coordinates in directions parallel to the magnetized plane acquire twisted boundary conditions and must be treated separately. Considering strings ending on branes A and B , it is convenient to introduce the combinations $Z_{AB}^\pm = (X_{AB}^1 \pm iX_{AB}^2)/\sqrt{2}$. These combinations diagonalize the boundary conditions and yield the mode expansions

$$\partial_z Z_{AB}^\pm = -i \sqrt{2\alpha'} \sum_{n \in \mathbf{Z}} \alpha_{n \pm \epsilon_{AB}}^\pm z^{-n-1 \pm \epsilon_{AB}}, \quad (2.5)$$

where we defined

$$\tan(\pi \epsilon_{AB}) \equiv 2\pi\alpha'(B^A - B^B). \quad (2.6)$$

After canonical quantization, the modes introduced above satisfy standard commutation relations, except for magnetized directions, where one finds

$$[\alpha_{n+\epsilon_{AB}}^+, \alpha_{m-\epsilon_{AB}}^-] = (n + \epsilon_{AB}) \delta_{n+m}. \quad (2.7)$$

As usual in covariant quantization, not all states in the Fock space obtained by acting with the creation modes on the $\text{SL}(2, \mathbf{R})$ -invariant vacuum $|0\rangle$ are physical: we need to select only the states belonging to the cohomology of the world-sheet BRST charge

$$Q_B^W = \oint \frac{dz}{2\pi i} c \left(-\frac{1}{4\alpha'} \partial X^M \partial X_M + (\partial c)b \right). \quad (2.8)$$

In the bosonic theory, the lowest-lying physical state is a tachyon $|\mathbf{k}\rangle \equiv c_1|k, 0\rangle$, with mass-shell condition $k^2 = -m^2 = 1/\alpha'$. The next mass level comprises $(\mathcal{D} + 2)$ massless states, which will be the focus of our analysis in the field theory limit: one finds two unphysical states, two null states, and $(\mathcal{D} - 2)$ physical polarization states appropriate for massless gauge bosons. A crucial ingredient of our analysis is the mapping between these string states and the space-time states in the limiting quantum field theory: as noticed for instance in chapter 4 of [62], the action of the worldsheet BRST charge (2.8) on the $(\mathcal{D} + 2)$ massless states mirrors the linearized action of the space-time BRST charge for the $U(N)$ gauge symmetry: in particular, the states created by world-sheet ghost oscillators, $c_{-1}|\mathbf{k}\rangle$ and $b_{-1}|\mathbf{k}\rangle$, behave as the spacetime ghosts C and \bar{C} . Acting with the α_{-1}^M oscillators, on the other hand, generates d states along the D-brane, and $n_s = \mathcal{D} - d$ states associated to the n_s directions transverse to the D-brane, representing respectively the d polarisations of the gauge vectors (including two unphysical ones), and n_s adjoint scalars. To be precise, the world-sheet BRST charge Q_B^W acts as

$$Q_B^W b_{-1}|\mathbf{k}\rangle = \sqrt{2\alpha'} k \cdot \alpha_{-1}|\mathbf{k}\rangle; \quad Q_B^W \alpha_{-1}^M|\mathbf{k}\rangle = \sqrt{2\alpha'} k^M c_{-1}|\mathbf{k}\rangle; \quad Q_B^W c_{-1}|\mathbf{k}\rangle = 0, \quad (2.9)$$

while the linearised space-time BRST transformation δ_B acts as

$$\delta_B(\bar{C}^a) \sim \partial \cdot Q^a; \quad \delta_B(Q_\mu^a) \sim \partial_\mu C^a; \quad \delta_B(Q_I^a) \sim 0; \quad \delta_B(C^a) \sim 0, \quad (2.10)$$

where a is an adjoint index, Q_μ^a and Q_I^a stand for a gluon mode and a scalar, depending on whether X^M is parallel or perpendicular to the D-brane, and $k^M = \{k^\mu, 0\}$.

This simple relation between world-sheet and space-time states is preserved in perturbation theory, when the string coupling is switched on and non-linear terms in the BRST operators must be taken into account. This is expected, since, in a perturbative analysis, fields propagating between interaction vertices are free. In practice, we will test this statement by calculating a string diagram with the world-sheet topology of a degenerating double-annulus, and identifying the contributions coming from the various massless states listed above, as they propagate through the diagram. We will show that each contribution matches the gauge theory result, where the corresponding space-time fields propagate in the matching edge of the relevant Feynman diagram, provided that the gauge used in field theory is the nonlinear Gervais-Neveu gauge, introduced in [16]. In this way, we can identify individual Feynman diagrams in the target field theory directly at the level of the string amplitude, picking a specific boundary of the string moduli space, and identifying the string states as they propagate along the degenerating surface.

A similar analysis holds also in the superstring case. In the RNS formalism one needs to introduce the extra world-sheet fields ψ^μ , β and γ , that are the partners under world-sheet supersymmetry of the ∂X^μ , b and c fields mentioned above. The monodromies for these new fields will be the same as those of their partners, except for a possible extra sign, which is allowed for fields of half-integer weight, and distinguishes the Ramond from the Neveu-Schwarz sectors. In this paper we will focus on the Neveu-Schwarz contributions: the analysis of the states at the first mass level, above the tachyonic ground state $|\mathbf{k}\rangle$, parallels that of the bosonic case. The only difference is that the relevant modes are $\psi_{-1/2}$, $\beta_{-1/2}$ and $\gamma_{-1/2}$: in the superstring partition function, the low energy limit will be performed by focusing on the contributions of states with half-integer weight.

3 The superstring partition function for the NS sector

From the world-sheet point of view, the interaction among D-branes is described by the string vacuum amplitude (the partition function) with boundaries, as depicted in figure 2. The case of two magnetized D-branes, corresponding to a one loop-amplitude, has been well studied [12–14, 63]. Here we will focus on planar world-sheets, and most of what we will say in this section applies to surfaces with $(h + 1)$ borders, corresponding to h -loop open superstring diagrams, but restricted to the NS sector, where the super-Schottky formalism described in ref. [30] can be used. In particular, as discussed in section 2, we consider parallel magnetized D-branes that can be separated in the directions transverse to their world-volumes. As a consequence, and as depicted in figure 4 for a (two-loop) surface with three boundaries, the partition function depends on two set of variables: the relative distances among D-branes, and the magnetic field gradients between pairs of D-branes.

To be precise, let us label the $(h + 1)$ world-sheet borders with $i = 0, 1, \dots, h$. Then we can label the D-brane to which the i -th border is attached with the integer A_i , with $A_i \in \{1, \dots, N\}$, and $A_i \leq A_{i+1}$. To get the full amplitude, we will have to sum over the

A_i 's. Having fixed A_0, \dots, A_h , we can take the A_0 -th brane as a reference and define

$$\begin{aligned} \mathbf{d}_I^i &= Y_I^{A_0} - Y_I^{A_i} \quad (I = d, \dots, \mathcal{D} - 1), \\ \tan(\pi\epsilon^i) &= 2\pi\alpha' g (B^{A_0} - B^{A_i}). \end{aligned} \quad (3.1)$$

The variables ϵ^i thus form an h -dimensional vector, which we will denote by $\vec{\epsilon}$; similarly, the variables \mathbf{d}_I^i , which have dimension of length, form n_s h -dimensional vectors, which we will label $\vec{\mathbf{d}}_I$. The classical mass of the string stretching between the A_0 -th brane and the A_i -th brane is then given by

$$m_i^2 = \frac{1}{(2\pi\alpha')^2} \sum_{I=d}^{\mathcal{D}-1} (\mathbf{d}_I^i)^2. \quad (3.2)$$

Notice finally that, for $h = 2$, as depicted in figure 4, we make a slight variation in this notation by flipping the sign of the second component of the two-dimensional vectors $\vec{\epsilon}$ and $\vec{\mathbf{d}}_I$, which will be useful to take full advantage of the extra symmetry at two loops.

The string partition function in this setup can be written as follows. For our purposes, it is useful to keep separate the contributions of the different conformal field theory sectors, which leads to the expression

$$\mathbf{Z}_h(\vec{\epsilon}, \vec{\mathbf{d}}) = \mathcal{N}_h^{(\vec{\epsilon})} \int d\boldsymbol{\mu}_h \mathbf{F}_{\text{gh}}(\boldsymbol{\mu}) \mathbf{F}_{\text{scal}}^{(\vec{\mathbf{d}})}(\boldsymbol{\mu}) \mathbf{F}_{\parallel}^{(\vec{\epsilon})}(\boldsymbol{\mu}) \mathbf{F}_{\perp}(\boldsymbol{\mu}). \quad (3.3)$$

Here $\mathcal{N}_h^{(\vec{\epsilon})}$ is a field-dependent normalization factor, to be discussed in section 4.4, and we denoted the contributions of the world-sheet ghost systems b, c and β, γ by \mathbf{F}_{gh} , that of the string fields X_I, ψ_I perpendicular to the D-branes by $\mathbf{F}_{\text{scal}}^{(\vec{\mathbf{d}})}$, while the contribution of the fields along the D-branes has been separated into sectors parallel ($\mathbf{F}_{\parallel}^{(\vec{\epsilon})}$) and perpendicular (\mathbf{F}_{\perp}) to the magnetized directions. Finally, $\boldsymbol{\mu}$ denotes collectively the supermoduli: here we use the super-Schottky formalism, reviewed in appendix A, where the supermoduli are the sewing parameters $e^{i\pi\varsigma_i} k_i^{1/2}$ (with $\varsigma_i \in \{0, 1\}$) and the fixed points $(u_i|\theta_i), (v_i|\phi_i)$ of h super-projective transformations $i = 1, \dots, h$. Note that we explicitly associate with each Schottky multiplier k_i the phase ς_i associated with the NS spin structure around the b_i homology cycle. In this parametrization the measure $d\boldsymbol{\mu}_h$ reads [30]

$$d\boldsymbol{\mu}_h = \left[\frac{\sqrt{(\mathbf{v}_1 - \mathbf{u}_1)(\mathbf{u}_1 - \mathbf{v}_2)(\mathbf{v}_2 - \mathbf{v}_1)}}{d\mathbf{v}_1 d\mathbf{u}_1 d\mathbf{v}_2} d\Theta_{\mathbf{v}_1 \mathbf{u}_1 \mathbf{v}_2} \right] \prod_{i=1}^h \frac{dk_i e^{i\pi\varsigma_i}}{k_i^{3/2}} \frac{d\mathbf{u}_i d\mathbf{v}_i}{\mathbf{v}_i - \mathbf{u}_i}, \quad (3.4)$$

where we denote superconformal coordinates in boldface, and the notation $\mathbf{v}_i - \mathbf{u}_i$ indicates the supersymmetric difference

$$\mathbf{v}_i - \mathbf{u}_i \equiv v_i - u_i + \theta_i \phi_i. \quad (3.5)$$

The square parenthesis in eq. (3.4) takes into account the super-projective invariance of the integrand, which allows us to fix three bosonic and two fermionic variables. $\Theta_{\mathbf{v}_1 \mathbf{u}_1 \mathbf{v}_2}$ is the fermionic super-projective invariant which can be constructed with three fixed points,

defined in refs. [20, 64], and given explicitly in eq. (A.12). If we specialize eq. (3.4) to $h = 2$ we find

$$d\boldsymbol{\mu}_2 = e^{i\pi(\varsigma_1 + \varsigma_2)} \frac{dk_1}{k_1^{3/2}} \frac{dk_2}{k_2^{3/2}} \frac{d\mathbf{u}_2 d\Theta_{\mathbf{v}_1 \mathbf{u}_1 \mathbf{v}_2}}{\mathbf{v}_2 - \mathbf{u}_2} \sqrt{\frac{(\mathbf{u}_1 - \mathbf{v}_2)(\mathbf{v}_2 - \mathbf{v}_1)}{\mathbf{v}_1 - \mathbf{u}_1}}. \quad (3.6)$$

Let us now examine in turn the various factors in the integrand of eq. (3.3). The ghost contribution is independent of both the magnetic fields and the D-brane separations, so we can use the result of ref. [30], which reads

$$\mathbf{F}_{\text{gh}}(\boldsymbol{\mu}) = \frac{(1 - k_1)^2 (1 - k_2)^2}{(1 + e^{i\pi\varsigma_1} k_1^{1/2})^2 (1 + e^{i\pi\varsigma_2} k_2^{1/2})^2} \prod'_\alpha \prod_{n=2}^\infty \left(\frac{1 + k_\alpha^n}{1 + e^{i\pi\vec{\zeta} \cdot \vec{N}_\alpha} k_\alpha^{n-\frac{1}{2}}} \right)^2. \quad (3.7)$$

In eq. (3.7), the notation \prod'_α means that the product is over all primary classes of the super Schottky group: a primary class is an equivalence class of primitive super Schottky group elements, i.e. those elements which cannot be written as powers of another element; two primitive elements are in the same primary class if one is related to the other by a cyclic permutation of its factors, or by inversion. The vector \vec{N}_α has h integer-valued components, and is defined as follows: the i -th entry counts how many times the generator \mathbf{S}_i enters in the element of the super Schottky group \mathbf{T}_α : more precisely, we define $N_\alpha^i = 0$ for $\mathbf{T}_\alpha = \mathbf{1}$ and $N_\alpha^i = N_\beta^i \pm 1$ for $\mathbf{T}_\alpha = \mathbf{S}_i^{\pm 1} \mathbf{T}_\beta$. Finally, also $\vec{\zeta}$ is a vector with h components, with the i -th component denoting the spin structure along the b_i cycle, as noted above.

In fact, we need to be more precise about the notation in eq. (3.7), because the half-integer powers of k_α could indicate either of the two branches of the function. The notation is to be understood in the following way: when the spin structure is $\vec{\zeta} = 0$, we define the eigenvalue of the Schottky group element \mathbf{T}_α with the smallest absolute value to be $-k_\alpha^{1/2}$, see eq. (A.16). In particular, we take $k_i^{1/2}$ to be *positive*¹ for $i = 1, \dots, h$. This corresponds to the fact that spinors are anti-periodic around a homology cycle with zero spin structure (see, for example, ref. [65]). Furthermore, we expect the partition function to be symmetric under the exchange of the homology cycles b_1, b_2 and $b_1^{-1} \cdot b_2$ (depicted in figure 5), and one can verify that $k^{1/2}(\mathbf{S}_1^{-1} \mathbf{S}_2)$ is always positive whenever $k_1^{1/2}$ and $k_2^{1/2}$ have the same sign. Our convention puts all three multipliers on the same footing. Note that $k_\alpha^{1/2}$ is not in general positive when \mathbf{T}_α is not a generator: for example, the eigenvalues of $\mathbf{T}_\alpha = \mathbf{S}_1 \mathbf{S}_2$ are positive when the spin structure is zero, so that $k^{1/2}(\mathbf{S}_1 \mathbf{S}_2)$, as computed in eq. (A.25), is negative.

The scalar contribution to eq. (3.3) depends on the separation between the D-branes in the transverse directions, as shown in figure 3. We can write $\mathbf{F}_{\text{scal}}^{(\vec{d})}$ as a product over the super Schottky group, capturing the non-zero mode contribution, times a new factor $\mathcal{Y}(\boldsymbol{\mu}, \vec{d})$, as

$$\mathbf{F}_{\text{scal}}^{(\vec{d})}(\boldsymbol{\mu}) = \mathcal{Y}(\boldsymbol{\mu}, \vec{d}) \prod'_\alpha \prod_{n=1}^\infty \left(\frac{1 + e^{i\pi\vec{\zeta} \cdot \vec{N}_\alpha} k_\alpha^{n-1/2}}{1 - k_\alpha^n} \right)^{n_s}. \quad (3.8)$$

The explicit form of \mathcal{Y} can be found by repeating the calculation performed in ref. [66] for the bosonic theory, and replacing the period matrix τ with the super-period matrix $\boldsymbol{\tau}$

¹This convention is the opposite to the one used in [11].

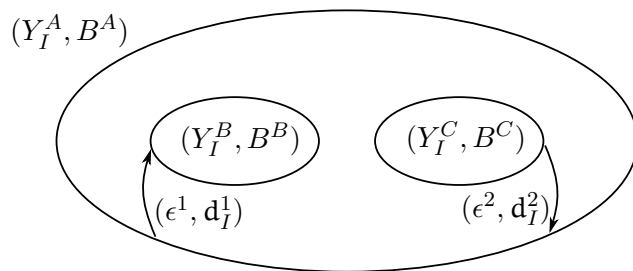


Figure 4. The double annulus world-sheet, with three boundaries labeled with $i = 0, 1, 2$ attached to three D-branes, with Chan-Paton factors A, B, C. The relative positions and background field strengths of branes B and C with respect to brane A determine the masses and the twisted boundary conditions, as described in the text.

discussed in appendix A.2.2. We find

$$\mathcal{Y}(\boldsymbol{\mu}, \vec{\mathbf{d}}) \equiv \prod_{I=1}^{n_s} \exp\left(-\frac{\vec{\mathbf{d}}_I \cdot \boldsymbol{\tau} \cdot \vec{\mathbf{d}}_I}{2\pi i \alpha'}\right). \quad (3.9)$$

It is instructive, and useful for our later implementation, to consider explicitly the $h = 2$ case. Let the $i = 0, 1, 2$ borders of the world-sheet be on the D-branes labelled by A, B and C, respectively. As mentioned above, it is useful in this special $h = 2$ case to define the $i = 2$ component \mathbf{d}_I^2 with the opposite sign with respect to eq. (3.1), so we have $\mathbf{d}_I^1 = Y_I^A - Y_I^B$ and $\mathbf{d}_I^2 = Y_I^C - Y_I^A$. By so doing, we can then define an additional (redundant) quantity, describing the displacement between the D-branes attached to the $i = 1$ and $i = 2$ borders, as $\mathbf{d}_I^3 = Y_I^B - Y_I^C$. Now the three distances \mathbf{d}_I^i for $i = 1, 2, 3$ are on an equal footing, reflecting the symmetry of the world-sheet topology, and we have $\mathbf{d}_I^1 + \mathbf{d}_I^2 + \mathbf{d}_I^3 = 0$ (see figure 4). One may easily verify that the product over the n_s transverse directions in eq. (3.9) evaluates to a function of the squared masses m_i^2 , defined as in eq. (3.2). One finds

$$\mathcal{Y}(\boldsymbol{\mu}, \vec{\mathbf{d}}) = \exp\left[2\pi i \alpha' (m_1^2 \boldsymbol{\tau}_{11} + m_2^2 \boldsymbol{\tau}_{22} + (m_3^2 - m_1^2 - m_2^2) \boldsymbol{\tau}_{12})\right]. \quad (3.10)$$

Finally, let us turn to the contribution of the world-sheet fields X^μ, ψ^μ along the world-volume direction of the D-branes. In absence of magnetic fields, the result can be found in ref. [30] and it reads

$$\mathbf{F}_{\text{gl}}^{(0)}(\boldsymbol{\mu}) = [\det(\text{Im } \boldsymbol{\tau})]^{-d/2} \prod_{\alpha} \prod_{n=1}^{\infty} \left(\frac{1 + e^{i\pi \vec{\zeta} \cdot \vec{N}_{\alpha}} k_{\alpha}^{n-1/2}}{1 - k_{\alpha}^n}\right)^d. \quad (3.11)$$

In the presence of constant background gauge fields, $\mathbf{F}_{\text{gl}}^{(0)}$ gets modified, since string coordinates along the D-branes are sensitive to such backgrounds. The relevant modification to the bosonic theory was derived in ref. [15]. Using the techniques described in refs. [15, 33, 67], it is possible to generalize this construction to the Neveu-Schwarz spin structure of the RNS superstring [11]. The result is that switching on the background fields

amounts to multiplying $\mathbf{F}_{\text{gl}}^{(0)}$ by a factor, as

$$\mathbf{F}_{\text{gl}}^{(0)}(\boldsymbol{\mu}) \longrightarrow \mathbf{F}_{\text{gl}}^{(\vec{\epsilon})}(\boldsymbol{\mu}) = \mathcal{R}(\boldsymbol{\mu}, \vec{\epsilon}) \mathbf{F}_{\text{gl}}^{(0)}(\boldsymbol{\mu}), \quad (3.12)$$

where, assuming the background fields to be non-zero only in one plane, we have

$$\begin{aligned} \mathcal{R}(\boldsymbol{\mu}, \vec{\epsilon}) = e^{-i\pi\vec{\epsilon}\cdot\boldsymbol{\tau}\cdot\vec{\epsilon}} \frac{\det(\text{Im } \boldsymbol{\tau})}{\det(\text{Im } \boldsymbol{\tau}_{\vec{\epsilon}})} \prod_{\alpha} \prod_{n=1}^{\infty} \left[\left(\frac{1 + e^{i\pi\vec{\zeta}\cdot\vec{N}_{\alpha}} k_{\alpha}^{n-1/2}}{1 - k_{\alpha}^n} \right)^{-2} \right. \\ \left. \times \frac{(1 + e^{i\pi(2\vec{\epsilon}\cdot\boldsymbol{\tau} + \vec{\zeta})\cdot\vec{N}_{\alpha}} k_{\alpha}^{n-1/2}) (1 + e^{-i\pi(2\vec{\epsilon}\cdot\boldsymbol{\tau} + \vec{\zeta})\cdot\vec{N}_{\alpha}} k_{\alpha}^{n-1/2})}{(1 - e^{2\pi i\vec{\epsilon}\cdot\boldsymbol{\tau}\cdot\vec{N}_{\alpha}} k_{\alpha}^n) (1 - e^{-2\pi i\vec{\epsilon}\cdot\boldsymbol{\tau}\cdot\vec{N}_{\alpha}} k_{\alpha}^n)} \right]. \end{aligned} \quad (3.13)$$

The matrix $\boldsymbol{\tau}_{\vec{\epsilon}}$ is the supersymmetric analogue of the twisted (or Prym) period matrix, the bosonic version of which was computed with the sewing method in [33, 35]. Its calculation is outlined in appendix B.2.

Inspecting eq. (3.13), we see that $\mathbf{F}_{\text{gl}}^{(\vec{\epsilon})}$ can be factorized as the product of a term $\mathbf{F}_{\parallel}^{(\vec{\epsilon})}$, capturing the contribution along the magnetized plane, times an ϵ -independent term \mathbf{F}_{\perp} arising from the unmagnetized directions. In the field theory limit, $\mathbf{F}_{\parallel}^{(\vec{\epsilon})}$ will generate the contributions of gluons polarized in the plane of the background field, while \mathbf{F}_{\perp} will give rise to gluons polarized in the transverse directions. Explicitly, we have

$$\mathbf{F}_{\perp}(\boldsymbol{\mu}) = [\det(\text{Im } \boldsymbol{\tau})]^{-\frac{d-2}{2}} \prod_{\alpha} \prod_{n=1}^{\infty} \left(\frac{1 + e^{i\pi\vec{\zeta}\cdot\vec{N}_{\alpha}} k_{\alpha}^{n-1/2}}{1 - k_{\alpha}^n} \right)^{d-2}, \quad (3.14)$$

$$\mathbf{F}_{\parallel}^{(\vec{\epsilon})}(\boldsymbol{\mu}) = \frac{e^{-i\pi\vec{\epsilon}\cdot\boldsymbol{\tau}\cdot\vec{\epsilon}}}{\det(\text{Im } \boldsymbol{\tau}_{\vec{\epsilon}})} \prod_{\alpha} \prod_{n=1}^{\infty} \frac{(1 + e^{i\pi(2\vec{\epsilon}\cdot\boldsymbol{\tau} + \vec{\zeta})\cdot\vec{N}_{\alpha}} k_{\alpha}^{n-1/2}) (1 + e^{-i\pi(2\vec{\epsilon}\cdot\boldsymbol{\tau} + \vec{\zeta})\cdot\vec{N}_{\alpha}} k_{\alpha}^{n-1/2})}{(1 - e^{2\pi i\vec{\epsilon}\cdot\boldsymbol{\tau}\cdot\vec{N}_{\alpha}} k_{\alpha}^n) (1 - e^{-2\pi i\vec{\epsilon}\cdot\boldsymbol{\tau}\cdot\vec{N}_{\alpha}} k_{\alpha}^n)}. \quad (3.15)$$

Focusing now on the $h = 2$ case, we can use super-projective invariance to fix three bosonic and two fermionic moduli. A convenient gauge choice in the super Schottky formalism is to specify the positions of the fixed points, given in terms of homogeneous coordinates² on $\mathbb{CP}^{1|1}$, as

$$|\mathbf{u}_1\rangle = (0, 1|0)^t, \quad |\mathbf{v}_1\rangle = (1, 0|0)^t, \quad |\mathbf{u}_2\rangle = (u, 1|\theta)^t, \quad |\mathbf{v}_2\rangle = (1, 1|\phi)^t, \quad (3.16)$$

with $(0 < u < 1)$, which leads to

$$\Theta_{\mathbf{v}_1\mathbf{u}_1\mathbf{v}_2} = \phi, \quad \mathbf{v}_2 - \mathbf{u}_2 = 1 - u + \theta\phi, \quad \sqrt{\frac{(\mathbf{u}_1 - \mathbf{v}_2)(\mathbf{v}_2 - \mathbf{v}_1)}{\mathbf{v}_1 - \mathbf{u}_1}} = 1. \quad (3.17)$$

Implementing this projective gauge fixing in eq. (3.3), we can finally express the $h = 2$ partition function as

$$\mathbf{Z}_2(\vec{\epsilon}, \vec{\mathbf{d}}) = e^{i\pi(\varsigma_1 + \varsigma_2)} \int \frac{dk_1}{k_1^{3/2}} \frac{dk_2}{k_2^{3/2}} \frac{du}{y} d\theta d\phi \mathbf{F}_{\text{gh}}(\boldsymbol{\mu}) \mathbf{F}_{\parallel}^{(\vec{\epsilon})}(\boldsymbol{\mu}) \mathbf{F}_{\perp}(\boldsymbol{\mu}) \mathbf{F}_{\text{scal}}^{(\vec{\mathbf{d}})}(\boldsymbol{\mu}), \quad (3.18)$$

where we defined

$$y \equiv (\mathbf{u}_1, \mathbf{v}_1, \mathbf{u}_2, \mathbf{v}_2) = 1 - u + \theta\phi, \quad (3.19)$$

in terms of the bosonic super-projective invariant built out of four points, $(\mathbf{z}_1, \mathbf{z}_2, \mathbf{z}_3, \mathbf{z}_4)$, see eq. (A.13).

²The relation between the super-conformal and homogeneous coordinates is given in eq. (A.5).

4 Taking the field theory limit

4.1 Expanding in powers of the multipliers

We are interested in computing the $\alpha' \rightarrow 0$ limit of the integrand of the superstring amplitude. In this limit, we expect massive string states to decouple, so that one is left with the massless spectrum. Possible contributions from the tachyon ground state cancel after GSO projection in the superstring case, or should be discarded by hand in the bosonic case. It is in principle non trivial to take this limit before integration over (super) moduli, since this requires constructing a map between the dimensionless moduli of the (super) Riemann surface and the dimensionful quantities that arise in the computation of field theory Feynman diagrams. This task is considerably simplified in the Schottky parametrization, where, as discussed for example in ref. [11], the contributions of individual string states can be identified by performing a Laurent expansion of the integrand of the string partition function in powers of the multipliers. One finds a correspondence between the order of expansion and the mass level of the string, and furthermore, within each mass level, one can track individual states by tracing the origin of each term to a specific factor in the string integrand.

The main difference between the bosonic string and the RNS superstring is that for the latter, which we discuss here, the expansion is in powers of $k_i^{1/2}$ rather than k_i , as is already apparent from our discussion in section 3. More precisely, since the measure of integration contains a factor $k_i^{-3/2}$, a term proportional to $k_i^{(n-3)/2}$ corresponds to a contribution from a state belonging to the n -th mass level circulating in the i -th string loop (where $n = 0$ corresponds to the tachyonic ground state). Therefore, all terms with $n > 1$ acquire a positive mass squared, $m^2 = (n - 1)/(2\alpha')$, and decouple in the limit $\alpha' \rightarrow 0$. We conclude that it is necessary to expand the various factors in the integrand of eq. (3.18) only up to terms of order $k_i^{1/2}$, in order to get the complete massless field theory amplitude.

This task is made possible by the fact that the multipliers of only finitely many super-Schottky group elements contribute at order $k_1^{1/2} k_2^{1/2}$. The reason is that the leading-order behaviour of the multiplier $k_\alpha = k(\mathbf{T}_\alpha)$ is related in a simple way to the index N_α^i introduced in section 3: one may verify that

$$k^{1/2}(\mathbf{S}_i^{\pm 1} \mathbf{T}_\alpha) = \mathcal{O}(k_i^{1/2} k_\alpha^{1/2}), \tag{4.1}$$

unless of course the left-most factor of \mathbf{T}_α is $\mathbf{S}_i^{\mp 1}$. Thus, for every super Schottky group element \mathbf{T}_α not in the primary class of an element in the set $\{\mathbf{S}_1, \mathbf{S}_2, \mathbf{S}_1 \mathbf{S}_2, \mathbf{S}_1^{-1} \mathbf{S}_2\}$, the multiplier $k_\alpha^{1/2}$ vanishes faster than $k_i^{1/2}$ for $k_i \rightarrow 0$. This enables us to easily compute expressions for all the factors in eq. (3.3), up to the relevant order.

Let us begin with \mathbf{F}_{gh} , defined in eq. (3.7). One immediately sees that the expansion of the infinite product starts at $\mathcal{O}(k_i^{3/2})$, and the numerator of the first factor can similarly be dropped. \mathbf{F}_{gh} becomes simply

$$\mathbf{F}_{\text{gh}}(\boldsymbol{\mu}) = (1 - 2 e^{i\pi\varsigma_1} k_1^{1/2})(1 - 2 e^{i\pi\varsigma_2} k_2^{1/2}) + \mathcal{O}(k_i). \tag{4.2}$$

Next, we compute \mathbf{F}_\perp , defined in eq. (3.14). Using the expressions for the multipliers $k^{1/2}(\mathbf{S}_1^{-1}\mathbf{S}_2)$ and $k^{1/2}(\mathbf{S}_1\mathbf{S}_2)$, given in eq. (A.25), we find

$$\mathbf{F}_\perp(\boldsymbol{\mu}) = [\det(\text{Im } \boldsymbol{\tau})]^{-\frac{d-2}{2}} \left[1 + (d-2)(e^{i\pi\varsigma_1} k_1^{1/2} + e^{i\pi\varsigma_2} k_2^{1/2}) \right. \\ \left. + (d-2) \left(\frac{y}{u} - y + d-2 \right) e^{i\pi(\varsigma_1+\varsigma_2)} k_1^{1/2} k_2^{1/2} \right] + \mathcal{O}(k_i). \quad (4.3)$$

The expansion of the determinant of the super period matrix is given in eq. (A.33), and, substituted here, leads to the factor

$$[\det(\text{Im } \boldsymbol{\tau})]^{-\frac{d-2}{2}} = \left[\frac{4\pi^2}{\log k_1 \log k_2 - \log^2 u} \right]^{\frac{d-2}{2}} \\ \times \left[1 + (d-2) \frac{y}{u} \theta\phi \frac{e^{i\pi\varsigma_1} k_1^{1/2} \log k_1 + e^{i\pi\varsigma_2} k_2^{1/2} \log k_2}{\log k_1 \log k_2 - (\log u)^2} \right] + \mathcal{O}(k_i). \quad (4.4)$$

Notice that logarithmic dependence on (super) moduli must be retained exactly: indeed, as shown in ref. [11] and discussed here in section 4.3, it will turn into polynomial dependence on Schwinger parameters in the field theory limit.

The expansion of the factor $\mathbf{F}_\parallel^{(\vec{\epsilon})}$, also given in eq. (3.14), is more intricate, as well as more interesting, because of the dependence on the external fields. Writing

$$\mathbf{F}_\parallel^{(\vec{\epsilon})}(\boldsymbol{\mu}) = \frac{e^{-i\pi\vec{\epsilon}\cdot\boldsymbol{\tau}\cdot\vec{\epsilon}}}{\det(\text{Im } \boldsymbol{\tau}_\vec{\epsilon})} \widehat{\mathcal{R}}(\boldsymbol{\mu}, \vec{\epsilon}), \quad (4.5)$$

where $\widehat{\mathcal{R}}$ is the background-field dependent factor of the infinite product appearing in eq. (3.15), we see that we can separately expand the three factors. The determinant of the twisted super period matrix is by far the most intricate contribution. It is discussed in appendix B, and a complete expression with the exact dependence on the fields, through $\vec{\epsilon}$, is very lengthy. We will see in section 4.3, however, that in the field theory limit we must expand in powers of the components of $\vec{\epsilon}$ as well: at that stage, we will be able to write a completely explicit expression also for $\det(\text{Im } \boldsymbol{\tau}_\vec{\epsilon})$. The exponential factor in the numerator of eq. (4.5) can be computed using the expression for $\boldsymbol{\tau}$ in eq. (A.32), and is given by

$$e^{-i\pi\vec{\epsilon}\cdot\boldsymbol{\tau}\cdot\vec{\epsilon}} = k_1^{-\epsilon_1^2/2} k_2^{-\epsilon_2^2/2} u^{-\epsilon_1\epsilon_2} \left[1 + \frac{y}{u} \theta\phi \left(e^{i\pi\varsigma_2} k_2^{1/2} \epsilon_1^2 + e^{i\pi\varsigma_1} k_1^{1/2} \epsilon_2^2 \right) \right] + \mathcal{O}(k_i). \quad (4.6)$$

Finally, the remaining factor in $\mathbf{F}_\parallel^{(\vec{\epsilon})}$ is given by

$$\widehat{\mathcal{R}}(\boldsymbol{\mu}, \vec{\epsilon}) = 1 + e^{i\pi\varsigma_1} k_1^{1/2} g_{12}^+ + e^{i\pi\varsigma_2} k_2^{1/2} g_{21}^+ \\ + e^{i\pi(\varsigma_1+\varsigma_2)} k_1^{1/2} k_2^{1/2} \left[g_{12}^+ g_{21}^+ - 2\theta\phi \frac{y}{u} (\epsilon_1 g_{12}^- + \epsilon_2 g_{21}^-) \right. \\ \left. - \frac{1}{2} \left(\left(y - \frac{y}{u} \right) g_{12}^+ g_{21}^+ + \left(y + \frac{y}{u} \right) g_{12}^- g_{21}^- \right) \right] + \mathcal{O}(k_i), \quad (4.7)$$

where we defined the factors

$$g_{ij}^{\pm} = k_i^{\epsilon_i} u^{\epsilon_j} \pm k_i^{-\epsilon_i} u^{-\epsilon_j}. \quad (4.8)$$

The last required ingredient is $\mathbf{F}_{\text{scal}}^{(\vec{d})}$, defined in eq. (3.8). Combining eq. (3.10) with eq. (A.32), we get

$$\begin{aligned} \mathcal{Y}(\boldsymbol{\mu}, \vec{d}) &= k_1^{\alpha' m_1^2} k_2^{\alpha' m_2^2} u^{\alpha'(m_3^2 - m_1^2 - m_2^2)} \\ &\times \left[1 - 2\alpha' \frac{y}{u} (e^{i\pi\varsigma_1} k_1^{1/2} m_2^2 + e^{i\pi\varsigma_2} k_2^{1/2} m_1^2) \right] + \mathcal{O}(k_i). \end{aligned} \quad (4.9)$$

The remaining, mass-independent, factor in $\mathbf{F}_{\text{scal}}^{(\vec{d})}$ in eq. (3.8) is easily expanded, getting

$$\mathbf{F}_{\text{scal}}^{(0)}(\boldsymbol{\mu}) = 1 + n_s (e^{i\pi\varsigma_1} k_1^{1/2} + e^{i\pi\varsigma_2} k_2^{1/2}) + n_s e^{i\pi(\varsigma_1 + \varsigma_2)} k_1^{1/2} k_2^{1/2} \left(\frac{y}{u} - y + n_s \right). \quad (4.10)$$

This completes the list of the factors in eq. (3.18). It is now straightforward to combine them, and expand the resulting polynomial in $k_i^{1/2}$ to the relevant order. Before proceeding, however, we must consider more carefully our choice of variables in view of the field theory limit.

4.2 A parametrization for the symmetric degeneration

In order to go beyond the specification of the mass states circulating in the string loops, and identify the contribution of individual Feynman diagrams in the field theory limit, we must refine our parametrization of (super) moduli space. Let us now, in particular, concentrate on Feynman diagrams with the symmetric topology depicted in the first two lines of figure 1. While individual Feynman diagrams will not be symmetric under the exchange of any two lines when the propagating states are different, we expect that, when summing over all states at a given mass level, the result should be fully symmetric, since there are no features distinguishing the three propagators at the level of the world-sheet geometry. This symmetry requirement will guide our choice of parametrization for the region of moduli space close to this degeneration, along the lines already discussed in ref. [11].

It is clear that the parametrization in terms of the bosonic moduli $k_1^{1/2}$, $k_2^{1/2}$ and $u \equiv 1 - y + \theta\phi$ will not be sufficiently symmetric, since the first two chosen moduli are multipliers of super-Schottky group generators, while the third one is a cross-ratio of the fixed points. To present the integration measure in a sufficiently symmetric way, we must parametrize it to be symmetric under permutations of the super-Schottky group elements \mathbf{S}_1 , \mathbf{S}_2 and $\mathbf{S}_1^{-1}\mathbf{S}_2$. The reason for this is that the homology cycles b_1 , b_2 and $(b_1^{-1} \cdot b_2)$ lift to these super-Schottky group elements on the covering surface $\mathbf{CP}^{1|1} - \Lambda$, and any two of b_1 , b_2 and $(b_1^{-1} \cdot b_2)$ (along with the appropriate choice of a -cycles) constitute a good canonical homology basis (see figure 5a). Our choice of \mathbf{S}_1 and \mathbf{S}_2 as the generators is arbitrary, so, in order to preserve modular invariance, the measure must be parametrized to display the symmetry under permutations of \mathbf{S}_1 , \mathbf{S}_2 and $\mathbf{S}_1^{-1}\mathbf{S}_2$. To reinforce this point, note that any other homology cycle built out of b cycles will intersect itself, as is the case for example for the $(b_1 \cdot b_2)$ cycle, depicted in figure 5b.

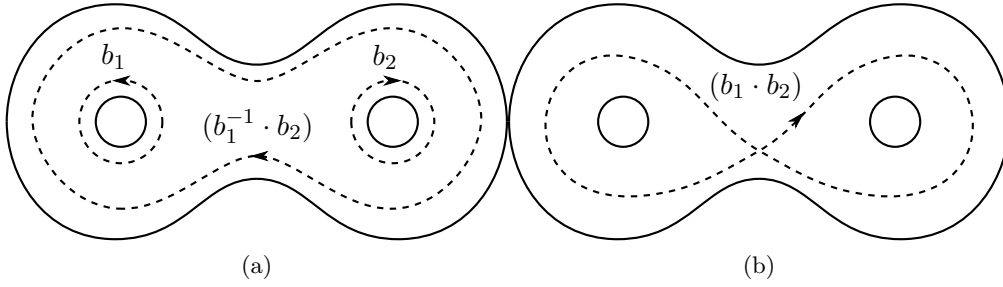


Figure 5. Two types of homology cycles on the double annulus.

A natural way to symmetrize the measure is to use the multiplier of $\mathbf{S}_1^{-1}\mathbf{S}_2$ as the third bosonic modulus, instead of u . Defining $-e^{i\pi\varsigma_3}k_3^{1/2}$ to be the eigenvalue of $\mathbf{S}_1^{-1}\mathbf{S}_2$ with the smallest absolute value, so that k_3 is the multiplier of that super Schottky group element, one can compute $k_3^{1/2}$ using eq. (A.24). It is related to y implicitly through

$$y = \frac{(1 - k_1)(1 - k_2) + \theta\phi \left[(1 + e^{i\pi\varsigma_1}k_1^{1/2})(1 + e^{i\pi\varsigma_2}k_2^{1/2})(1 + e^{i\pi(\varsigma_1+\varsigma_2)}k_1^{1/2}k_2^{1/2}) \right]}{1 + k_1k_2 + k_1^{1/2}k_2^{1/2}(k_3^{1/2} + k_3^{-1/2})}. \quad (4.11)$$

In these definitions, ς_3 is the spin structure around the $b_3 \equiv b_1^{-1} \cdot b_2$ homology cycle, and therefore it is given simply by $\varsigma_3 = \varsigma_1 + \varsigma_2 \pmod{2}$. $k_3^{1/2}$ is then positive, just as $k_1^{1/2}$ and $k_2^{1/2}$ are.

As discussed in ref. [11], the field theory limit becomes particularly transparent if one factors the three multipliers k_i in order to assign a parameter to each section of the Riemann surface that will degenerate into an individual field theory propagator. This is done by defining

$$k_1^{1/2} = \sqrt{p_1}\sqrt{p_3} \quad k_2^{1/2} = \sqrt{p_2}\sqrt{p_3} \quad k_3^{1/2} = \sqrt{p_1}\sqrt{p_2}, \quad (4.12)$$

where $\sqrt{p_i}$ is defined to be positive. In analogy to the discussion of ref. [11], each p_i will be interpreted, in the field theory limit, as the logarithm of the Schwinger proper time associated to a propagator.

For bosonic strings, the discussion leading to eq. (4.12) was sufficient to construct a symmetric measure of integration, prepared for the symmetric degeneration in the field theory limit. In the present case, instead, one must also worry about fermionic moduli: our current choice of θ and ϕ as moduli will not yield a symmetric measure, since they are super-projective invariants built out of the fixed points of \mathbf{S}_1 and \mathbf{S}_2 only. In order to find the proper Grassmann variables of integration, we take advantage of the fact that we are allowed to rescale θ and ϕ with arbitrary functions of the moduli, since such a rescaling automatically cancels with the Berezinian of the corresponding change of integration variables. Such a rescaling of course leaves the integral invariant, but it can be used to move contributions between the various factors of the integrand, in such a way that individual factors respect the overall exchange symmetry of the diagram, as we wish to do here. In order to find a pair of odd moduli invariant under permutations of \mathbf{S}_1 , \mathbf{S}_2 , $\mathbf{S}_1^{-1}\mathbf{S}_2$, we

proceed as follows. Define

$$\hat{\theta}_{ij} = c_{ij} \Theta_{\mathbf{v}_i \mathbf{u}_i \mathbf{u}_j}, \quad \hat{\phi}_{ij} = c_{ij} \Theta_{\mathbf{v}_i \mathbf{u}_i \mathbf{v}_j}, \quad (4.13)$$

for $(ij) = (12), (23), (31)$. For the factors c_{ij} we make the choice

$$c_{12} = [e^{i\pi\varsigma_3} (1 + q_1 q_2)(1 - q_1 q_3)(1 - q_2 q_3)]^{-1/2}, \quad (4.14)$$

with c_{23} and c_{31} obtained by permuting the indices (123), and where \mathbf{u}_3 and \mathbf{v}_3 are the fixed points of the transformation $\mathbf{S}_1^{-1} \mathbf{S}_2$. In eq. (4.14), we have introduced the symbols q_i , $i = 1, 2, 3$, defined by³

$$q_1 = e^{i\pi\varsigma_2} \sqrt{p_1}, \quad q_2 = e^{i\pi\varsigma_1} \sqrt{p_2}, \quad q_3 = e^{i\pi\varsigma_3} \sqrt{p_3}. \quad (4.15)$$

With this choice for c_{ij} , one can check that

$$e^{i\pi\varsigma_3} d\hat{\theta}_{12} d\hat{\phi}_{12} = e^{i\pi\varsigma_1} d\hat{\theta}_{23} d\hat{\phi}_{23} = e^{i\pi\varsigma_2} d\hat{\theta}_{31} d\hat{\phi}_{31}, \quad (4.16)$$

so that the Grassmann measure of integration has the required symmetry.

It is not difficult to rewrite the various objects computed in section 4.1 in terms of the new variables, and expand the results to the required order in p_i . In order to do so, we use

$$\theta\phi = q_3(1 + q_1 q_2) \hat{\theta}_{12} \hat{\phi}_{12} + \mathcal{O}(p_i), \quad (4.17)$$

as well as

$$u = p_3 [1 + \hat{\theta}_{12} \hat{\phi}_{12} (q_3 - q_1 - q_2 + q_1 q_2 q_3)] + \mathcal{O}(p_1, p_2, p_3^2). \quad (4.18)$$

With these results, it is straightforward to verify the symmetry of the full string integrand. In particular, we find that the product of the two-loop measure of integration times the ghost factor is given by

$$\begin{aligned} d\boldsymbol{\mu}_2 \mathbf{F}_{\text{gh}}(\boldsymbol{\mu}) &= \prod_{i=1}^3 \left[\frac{dp_i}{p_i^{3/2}} \frac{1 - e^{i\pi\varsigma_i} k_i^{1/2}}{\sqrt{1 + p_i}} \right] d\hat{\theta}_{12} d\hat{\phi}_{12} \frac{1}{\sqrt{1 + p_1 p_2 p_3}} \\ &= \prod_{i=1}^3 \left[\frac{dp_i}{q_i^3} \right] d\hat{\theta}_{12} d\hat{\phi}_{12} (1 - q_1 q_3 - q_2 q_3 - q_1 q_2) + \mathcal{O}(p_i), \end{aligned} \quad (4.19)$$

where the contribution of the spin structure to $d\boldsymbol{\mu}_2$ in eq. (3.6) has been absorbed in $d\hat{\theta}_{12} d\hat{\phi}_{12}$. Similarly, the contribution of the orbital modes defined in eq. (4.7) becomes

$$\begin{aligned} \widehat{\mathcal{R}}(\boldsymbol{\mu}, \vec{\epsilon}) &= 1 + \{ q_1 q_2 (p_1^{\epsilon_1} p_2^{-\epsilon_2} - p_1^{-\epsilon_1} p_2^{\epsilon_2}) [1 - \hat{\theta}_{12} \hat{\phi}_{12} q_3 (\epsilon_1 - \epsilon_2)] \\ &\quad + \text{cyclic permutations} \} + \mathcal{O}(p_i). \end{aligned} \quad (4.20)$$

³Note that the spin structures of q_1 and q_2 are swapped compared with what one might expect. This, however, is reasonable, because the q_i defined in this way factorize the NS sewing parameters $e^{i\pi\varsigma_i} k_i^{1/2}$ as follows: $e^{i\pi\varsigma_1} k_1^{1/2} = q_1 q_3$, $e^{i\pi\varsigma_2} k_2^{1/2} = q_2 q_3$, $e^{i\pi\varsigma_3} k_3^{1/2} = q_1 q_2$.

Here, and in the rest of this section, we understand ‘cyclic permutations’ to mean cyclic permutations of the indices (1, 2, 3) for p_i , q_i , ϵ_i and m_i^2 , where $\epsilon_3 \equiv -\epsilon_1 - \epsilon_2$.⁴ The indices of $\hat{\theta}_{12} \hat{\phi}_{12}$, on the other hand, are not permuted.

In order to reconstruct the full contribution of fields in the directions parallel to the magnetized plane, we still need the other factors appearing in eq. (4.6). The exponential factor takes the form

$$e^{-i\pi\vec{\tau}\cdot\vec{\tau}} = p_1^{-\epsilon_1^2/2} p_2^{-\epsilon_2^2/2} p_3^{-\epsilon_3^2/2} \left[1 - \frac{1}{2} \hat{\theta}_{12} \hat{\phi}_{12} (q_1 (\epsilon_1^2 - \epsilon_2^2 - \epsilon_3^2) + q_1 q_2 q_3 \epsilon_1^2 + \text{cycl. perm.}) \right] + \mathcal{O}(p_i). \quad (4.21)$$

The last factor in eq. (4.6) is the twisted determinant $\det(\text{Im } \tau_{\vec{\epsilon}})$, whose calculation is described in appendix B. The result for generic values of u is a lengthy combination of hypergeometric functions, which however simplifies drastically in the limit we are considering here, where u , proportional to p_3 , is small.

In this limit (B.33) reads

$$\begin{aligned} \det(\text{Im } \tau_{\vec{\epsilon}}) &= \frac{1}{4\pi^2} \Gamma(-\epsilon_1) \Gamma(-\epsilon_2) \Gamma(-\epsilon_3) \left\{ p_1^{\epsilon_1/2} p_2^{\epsilon_2/2} p_3^{\epsilon_3/2} (\epsilon_1 p_1^{-\epsilon_1/2} + \epsilon_2 p_2^{-\epsilon_2/2} + \epsilon_3 p_3^{-\epsilon_3/2}) \right. \\ &\quad + \hat{\theta}_{12} \hat{\phi}_{12} [q_1 (p_1^{\epsilon_1/2} p_2^{-\epsilon_2/2} p_3^{-\epsilon_3/2} + p_1^{-\epsilon_1/2} p_2^{\epsilon_2/2} p_3^{\epsilon_3/2}) p_1^{\epsilon_1/2} \epsilon_2 \epsilon_3 + \text{cycl. perm.}] \\ &\quad + \hat{\theta}_{12} \hat{\phi}_{12} q_1 q_2 q_3 p_1^{-3\epsilon_1/2} p_2^{-3\epsilon_2/2} p_3^{-3\epsilon_3/2} \\ &\quad \left. \times [p_1^{2\epsilon_1} p_2^{2\epsilon_2} p_3^{\epsilon_3} (2\epsilon_3^2 - \epsilon_1 \epsilon_2) + p_3^{3\epsilon_3} (2\epsilon_3 (p_1^{2\epsilon_1} \epsilon_2 + p_2^{2\epsilon_2} \epsilon_1) - p_1^{\epsilon_1} p_2^{\epsilon_2} \epsilon_1 \epsilon_2) + \text{cycl. perm.}] \right\} \\ &\quad + (\epsilon_i \leftrightarrow -\epsilon_i) + \mathcal{O}(p_i). \end{aligned} \quad (4.22)$$

Next, we need the contribution of the untwisted gluon sector, given in eq. (4.3). In the current parametrization it reads

$$\mathbf{F}_{\perp}(\boldsymbol{\mu}) = [\det(\text{Im } \boldsymbol{\tau})]^{-(d-2)/2} [1 - (d-2)(q_1 q_3 + q_2 q_3 + q_1 q_2)] + \mathcal{O}(p_i), \quad (4.23)$$

where the determinant of the period matrix, given by eq. (A.33), becomes

$$\begin{aligned} \det(\text{Im } \boldsymbol{\tau}) &= \frac{1}{4\pi^2} \left\{ \log p_1 \log p_2 + \log p_2 \log p_3 + \log p_3 \log p_1 \right. \\ &\quad \left. - 2 \hat{\theta}_{12} \hat{\phi}_{12} [(q_1 - q_1 q_2 q_3) \log p_1 + \text{cycl. perm.}] \right\} + \mathcal{O}(p_i). \end{aligned} \quad (4.24)$$

Finally, we need the ingredients for the scalar sector, given above in eq. (4.9) and eq. (4.10). The mass contribution takes the form

$$\begin{aligned} \mathcal{Y}(\boldsymbol{\mu}, \vec{\mathbf{d}}) &= p_1^{\alpha' m_1^2} p_2^{\alpha' m_2^2} p_3^{\alpha' m_3^2} [1 + \alpha' \hat{\theta}_{12} \hat{\phi}_{12} (q_1 (m_1^2 - m_2^2 - m_3^2) \\ &\quad + q_1 q_2 q_3 m_1^2 + \text{cycl. perm.})] + \mathcal{O}(p_i), \end{aligned} \quad (4.25)$$

while the mass-independent factor is given by

$$\mathbf{F}_{\text{scal}}^{(0)}(\boldsymbol{\mu}) = 1 + n_s (q_1 q_3 + q_2 q_3 + q_1 q_2) + \mathcal{O}(p_i). \quad (4.26)$$

This completes the list of ingredients needed for the analysis of the symmetric degeneration of the surface. We now turn to the calculation of the $\alpha' \rightarrow 0$ limit.

⁴Recall that, in the $h = 2$ case, we define ϵ_2 with the opposite sign with respect to eq. (3.1), to exploit the symmetry of the worldsheet.

4.3 Mapping moduli to Schwinger parameters

The last, crucial step needed to take the field theory limit is the mapping between the dimensionless moduli and the dimensionful quantities that enter field theory Feynman diagrams. This α' -dependent change of variables sets the space-time scale of the scattering process and selects those terms in the string integrand that are not suppressed by powers of the string tension. The basic ideas underlying the choice of field theory variables have been known for a long time (see for example ref. [68]), and were recently refined for the case of multi-loop gluon amplitudes in ref. [11]. The change from bosonic strings to superstrings does not significantly affect those arguments: in the present case we will see that integration over odd moduli will simply provide a more refined tool to project out unwanted contributions, once the Berezin integration is properly handled.

Following ref. [11], we introduce dimensionful field-theoretic quantities with the change of variables

$$p_i = \exp\left[-\frac{t_i}{\alpha'}\right], \quad \epsilon_i = 2\alpha'gB_i + \mathcal{O}(\alpha'^3), \quad i = 1, 2, 3. \quad (4.27)$$

These definitions make it immediately obvious that terms of the form $p_i^{c\epsilon_i}$ must be treated exactly, as we have done. On the other hand, terms proportional to high powers of ϵ_i are suppressed by powers of α' in the field theory limit, which is the source of further simplifications in our final expressions.

For completeness, we give here the results for the various factors in eq. (3.3) as Taylor expansions powers of q_i (that is, in half-integer powers of p_i), but with the field- and mass-dependent coefficients of the leading terms worked out exactly. Beginning with the contribution of gluon modes perpendicular to the magnetic fields, $\mathbf{F}_\perp(\boldsymbol{\mu})$, we find

$$\begin{aligned} \mathbf{F}_\perp(\boldsymbol{\mu}) &= \left[\frac{(2\pi\alpha')^2}{\Delta_0}\right]^{d/2-1} \left\{ 1 + (d-2) \left[q_1q_2 + q_2q_3 + q_3q_1 \right. \right. \\ &\quad \left. \left. - \alpha' \hat{\theta}_{12} \hat{\phi}_{12} \frac{1}{\Delta_0} (t_1q_1 + t_2q_2 + t_3q_3 + (d-3)(t_1+t_2+t_3)q_1q_2q_3) \right] + \mathcal{O}((\alpha')^2, p_i) \right\} \\ &\equiv \left[\frac{(2\pi\alpha')^2}{\Delta_0}\right]^{d/2-1} \sum_{m,n,p=0}^{\infty} q_1^m q_2^n q_3^p \widehat{\mathbf{F}}_\perp^{(mnp)}(t_i), \end{aligned} \quad (4.28)$$

where we defined

$$\Delta_0 = t_1t_2 + t_2t_3 + t_3t_1, \quad (4.29)$$

which we recognize as the first Symanzik polynomial [69] of graphs with the topology of those in the first two lines of figure 1, expressed in terms of standard Schwinger parameters.

The result for the contribution of gluon modes parallel to the magnetic field is more interesting, as one begins to recognize detailed structures that are known to arise in the corresponding field theory. Multiplying eq. (4.20) by eq. (4.21), and dividing by eq. (4.22),

one finds

$$\begin{aligned}
 \mathbf{F}_{\parallel}^{(\vec{\epsilon})}(\boldsymbol{\mu}) &= \frac{(2\pi\alpha')^2}{\Delta_B} \left\{ 1 + 2 \left[\cosh(2g(B_1 t_1 - B_2 t_2)) q_1 q_2 \right. \right. \\
 &\quad \left. \left. - \alpha' \hat{\theta}_{12} \hat{\phi}_{12} \frac{1}{\Delta_B} \frac{\sinh(gB_1 t_1)}{gB_1} \cosh(g(2B_1 t_1 - B_2 t_2 - B_3 t_3)) (q_1 + q_1 q_2 q_3) \right. \right. \\
 &\quad \left. \left. + \text{cycl. perm.} \right] + \mathcal{O}(\alpha'^2) + \mathcal{O}(p_i) \right\} \\
 &\equiv \frac{(2\pi\alpha')^2}{\Delta_B} \sum_{m,n,p=0}^{\infty} q_1^m q_2^n q_3^p \widehat{\mathbf{F}}_{\parallel}^{(mnp)}(t_i, B_i),
 \end{aligned} \tag{4.30}$$

where

$$\Delta_B = \frac{\cosh[g(B_1 t_1 - B_2 t_2 - B_3 t_3)]}{2g^2 B_2 B_3} + \text{cycl. perm.} \tag{4.31}$$

Using the fact that $B_1 + B_2 + B_3 = 0$, one can verify that Δ_B can be understood as the charged generalization of the first Symanzik polynomial for this graph topology, and indeed for vanishing fields Δ_B tends to Δ_0 . It is then easy to see that $\mathbf{F}_{\parallel}^{(\vec{\epsilon})}(\boldsymbol{\mu})$, in the same limit, reproduces $\mathbf{F}_{\perp}(\boldsymbol{\mu})$ with the replacement $d - 2 \rightarrow 2$, as expected.

The contribution from the D-brane world-volume scalars can be obtained combining eq. (4.25) and eq. (4.26). One finds

$$\begin{aligned}
 \mathbf{F}_{\text{scal}}^{(\vec{d})}(\boldsymbol{\mu}) &= e^{-t_1 m_1^2} e^{-t_2 m_2^2} e^{-t_3 m_3^2} [1 + n_s (q_1 q_2 + q_2 q_3 + q_3 q_1) \\
 &\quad + \alpha' \hat{\theta}_{12} \hat{\phi}_{12} ((m_1^2 - m_2^2 - m_3^2) q_1 - (n_s - 1) m_1^2 q_1 q_2 q_3 + \text{cycl. perm.})] + \mathcal{O}(p_i) \\
 &\equiv \prod_{i=1}^3 [e^{-t_i m_i^2}] \sum_{m,n,p=0}^{\infty} q_1^m q_2^n q_3^p \widehat{\mathbf{F}}_{\text{scal}}^{(mnp)}(t_i, m_i),
 \end{aligned} \tag{4.32}$$

where one recognizes the exponential dependence on particle masses, each multiplied by the Schwinger parameter of the corresponding propagator, which is characteristic of massive field-theory Feynman diagrams. Note that the masses m_i^2 appearing in eq. (4.32) arise via symmetry breaking from the distance between D-branes, and therefore represent classical shifts of the string spectrum: below, for brevity, we will often call ‘massless’ all string states that would be massless in the absence of symmetry breaking.

The final factor, including the integration measure and the contribution from the ghosts, can be read off eq. (4.19), and can be organized as

$$d\boldsymbol{\mu}_2 \mathbf{F}_{\text{gh}}(\boldsymbol{\mu}) = \prod_{i=1}^3 \left[\frac{dp_i}{q_i^3} \right] d\hat{\theta}_{12} d\hat{\phi}_{12} \sum_{m,n,p=0}^{\infty} q_1^m q_2^n q_3^p \widehat{\mathbf{F}}_{\text{gh}}^{(mnp)}. \tag{4.33}$$

The complete integrand of eq. (3.3) is the product of \mathbf{F}_{\perp} from eq. (4.28), \mathbf{F}_{\parallel} from eq. (4.30), \mathbf{F}_{scal} from eq. (4.32) and $d\boldsymbol{\mu}_2 \mathbf{F}_{\text{gh}}$ from eq. (4.33). In the proximity of the symmetric degeneration, it can be organized in a power series in terms of the variables q_i , as we have

done for individual factors. We write

$$d\mathbf{Z}_2^{\text{sym}}(\boldsymbol{\mu}) = \prod_{i=1}^3 \left[\frac{dp_i}{q_i^3} e^{-t_i m_i^2} \right] d\hat{\theta}_{12} d\hat{\phi}_{12} \frac{(2\pi\alpha')^d}{\Delta_0^{d/2-1} \Delta_B} \times \sum_{m,n,p=0}^{\infty} q_1^m q_2^n q_3^p \widehat{\mathbf{F}}^{(mnp)}(t_i, m_i, B_i). \quad (4.34)$$

It is now straightforward to extract the contribution of massless states, which is contained in the coefficient $\widehat{\mathbf{F}}^{(111)}(t_i, m_i, B_i)$. For bosonic strings, one had to discard the contribution of the tachyonic ground state by hand: in this case, one can simply implement the GSO projection and observe the expected decoupling of the tachyon. We now turn to the analysis of this point.

4.4 The symmetric degeneration after GSO projection

Starting with the expression in eq. (4.34), we can now describe more precisely the connection between the powers of the multipliers and the mass eigenstates circulating in the loops. For the symmetric degeneration, we now see that the power of p_i corresponds to the mass level of the state propagating in the i -th edge of the diagram. Indeed one observes that

$$\frac{dp_i}{p_i^{3/2}} (p_i^{1/2})^n = -\frac{1}{\alpha'} dt_i e^{-\frac{n-1}{2\alpha'} t_i}, \quad (4.35)$$

and one recognizes that $dt_i e^{-\frac{n-1}{2\alpha'} t_i}$ is a factor one would expect to see in a Schwinger-parameter propagator for a field with squared mass $m^2 = \frac{n-1}{2\alpha'}$. In particular, if $n = 0$, then the state propagating in the i -th edge will be a tachyon, and will have to be removed by the GSO projection.

A cursory look at \mathbf{F}_{\parallel} in eq. (4.30), \mathbf{F}_{\perp} in eq. (4.28), \mathbf{F}_{scal} in eq. (4.32) and $d\boldsymbol{\mu}_2 \mathbf{F}_{\text{gh}}$ in eq. (4.19), would suggest that tachyons can propagate simultaneously in any number of edges of the diagram: indeed, we can find terms proportional to $\prod_i dp_i/q_i^3$ times 1, q_1 , $q_1 q_2$, $q_1 q_2 q_3, \dots$, which correspond respectively to three, two, one or no edges with propagating tachyons. A closer inspection shows, however, that the nilpotent object $\hat{\theta}_{12} \hat{\phi}_{12}$ multiplies only terms with an *odd* number of factors of q_i , a property which is preserved when we multiply terms together. Since the Berezin integral over $d\hat{\theta}_{12} d\hat{\phi}_{12}$ picks out the coefficient of $\hat{\theta}_{12} \hat{\phi}_{12}$, it follows that, after carrying out the Berezin integration, each term must contain an odd number of factors of q_i .

As a consequence, after Berezin integration and truncation of the integrand to $\mathcal{O}(p_i^0)$, eq. (4.34) will be written as a sum of four terms, proportional to $\prod_{i=1}^3 dp_i/p_i^{3/2}$ multiplied by the factors

$$q_1 = e^{i\pi\epsilon_2} \sqrt{p_1}, \quad q_2 = e^{i\pi\epsilon_1} \sqrt{p_2}, \quad q_3 = e^{i\pi\epsilon_3} \sqrt{p_3}, \quad q_1 q_2 q_3 = \sqrt{p_1 p_2 p_3}. \quad (4.36)$$

The first three terms in eq. (4.36) carry the contributions of tachyons propagating in loops: since we wish to excise tachyons from the spectrum, we need to implement a GSO projection in such a way that these three terms vanish. This is achieved by simply averaging

the amplitude over the four spin structures $(\varsigma_1, \varsigma_2) \in \{(0, 0), (1, 0), (0, 1), (1, 1)\}$; one clearly sees that the first three terms in eq. (4.36) vanish while the fourth term is independent of $\vec{\zeta}$ and thus unaffected. Therefore the GSO-projected amplitude is free of tachyons while the massless sector is intact, as desired.

We are now in a position to take the field theory limit for the symmetric degeneration. The only missing ingredient is the normalization factor $\mathcal{N}_h^{(\vec{\epsilon})}$ introduced in eq. (3.3). It is given by

$$\mathcal{N}_2^{(\vec{\epsilon})} = \frac{C_2}{\cos(\pi\epsilon_1)\cos(\pi\epsilon_2)}, \quad (4.37)$$

where C_h is the normalization factor for an h -loop string amplitude in terms of the d -dimensional Yang-Mills coupling g_d , calculated in appendix A of ref. [68]. For $h = 2$ it is given by

$$C_2 = \frac{g_d^2}{(4\pi)^d} \frac{(\alpha')^2}{(2\pi\alpha')^d}. \quad (4.38)$$

The denominator in eq. (4.37) arises from the Born-Infeld contribution to the normalization of the boundary state (see for example ref. [70]). It does not contribute to the field theory limit, since $\cos(\pi\epsilon_1)\cos(\pi\epsilon_2) = 1 + \mathcal{O}(\alpha'^2)$, after expressing the twists ϵ_i in terms of the background field strengths via eq. (4.27).

Applying the GSO projection to eq. (4.34), and using $dp_i/p_i = -dt_i/\alpha'$, we finally find that the QFT limit of the partition function can be represented succinctly by

$$Z_{2,\text{QFT}}^{\text{sym}}(m_i, B_i) = \frac{g_d^2}{(4\pi)^d} \int \prod_{i=1}^3 dt_i e^{-t_i m_i^2} \frac{1}{\Delta_0^{(d-2)/2} \Delta_B} \times \lim_{\alpha' \rightarrow 0} \left[-\frac{1}{\alpha'} \int d\hat{\theta}_{12} d\hat{\phi}_{12} \widehat{\mathbf{F}}^{(111)}(t_i, m_i, B_i) \right], \quad (4.39)$$

where the limit on the second line is finite after Berezin integration. In order to see that, and in order to give our results as explicitly as possible, we define (for simplicity we omit the arguments of the functions \mathbf{f})

$$\mathbf{f}_{\text{gh}}^{(mnp)} = \begin{cases} -\frac{1}{\alpha'} \partial_{\hat{\theta}_{12}} \partial_{\hat{\phi}_{12}} \widehat{\mathbf{F}}_{\text{gh}}^{(mnp)} & \text{if } m+n+p \text{ is odd,} \\ \widehat{\mathbf{F}}_{\text{gh}}^{(mnp)} & \text{if } m+n+p \text{ is even,} \end{cases} \quad (4.40)$$

and similarly for $\mathbf{f}_{\parallel}^{(mnp)}(t_i, B_i)$, $\mathbf{f}_{\perp}^{(mnp)}(t_i)$ and $\mathbf{f}_{\text{scal}}^{(mnp)}(t_i, m_i)$. With our definitions, one easily sees that

$$\mathbf{f}_{\text{gh}}^{(000)} = \mathbf{f}_{\parallel}^{(000)} = \mathbf{f}_{\perp}^{(000)} = \mathbf{f}_{\text{scal}}^{(000)} = 1. \quad (4.41)$$

Performing the Berezin integration is then a simple matter of combinatorics, and one finds

$$Z_{2,\text{QFT}}^{\text{sym}}(m_i, B_i) = \frac{g_d^2}{(4\pi)^d} \int \prod_{i=1}^3 dt_i e^{-t_i m_i^2} \frac{1}{\Delta_0^{(d-2)/2} \Delta_B} \times [\mathbf{f}_{\parallel}^{(111)}(t_i, B_i) + \mathbf{f}_{\parallel}^{(110)}(t_i, B_i) \mathbf{f}_{\perp}^{(001)}(t_i) + (25 \text{ more terms})]. \quad (4.42)$$

We can read off the various terms in the integrand by picking the coefficients of the appropriate factors of q_i from \mathbf{F}_{\parallel} in eq. (4.30), \mathbf{F}_{\perp} in eq. (4.28), \mathbf{F}_{scal} in eq. (4.32) and $d\mu_2 \mathbf{F}_{\text{gh}}$ in eq. (4.19), and then selecting the coefficient of $\hat{\theta}_{12} \hat{\phi}_{12}$, divided by α' . We find

$$\begin{aligned}
 \mathbf{f}_{\parallel}^{(111)} &= \frac{2}{\Delta_B} \frac{\sinh(gB_1 t_1)}{gB_1} \cosh [g(2B_1 t_1 - B_2 t_2 - B_3 t_3)] + \text{cycl. perm.}, \\
 \mathbf{f}_{\parallel}^{(110)} \mathbf{f}_{\perp}^{(001)} &= \frac{2}{\Delta_0} (d-2) t_3 \cosh [2g(B_1 t_1 - B_2 t_2)], \\
 \mathbf{f}_{\parallel}^{(001)} \mathbf{f}_{\perp}^{(110)} &= \frac{2}{\Delta_B} (d-2) \frac{\sinh(gB_3 t_3)}{gB_3} \cosh [g(2B_3 t_3 - B_1 t_1 - B_2 t_2)], \\
 \mathbf{f}_{\perp}^{(111)} &= \frac{1}{\Delta_0} (d-2)(d-3)(t_1 + t_2 + t_3), \\
 \mathbf{f}_{\text{gh}}^{(110)} \mathbf{f}_{\parallel}^{(001)} &= -\frac{2}{\Delta_B} \frac{\sinh(gB_3 t_3)}{gB_3} \cosh [g(2B_3 t_3 - B_1 t_1 - B_2 t_2)], \\
 \mathbf{f}_{\text{gh}}^{(110)} \mathbf{f}_{\perp}^{(001)} &= -\frac{1}{\Delta_0} (d-2) t_3, \\
 \mathbf{f}_{\text{gh}}^{(110)} \mathbf{f}_{\text{scal}}^{(001)} &= m_3^2 - m_1^2 - m_2^2, \\
 \mathbf{f}_{\text{scal}}^{(110)} \mathbf{f}_{\parallel}^{(001)} &= \frac{2}{\Delta_B} n_s \frac{\sinh(gB_3 t_3)}{gB_3} \cosh [g(2B_3 t_3 - B_1 t_1 - B_2 t_2)], \\
 \mathbf{f}_{\text{scal}}^{(110)} \mathbf{f}_{\perp}^{(001)} &= \frac{1}{\Delta_0} (d-2) n_s t_3, \\
 \mathbf{f}_{\parallel}^{(110)} \mathbf{f}_{\text{scal}}^{(001)} &= 2(m_1^2 + m_2^2 - m_3^2) \cosh [2g(B_1 t_1 - B_2 t_2)], \\
 \mathbf{f}_{\perp}^{(110)} \mathbf{f}_{\text{scal}}^{(001)} &= (d-2)(m_1^2 + m_2^2 - m_3^2), \\
 \mathbf{f}_{\text{scal}}^{(111)} &= (n_s - 1)(m_1^2 + m_2^2 + m_3^2).
 \end{aligned} \tag{4.43}$$

The other terms in the integrand can be obtained from the above by cyclic symmetry.

We conclude by noting that eq. (4.42) does not give the complete 2-loop contribution to the vacuum amplitude with this topology, since the string theory calculation distinguishes the three D-branes where the world-sheet boundaries are attached. This is reflected in the integration region over the Schwinger parameters t_i , already discussed in ref. [15]: they are not integrated directly in the interval $0 < t_i < \infty$, as would be the case in field theory, but they are ordered, as $0 < t_3 < t_2 < t_1 < \infty$. In order to recover the full amplitude, with the correct color factors and integration region, one must sum over all possible attachments of the string world-sheet to the D-branes, effectively summing over the different values of the background fields B_i and masses m_i^2 . In the absence of external fields, this sum amounts just to the introduction of a symmetry and color factor; for non-vanishing B_i , it reconstructs the correct symmetry properties of the amplitude under permutations.

4.5 The incomplete degeneration

In the last three sections, 4.2, 4.3 and 4.4, we have given the tools to compute the field theory limit of the partition function in the vicinity of the symmetric degeneration, see figure 6a: our final result is summarized in eq. (4.42). The field theory two-loop effective action, however, includes also the Feynman diagrams with a quartic vertex depicted in the last two lines of figure 1.

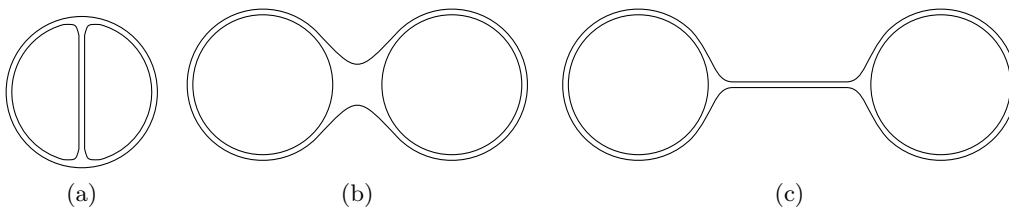


Figure 6. The symmetric (figure 6a), incomplete (figure 6b), and separating (figure 6c) degenerations of the two-loop vacuum amplitude.

The main feature of vacuum graphs with a four point vertex, which drives the corresponding choice of parametrization for the neighborhood of moduli space depicted in figure 6b, is the fact that such graphs have only two propagators, each one encompassing a complete loop, and furthermore they are symmetric under the exchange of the two loops. It is natural therefore to associate to each propagator a Schwinger parameter linked to the Schottky multiplier of the corresponding string loop. The fact that there are no further Schwinger parameters implies also that the third bosonic modulus must be integrated over its domain except for a small region around each boundary. We therefore call the configuration depicted in figure 6b the *incomplete* degeneration.

To compute the field theory limit for the incomplete degeneration, we must retrace our steps back to section 4.1, where the various factors in the partition function were expressed in terms of k_i and u (or y). We then relate the multipliers to Schwinger parameters as

$$k_i = e^{-t_i/\alpha'}, \quad (i = 1, 2), \quad (4.44)$$

and replace ϵ_i according to eq. (4.27).

As may be expected from the simplicity of the target graph, the string partition function simplifies drastically when the $\alpha' \rightarrow 0$ limit is taken in this way. One finds for example that the determinant of the (twisted) period matrix reduces to

$$\begin{aligned} [\det(\text{Im } \boldsymbol{\tau})]^{-1} &= \frac{(2\pi\alpha')^2}{t_1 t_2} + \mathcal{O}((\alpha')^3) \\ [\det(\text{Im } \boldsymbol{\tau}_{\tilde{\epsilon}})]^{-1} &= (2\pi\alpha')^2 \frac{gB_1}{\sinh(gB_1 t_1)} \frac{gB_2}{\sinh(gB_2 t_2)} + \mathcal{O}((\alpha')^3), \end{aligned} \quad (4.45)$$

while the hyperbolic functions appearing in the field theory limit arise in a direct way from combinations like

$$\begin{aligned} k_1^{\epsilon_1} u^{\epsilon_2} + k_1^{-\epsilon_1} u^{-\epsilon_2} &= 2 \cosh(2gB_1 t_1) + \mathcal{O}(\alpha'), \\ k_1^{\epsilon_1} k_2^{\epsilon_2} u^{\epsilon_1 + \epsilon_2} + k_1^{-\epsilon_1} k_2^{-\epsilon_2} u^{-\epsilon_1 - \epsilon_2} &= 2 \cosh(2g(B_1 t_1 + B_2 t_2)) + \mathcal{O}(\alpha'). \end{aligned} \quad (4.46)$$

The resulting expressions are very simple because, with no Schwinger parameter associated to u , factors of the form $u^{\pm \epsilon_i}$ do not contribute to the field theory limit. This is what makes it possible to perform the integration over the third bosonic modulus, and over the two fermionic moduli: indeed, in the parametrization considered here, the entire partition

function can be written explicitly, in the $\alpha' \rightarrow 0$ limit, in terms of just three simple integrals over the non-degenerating coordinates of super-moduli space. After GSO projection, one finds

$$\begin{aligned}
 d\mathbf{Z}_2^{\text{inc+sep}}(\boldsymbol{\mu}) &= \frac{(2\pi\alpha')^d}{(\alpha')^2} \prod_{i=1}^2 \left[\frac{dt_i e^{-t_i m_i^2} g B_i}{t_i^{d/2-1} \sinh(g B_i t_i)} \right] du d\theta d\phi \\
 &\times \left\{ \frac{1}{y} (d-2 + 2 \cosh(2g B_1 t_1) + n_s - 2) (d-2 + 2 \cosh(2g B_2 t_2) + n_s - 2) \right. \\
 &\quad - [d-2 + 2 \cosh(2g(B_1 t_1 + B_2 t_2)) + n_s] \\
 &\quad \left. + \frac{1}{u} [d-2 + 2 \cosh(2g(B_1 t_1 - B_2 t_2)) + n_s] \right\} + \mathcal{O}(e^{-t_i/\alpha'}, \alpha').
 \end{aligned} \tag{4.47}$$

As the notation suggests, eq. (4.47) in principle contains contributions from both the incomplete and the separating degenerations, and we now turn to the problem of disentangling them. We also see that in order to complete the calculation one just needs to determine three numerical constants, given by the following integrals over the non-degenerating super-moduli,

$$I_1 = \int_{\widehat{\mathfrak{M}}_{1|2}} du d\theta d\phi \frac{1}{y}, \quad I_2 = - \int_{\widehat{\mathfrak{M}}_{1|2}} du d\theta d\phi, \quad I_3 = \int_{\widehat{\mathfrak{M}}_{1|2}} du d\theta d\phi \frac{1}{u}. \tag{4.48}$$

To determine the domain of integration $\widehat{\mathfrak{M}}_{1|2}$ in eq. (4.48), and to identify the different degeneration limits, note that the separating, symmetric and incomplete degenerations all come from the region of super-moduli space in which the two Schottky multipliers k_1 and k_2 are small. In this limit, we can think of super moduli space as a 1|2-dimensional space parametrized by $(u|\theta, \phi)$. The separating degeneration corresponds to the limit $y \rightarrow 0$, while the symmetric degeneration corresponds to the limit $u \rightarrow 0$, and the incomplete degeneration comes from the region of super moduli space interpolating between the two limits. As pointed out in refs. [21, 71], however, this simple characterization must be made more precise, in particular with regards to the choice of parameters near the two degenerations.

First of all, we note that the first term in braces on the right-hand side of eq. (4.47), proportional to the integral I_1 , dominates in the limit $y \rightarrow 0$, and we expect it to represent the contributions of the one-particle reducible (1PR) Feynman diagrams, which we neglect. We can then concentrate on the evaluation of the integrals relevant for our purposes, which are I_2 and I_3 in eq. (4.48). They can be calculated using Stokes' theorem for a super-manifold with a boundary (see section 3.4 of [71]), since the integrands are easily expressed as total derivatives. We write

$$\begin{aligned}
 -du d\theta d\phi &\equiv d\nu_2, & \nu_2 &= -u d\theta d\phi, \\
 \frac{du}{u} d\theta d\phi &\equiv d\nu_3, & \nu_3 &= \log(u) d\theta d\phi.
 \end{aligned} \tag{4.49}$$

These expressions mean that the corresponding integrals are localized on the boundary of $\widehat{\mathfrak{M}}_{1|2}$, which consists of two loci associated with the two distinct ways in which the double

annulus world-sheet can completely degenerate: the symmetric degeneration of figure 6a, and the separating degeneration of figure 6c.

To use Stokes' theorem, it is important to characterize precisely the 0|2-dimensional boundary of the super-moduli-space region over which we are integrating. More precisely, we need to find bosonic functions of the worldsheet moduli $\xi_i(u, \theta, \phi)$, defined near the boundaries of $\widehat{\mathfrak{M}}_{1|2}$, such that the vanishing of ξ_i defines a compactification divisor \mathcal{D}_i . Such functions are called *canonical parameters* in section 6.3 of [21]. It is important to note that, for singular integrands such as those of I_1 and I_3 , it is not sufficient to define the canonical parameter ξ up to an overall factor, which may include nilpotent terms. For example, if we attempt to rescale $\xi = (1 + \theta\phi)\xi'$, then $\log \xi = \log \xi' + \theta\phi$, so that the Berezin integral $\int d\theta d\phi \log \xi$ does not coincide with $\int d\theta d\phi \log \xi'$.

In the small- u region, the proper choice of the canonical parameter ξ_{sym} is dictated by our parametrization of the symmetric degeneration: we must take $\xi_{\text{sym}} = p_3$, as defined in eq. (4.12), in order to properly glue together the two regions. Although p_3 and the cross-ratio u vanish at the same point, they are related by a non-trivial rescaling at leading order in the multipliers. Indeed

$$u = \frac{p_3}{1 + p_3}(1 + \theta\phi) + \mathcal{O}(k_i^{1/2}), \tag{4.50}$$

which affects the Berezin integral of eq. (4.49), as discussed above. Note that, not having introduced a parametrization for the separating degeneration, we would not have a similar guideline in the small- y region. Furthermore, the fact that the corresponding field theory diagram needs to be regulated,⁵ in order to make sense of the vanishing momentum flowing in the intermediate propagator, introduces an ambiguity also in the field theory result.

With this choice of parametrization, we can now use Stokes' theorem to determine the values of I_2 and I_3 . Taking $\xi_{\text{sep}} = y$ as a canonical parameter for the separating degeneration, we find

$$\begin{aligned} I_2 &= \lim_{\epsilon \rightarrow 0} \left[\int_{y=\epsilon} \nu_2 - \int_{p_3=\epsilon} \nu_2 \right], \\ &= \lim_{\epsilon \rightarrow 0} \left[- \int d\theta d\phi (1 - \epsilon + \theta\phi) + \int d\theta d\phi \frac{\epsilon}{1 + \epsilon} (1 + \theta\phi) \right] = 1, \end{aligned} \tag{4.51}$$

where we used $\int d\theta d\phi \theta\phi = -1$. Similarly

$$\begin{aligned} I_3 &= \lim_{\epsilon \rightarrow 0} \left[\int_{y=\epsilon} \nu_3 - \int_{p_3=\epsilon} \nu_3 \right], \\ &= \lim_{\epsilon \rightarrow 0} \left[\int d\theta d\phi (1 - \epsilon + \theta\phi) - \int d\theta d\phi \log \left[\frac{\epsilon}{1 + \epsilon} (1 + \theta\phi) \right] \right] = 0. \end{aligned} \tag{4.52}$$

Inserting these results into eq. (4.47), discarding the separating degeneration, and introducing the overall normalization given in eq. (4.38), we obtain our final expression for the

⁵Notice that, in the gauge we use, this Feynman diagram would not automatically vanish in a $U(N)$ theory, as the 3-point vertices contain also terms proportional to the symmetric color tensor d^{abc} .

contribution of diagrams with a four-point vertex to the field-theory effective action. It is given by

$$Z_{2,\text{QFT}}^{\text{inc}}(m_i, B_i) = \frac{g^2}{(4\pi)^d} \int_0^\infty \prod_{i=1}^2 \left[\frac{dt_i e^{-t_i m_i^2} g B_i}{t_i^{d/2-1} \sinh(g B_i t_i)} \right] \left(d - 2 + 2 \cosh(2g(B_1 t_1 + B_2 t_2)) + n_s \right). \quad (4.53)$$

In order to identify the contributions of individual Feynman diagrams to eq. (4.53), we can retrace the steps of the calculation and assign each term in our result to the appropriate world-sheet conformal field theory, as we did for the symmetric degeneration in eq. (4.42). We find that we can rewrite eq. (4.53) as

$$Z_{2,\text{QFT}}^{\text{inc}}(m_i, B_i) = -\frac{g^2}{(4\pi)^d} \int_0^\infty \prod_{i=1}^2 \left[\frac{dt_i e^{-t_i m_i^2} g B_i}{t_i^{d/2-1} \sinh(g B_i t_i)} \right] (\mathbf{f}_{\parallel}^{11} + \mathbf{f}_{\perp}^{11} + \mathbf{f}_{\text{scal}}^{11} + \mathbf{f}_{\text{gh}}^{11}), \quad (4.54)$$

where here the superscripts denote the powers of $k_i^{1/2}$ ($i = 1, 2$) from which the coefficients were extracted, and we have omitted the arguments of the functions \mathbf{f} for simplicity. The precise identification is

$$\mathbf{f}_{\parallel}^{11} = -2 \cosh(2g(B_1 t_1 + B_2 t_2)) \quad \mathbf{f}_{\perp}^{11} = -(d - 2), \quad \mathbf{f}_{\text{scal}}^{11} = -n_s, \quad \mathbf{f}_{\text{gh}}^{11} = 0. \quad (4.55)$$

A few remarks are in order. First of all we note that $\mathbf{f}_{\text{gh}}^{11}$ vanishes; this corresponds to the fact that, in the infinite product in $\mathbf{F}_{\text{gh}}(k_i, \eta)$ in eq. (3.11), n ranges from 2 to ∞ , not from 1 to ∞ as in the case of \mathbf{F}_{gl} and \mathbf{F}_{scal} . As a consequence, there is no term proportional to $k^{1/2}(\mathbf{S}_1 \mathbf{S}_2)$ in the partition function for the ghost systems. We will see that this corresponds to the fact that there is no quartic ghost vertex in the associated Yang-Mills theory. Next, we note that all terms associated with the four-point vertex diagram are not factorizable into the product of two contributions, proportional to $k_1^{1/2}$ and $k_2^{1/2}$ respectively. If, on the other hand, we had traced the origin of the terms associated with the separating degeneration, and proportional to the integral I_1 , we would have found that the factor multiplying $1/y$ in eq. (4.47) can be written as

$$(\mathbf{f}_{\parallel}^{10} + \mathbf{f}_{\perp}^{10} + \mathbf{f}_{\text{scal}}^{10} + \mathbf{f}_{\text{gh}}^{10})(\mathbf{f}_{\parallel}^{01} + \mathbf{f}_{\perp}^{01} + \mathbf{f}_{\text{scal}}^{01} + \mathbf{f}_{\text{gh}}^{01}). \quad (4.56)$$

This means that no contributions arise from the Schottky group elements $\mathbf{S}_1 \mathbf{S}_2$ and $\mathbf{S}_1^{-1} \mathbf{S}_2$, which would imply a genuine correlation between the two loops. Rather, as expected, these terms are simply the product of factors rising from individual disconnected loops. Finally, we note that the result $I_3 = 0$ is crucial in order to recover the correct field theory limit: indeed, as will be verified in the next section and shown in appendix C, no field theory diagram yields hyperbolic functions with the parameter dependence displayed on the last line of eq. (4.47). We see once again that the field theory limit, once the contributions of individual diagrams have been identified, provides non-trivial checks of the procedures used to perform the integration over super-moduli.

5 Yang-Mills theory in the background field Gervais-Neveu gauge

In order to make a precise comparison between string theory and field theory at the level of individual Feynman diagrams, as was done in a simple case in ref. [11], we need a precise characterization of the field-theory Lagrangian we are working with, including gauge fixing and ghost contributions. In principle, this presents no difficulties, since our target is a $U(N)$ Yang-Mills theory, albeit with a rather special gauge choice. There are however a number of subtleties, ranging from the special features of the background field framework, to issues of dimensional reduction, and to the need to break spontaneously the gauge symmetry in order to work with well-defined Feynman diagrams in the infrared limit, which altogether lead to a somewhat complicated and unconventional field theory setup. We will therefore devote this section to a detailed discussion of the field theory Lagrangian which arises from the field theory limit of our chosen string configuration.

The first layer of complexity is due to the fact that the string theory setup naturally corresponds to a field theory configuration with a non-trivial background field. In general, such a background field breaks the gauge symmetry: in our case, since we are working with mutually commuting gauge fields with constant field strengths, and we have a string configuration with separated D -brane sets, one will generically break the $U(N)$ gauge symmetry down to $U(1)^N$. We will have to adjust our notation to take this into account. Notice also that our background fields break Lorentz invariance as well, since only certain polarizations are non-vanishing. As a consequence, the polarizations of the quantum field will also be distinguished as parallel or perpendicular to the given background.

Furthermore, it is interesting to work in a generic space-time dimension d , and we will find it useful to work with massive scalar fields giving infrared-finite Feynman diagrams. We will therefore work with a d -dimensional gauge theory obtained by dimensional reduction from the dimension $\mathcal{D} > d$ appropriate to the string configuration. This yields $n_s = \mathcal{D} - d$ adjoint scalar fields minimally coupled to the d -dimensional gauge theory, and we will choose our background fields such that these fields acquire a non-vanishing expectation value, giving mass to some of the gauge fields.

Finally, as suggested originally in ref. [45], and recently confirmed by the analysis of ref. [11], covariantly quantized string theory picks a very special gauge in the field theory limit: a background field version of the non-linear gauge first introduced by Gervais and Neveu in ref. [16]. This gauge has certain simplifying features: for example at tree level and at one loop it gives simplified color-ordered Feynman rules which considerably reduce the combinatoric complexity of gauge-theory amplitudes [45]. Only at the two-loop level, however, the full complexity of the non-linear gauge fixing becomes apparent. One effect, for example, is that the diagonal $U(1)$ ‘photon’, which ordinarily is manifestly decoupled and never appears in ‘gluon’ diagrams, in this case has non-trivial, gauge-parameter dependent couplings to $SU(N)$ states, and the decoupling only happens when all relevant Feynman diagrams are summed.

In what follows, we adopt the following notations: we use calligraphic letters for matrix-valued $u(N)$ gauge fields, and ordinary capital letters for their component fields; we use $M, N, \dots = 1, \dots, \mathcal{D}$ for Lorentz indices in \mathcal{D} -dimensional Minkowski space before

dimensional reduction, and $\mu, \nu, \dots = 1, \dots, d$ for Lorentz indices in the d -dimensional reduced space-time; finally, $I, J, \dots = 1, \dots, n_s$ indices enumerate adjoint scalars, and $A, B, \dots = 1, \dots, N$ indices enumerate the components of $u(N)$ vectors and matrices. In this language, \mathcal{A}_M will denote the \mathcal{D} -dimensional classical background field, \mathcal{Q}_M the corresponding quantum field, while \mathcal{C} and $\bar{\mathcal{C}}$ are ghost and anti-ghost fields.

We will now proceed to write out the quantum lagrangian (including gauge-fixing and ghost terms) in terms of matrix-valued fields. We will then comment on the form taken by various terms in component notation, which is more directly related to the vertices appearing in diagrammatic calculations.

5.1 The $u(N)$ Lagrangian

We begin by constructing the \mathcal{D} -dimensional Yang-Mills Lagrangian, which, in the presence of a background gauge field, depends on the combination $\mathcal{A}_M + \mathcal{Q}_M$. The field-strength tensor \mathcal{F}_{MN} can be expressed in terms of the covariant derivative of the quantum field with respect to the background field, $\mathfrak{D}_M = \partial_M + ig[\mathcal{A}_M, \cdot]$, as

$$\begin{aligned} \mathcal{F}_{MN}(\mathcal{A} + \mathcal{Q}) &= -\frac{i}{g} [\mathfrak{D}_M^{\mathcal{A}+\mathcal{Q}}, \mathfrak{D}_N^{\mathcal{A}+\mathcal{Q}}] \\ &= \mathcal{F}_{MN}(\mathcal{A}) + \mathfrak{D}_M \mathcal{Q}_N - \mathfrak{D}_N \mathcal{Q}_M + ig[\mathcal{Q}_M, \mathcal{Q}_N], \end{aligned} \tag{5.1}$$

where $\mathcal{F}_{MN}(\mathcal{A})$ is the field strength tensor for the background field only, while $\mathfrak{D}_M^{\mathcal{A}+\mathcal{Q}}$ is the covariant derivative with respect to the complete gauge field. The classical Lagrangian for the quantum gauge field \mathcal{Q} can then be written as

$$\begin{aligned} \mathcal{L}_{\text{cl}} = \text{Tr} \left[\mathfrak{D}^M \mathcal{Q}^N \mathfrak{D}_N \mathcal{Q}_M - \mathfrak{D}^M \mathcal{Q}^N \mathfrak{D}_M \mathcal{Q}_N + 2ig \mathcal{F}_{MN} \mathcal{Q}^M \mathcal{Q}^N \right. \\ \left. + 2ig \mathfrak{D}^M \mathcal{Q}^N [\mathcal{Q}_M, \mathcal{Q}_N] + \frac{1}{2} g^2 [\mathcal{Q}_M, \mathcal{Q}_N] [\mathcal{Q}^M, \mathcal{Q}^N] \right], \end{aligned} \tag{5.2}$$

where Tr here denotes the trace over the $u(N)$ Lie algebra, and we have removed terms independent of \mathcal{Q} , as well as terms linear in \mathcal{Q} , because they are not relevant for our effective action calculation.

In anticipation of the string theory results, we now wish to fix the gauge using a background field version of the non-linear gauge condition introduced by Gervais and Neveu in ref. [16], setting

$$\mathcal{G}(\mathcal{A}, \mathcal{Q}) = \mathfrak{D}_M \mathcal{Q}^M + i\gamma g \mathcal{Q}_M \mathcal{Q}^M = 0, \tag{5.3}$$

where γ is a gauge parameter. The gauge-fixing Lagrangian \mathcal{L}_{gf} is then given by

$$\begin{aligned} \mathcal{L}_{\text{gf}} &= -\text{Tr} [(\mathcal{G}(\mathcal{A}, \mathcal{Q}))^2] \\ &= -\text{Tr} [\mathfrak{D}_M \mathcal{Q}^M \mathfrak{D}_N \mathcal{Q}^N + 2i\gamma g \mathfrak{D}_M \mathcal{Q}^M \mathcal{Q}_N \mathcal{Q}^N - \gamma^2 g^2 \mathcal{Q}_M \mathcal{Q}^M \mathcal{Q}_N \mathcal{Q}^N]. \end{aligned} \tag{5.4}$$

Notice that the overall covariant gauge-fixing parameter which would appear in front of eq. (5.4) has been set equal to one. Note also that this gauge fixing modifies not only the gluon propagator, as expected, but also the three- and four-gluon vertices. In particular, the symmetric nature of the quadratic term in the gauge-fixing function \mathcal{G} will generate

Feynman rules involving the symmetric $u(N)$ tensors d_{abc} , which in turn will induce spurious couplings between gluons and $u(1)$ photons.

Finally, we need the Lagrangian for the Faddeev-Popov ghost and anti-ghost fields, \mathcal{C} and $\bar{\mathcal{C}}$. It is defined as usual in terms of the gauge transformation of the gauge-fixing function, as

$$\mathcal{L}_{\text{gh}} = \text{Tr} [\bar{\mathcal{C}} \delta_{\mathcal{C}} \mathcal{G}(\mathcal{A}, \mathcal{Q})], \quad (5.5)$$

using \mathcal{C} as parameter of the gauge transformation. The result is

$$\begin{aligned} \mathcal{L}_{\text{gh}} = 2 \text{Tr} [& -\bar{\mathcal{C}} \mathfrak{D}_M \mathfrak{D}^M \mathcal{C} + i g \mathfrak{D}_M \bar{\mathcal{C}} [Q^M, \mathcal{C}] \\ & - i \gamma g \bar{\mathcal{C}} \{Q_M, \mathfrak{D}^M \mathcal{C}\} + \gamma g^2 \bar{\mathcal{C}} \{Q_M, [Q^M, \mathcal{C}]\}]. \end{aligned} \quad (5.6)$$

This completes the construction of the pure Yang-Mills Lagrangian in \mathcal{D} dimensions; next, we want to dimensionally reduce it to d dimensions. The reduction splits the \mathcal{D} -dimensional gauge fields (both classical and quantum) into a d -dimensional field and $n_s \equiv \mathcal{D} - d$ adjoint scalars, according to

$$\{\mathcal{A}_M\} \rightarrow \left\{ \mathcal{A}_\mu, \frac{1}{g} \mathcal{M}_I \right\}, \quad \{Q_M\} \rightarrow \{Q_\mu, \Phi_I\}, \quad (5.7)$$

with $\mu = 0, \dots, d-1$ and $I = 1, \dots, n_s$, and we have assumed that the classical background scalars take on constant values \mathcal{M}_I , which we will use to spontaneously break the gauge symmetry and give masses to selected components of the gauge field. Similarly, since we are neglecting the dependence of the fields on the reduced coordinates, the covariant derivative splits into a d -dimensional covariant derivative and a pure commutator with the background scalar fields, as

$$\{\mathfrak{D}_M\} \rightarrow \{\mathfrak{D}_\mu \equiv \partial_\mu + i g [\mathcal{A}_\mu, \cdot], i [\mathcal{M}_I, \cdot]\}. \quad (5.8)$$

Indeed, the \mathcal{D} -dimensional d'Alembertian differs from the d -dimensional one by a mass term: for any field X ,

$$\mathfrak{D}_M \mathfrak{D}^M X = \mathfrak{D}_\mu \mathfrak{D}^\mu X + [\mathcal{M}_I, [\mathcal{M}^I, X]]. \quad (5.9)$$

Notice that in this section we work with the metric $\eta = \text{diag}(+, -, \dots, -)$. However, when summing over reduced dimensions, our summation convention does not include the negative signature of the metric, and must be understood simply as a summation over flavor indices I . With these conventions, the gauge condition in eq. (5.3) becomes

$$\mathfrak{D}_\mu Q^\mu + i \gamma g Q_\mu Q^\mu - i [\mathcal{M}_I, \Phi^I] - i \gamma g \Phi_I \Phi^I = 0. \quad (5.10)$$

When these further changes are implemented in the Lagrangian, a number of non-trivial interaction vertices are generated. It is then useful to organize the dimensionally-reduced

Lagrangian as a sum of terms with different operator content. One can write

$$\begin{aligned}
 \mathcal{L}_{\mathcal{Q}^2} &= \text{Tr} \left[\mathcal{Q}^\mu \left(\mathfrak{D}_\nu \mathfrak{D}^\nu \mathcal{Q}_\mu + 4i g F_{\mu\rho} \mathcal{Q}^\rho + [\mathcal{M}_I, [\mathcal{M}^I, \mathcal{Q}_\mu]] \right) \right], \\
 \mathcal{L}_{\Phi^2} &= \text{Tr} \left[-\Phi_I \mathfrak{D}_\nu \mathfrak{D}^\nu \Phi^I - \Phi^I [\mathcal{M}_J, [\mathcal{M}^J, \Phi_I]] \right], \\
 \mathcal{L}_{\bar{\mathcal{C}}\mathcal{C}} &= \text{Tr} \left[-2\bar{\mathcal{C}} \mathfrak{D}_\mu \mathfrak{D}^\mu \mathcal{C} - 2\bar{\mathcal{C}} [\mathcal{M}_J, [\mathcal{M}^J, \mathcal{C}]] \right], \\
 \mathcal{L}_{\mathcal{Q}^3} &= -2i g \gamma \text{Tr} [\mathfrak{D}_\mu \mathcal{Q}^\mu \mathcal{Q}_\nu \mathcal{Q}^\nu] - 2i g \text{Tr} [\mathfrak{D}_\mu \mathcal{Q}_\nu [\mathcal{Q}^\mu, \mathcal{Q}^\nu]], \\
 \mathcal{L}_{\mathcal{Q}\Phi^2} &= 2i g \gamma \text{Tr} [\mathfrak{D}_\mu \mathcal{Q}^\mu \Phi_I \Phi^I] + 2i g \text{Tr} [\mathfrak{D}_\mu \Phi_I [\mathcal{Q}^\mu, \Phi^I]], \\
 \mathcal{L}_{\bar{\mathcal{C}}\mathcal{C}\mathcal{Q}} &= 2i g \text{Tr} [\mathfrak{D}_\mu \bar{\mathcal{C}} [\mathcal{Q}^\mu, \mathcal{C}]] - 2i \gamma g \text{Tr} [\bar{\mathcal{C}} \{ \mathcal{Q}_\mu, \mathfrak{D}^\mu \mathcal{C} \}], \\
 \mathcal{L}_{\Phi\mathcal{Q}^2} &= -2\gamma g \text{Tr} [[\mathcal{M}_I, \Phi^I] \mathcal{Q}_\mu \mathcal{Q}^\mu] - 2g \text{Tr} [[\mathcal{M}_I, \mathcal{Q}_\mu] [\Phi^I, \mathcal{Q}^\mu]], \\
 \mathcal{L}_{\Phi^3} &= 2\gamma g [[\mathcal{M}_I, \Phi^I] \Phi_J \Phi^J] + 2g \text{Tr} [[\mathcal{M}_I, \Phi_J] [\Phi^I, \Phi^J]], \\
 \mathcal{L}_{\Phi\bar{\mathcal{C}}\mathcal{C}} &= 2g \text{Tr} [[\mathcal{M}_I, \bar{\mathcal{C}}] [\Phi^I, \mathcal{C}]] - 2\gamma g \text{Tr} [\bar{\mathcal{C}} \{ \Phi^I, [\mathcal{M}_I, \mathcal{C}] \}], \\
 \mathcal{L}_{\mathcal{Q}^4} &= g^2 (\eta_{\rho\mu} \eta_{\nu\sigma} - (1 - \gamma^2) \eta_{\rho\nu} \eta_{\sigma\mu}) \text{Tr} [\mathcal{Q}^\mu \mathcal{Q}^\nu \mathcal{Q}^\rho \mathcal{Q}^\sigma], \\
 \mathcal{L}_{\mathcal{Q}^2\Phi^2} &= -2g^2 \text{Tr} [\Phi_I \mathcal{Q}^\mu \Phi^I \mathcal{Q}_\mu] + 2(1 - \gamma^2) g^2 \text{Tr} [\Phi_I \Phi^I \mathcal{Q}^\mu \mathcal{Q}_\mu], \\
 \mathcal{L}_{\Phi^4} &= g^2 \text{Tr} [\Phi_I \Phi_J \Phi^I \Phi^J] - (1 - \gamma^2) g^2 \text{Tr} [\Phi_I \Phi^I \Phi_J \Phi^J], \\
 \mathcal{L}_{\bar{\mathcal{C}}\mathcal{C}\mathcal{Q}^2} &= 2\gamma g^2 \text{Tr} [\bar{\mathcal{C}} \{ \mathcal{Q}_\mu, [\mathcal{Q}^\mu, \mathcal{C}] \}], \\
 \mathcal{L}_{\bar{\mathcal{C}}\mathcal{C}\Phi^2} &= -2\gamma g^2 \text{Tr} [\bar{\mathcal{C}} \{ \Phi_I, [\Phi^I, \mathcal{C}] \}].
 \end{aligned} \tag{5.11}$$

As is typical in cases of broken symmetry, the Lagrangian in eq. (5.11) displays a variety of interactions, and is considerably more intricate than the combination of eqs. (5.2), (5.4) and (5.6). In order to compute Feynman diagrams, and to compare with the string theory calculation, it is useful to write down an expression for the Lagrangian in terms of component fields as well. In order to do so, we now assume that the matrices \mathcal{A}_μ and \mathcal{M}_I are all mutually commuting: we can then pick a basis of $\mathfrak{u}(N)$ in which they are diagonal. In this basis, we write

$$\mathcal{M}_I = \text{diag}\{m_I^A\}, \quad \mathcal{A}_\mu = \text{diag}\{A_\mu^A\}, \quad A = 1, \dots, N. \tag{5.12}$$

Similarly, we write the quantum matrix fields as

$$\begin{aligned}
 [\mathcal{Q}_\mu]^{AB} &= \frac{1}{\sqrt{2}} Q_\mu^{AB}, & [\Phi_I]^{AB} &= \frac{1}{\sqrt{2}} \phi_I^{AB} \\
 [\bar{\mathcal{C}}]^{AB} &= \frac{1}{\sqrt{2}} \bar{c}^{AB}, & [\mathcal{C}]^{AB} &= \frac{1}{\sqrt{2}} c^{AB},
 \end{aligned} \tag{5.13}$$

all satisfying $X^{AB} = (X^{BA})^*$, since $\mathfrak{u}(N)$ matrices are Hermitian; the factors of $1/\sqrt{2}$ ensure that the matrix element fields are canonically normalized. Notice that, thanks to diagonal form of the classical field \mathcal{A}_μ , the covariant derivative \mathfrak{D}_μ does not mix matrix entries. Indeed, defining

$$A_\mu^{AB} \equiv A_\mu^A - A_\mu^B, \tag{5.14}$$

one can write

$$[\mathfrak{D}_\mu X]^{AB} = (\partial_\mu + i g A_\mu^{AB}) X^{AB}, \tag{5.15}$$

where indices on the right-hand side are not summed. In particular, the covariant derivative of diagonal entries reduces to the ordinary derivative. Motivated by this, we can define a covariant derivative D_μ acting directly on matrix entries, as opposed to $\mathfrak{u}(N)$ elements. Suppressing the A, B indices on the derivative symbol, we write

$$D_\mu X^{AB} = (\partial_\mu + ig A_\mu^{AB}) X^{AB} \quad \longrightarrow \quad [\mathfrak{D}_\mu X]^{AB} = D_\mu X^{AB}. \quad (5.16)$$

Note that D_μ is a derivation, obeying the Leibnitz rule

$$D_\mu (XY)^{AB} = (D_\mu X^A_C) Y^{CB} + X^A_B (D_\mu Y^{CB}), \quad (5.17)$$

so it can be partially integrated in any integrand with contracted color indices. Treating the mass matrices in a similar way, we define

$$m_I^{AB} \equiv m_I^A - m_I^B, \quad m_{AB}^2 \equiv \sum_{I=1}^{n_s} (m_I^{AB})^2. \quad (5.18)$$

This implies

$$[\mathcal{M}_I, X]^{AB} = m_I^{AB} X^{AB}, \quad [\mathcal{M}_I, [\mathcal{M}^I, X]]_{AB} = m_{AB}^2 X_{AB}, \quad (5.19)$$

where again on the right-hand side the indices A and B are fixed and not summed. As an example, the term quadratic in Φ in eq. (5.11) can be written in component notation as

$$\begin{aligned} \mathcal{L}_{\Phi^2} &= -\frac{1}{2} \phi_I^{AB} D_\mu D^\mu \phi^{BA,I} - \frac{1}{2} \phi_I^{AB} m_{ij}^2 \phi^{BA,I} \\ &= -\frac{1}{2} \sum_{A=1}^N \phi_I^{AA} \partial_\mu \partial^\mu \phi^{AA,I} - \sum_{1 \leq A < B}^N [(\phi_I^{AB})^* D_\mu D^\mu \phi^{AB,I} + m_{AB}^2 |\phi_I^{AB}|^2], \end{aligned} \quad (5.20)$$

which is the correctly normalized quadratic part of the Lagrangian for N massless real scalar fields ϕ^{AA} , and $\frac{1}{2}N(N-1)$ complex scalars ϕ^{AB} , $A < B$, with mass $|m_{AB}|$. To give a second example, the gauge-fixing condition in component notation reads

$$D^\mu Q_\mu^{AB} + i\gamma g Q_\mu^{AC} Q_C^{\mu,B} - im_I^{AB} \phi_I^{AB} - i\gamma g \phi_{I,C}^A \phi_I^{CB} = 0, \quad (5.21)$$

where C is summed over but there is no summation over A or B . Note that after dimensional reduction and spontaneous symmetry breaking the gauge fixing has become more unconventional from the d -dimensional point of view, involving scalar fields as well as gauge fields, and mass parameters.

We conclude this section by giving the explicit expression for the background field that we will be working with. We choose it so that, for each A , the abelian field strength $F_{\mu\nu}^A = \partial_\mu A_\nu^A - \partial_\nu A_\mu^A$ is a $U(1)$ magnetic field in the $\{x_1, x_2\}$ plane. A possible choice, already employed in ref. [11], is

$$A_\mu^A(x) = x_1 \eta_{\mu 2} B^A \quad \longrightarrow \quad F_{\mu\nu}^A = f_{\mu\nu} B^A, \quad (5.22)$$

where we defined the antisymmetric tensor

$$f_{\mu\nu} = \eta_{\mu 1} \eta_{\nu 2} - \eta_{\nu 1} \eta_{\mu 2}. \quad (5.23)$$

We now turn to the evaluation of selected two-loop vacuum diagrams, contributing to the effective action, which we can then compare with the corresponding expressions derived from string theory. Preliminarily, we collect useful expressions for the relevant coordinate-space propagators in the presence of the background field.

5.2 Propagators in a constant background field

The quantum field theory objects that we wish to compute, in order to compare with string theory results, are two-loop vacuum diagrams contributing to the effective action, and computed with our chosen background field, eq. (5.22). At two loops, these diagrams can be computed in a straightforward manner in coordinate space, directly from the path integral definition of the generating functional,

$$\begin{aligned}
 Z[J_\mu^{AB}, \eta^{AB}, \bar{\eta}^{AB}, J_I^{AB}] &= \int [DQ_\mu^{AB} D\bar{c}^{AB} Dc^{AB} D\phi_I^{AB}] \\
 &\times \exp \left[i \int d^d x \left(\mathcal{L}[Q_\mu^{AB}, \bar{c}^{AB}, c^{AB}, \phi_I^{AB}] \right. \right. \\
 &\quad \left. \left. + J_\mu^{AB} Q_{BA}^\mu + \bar{c}^{BA} \eta^{AB} + \bar{\eta}^{AB} c^{BA} + J_I^{AB} \phi_I^{BA} \right) \right],
 \end{aligned}
 \tag{5.24}$$

where J_μ , J_I , η and $\bar{\eta}$ are matrix sources for the fields in the complete Lagrangian \mathcal{L} . The only non-trivial step is the computation of the quantum field propagators in the presence of the background field: diagrams are then simply constructed by differentiating the free generating functional with respect to the external sources. For a background field of the form of eq. (5.22), the solution is well-known for the scalar propagator (see, for example, ref. [15]): we briefly describe it here, and discuss the generalization to vector fields.

For scalar fields, the propagator in the presence of the background in eq. (5.22) can be expressed in terms of a heat kernel as

$$G^{AB}(x, y) = \int_0^\infty dt \mathcal{K}^{AB}(x, y; t),
 \tag{5.25}$$

where, defining $B_{AB} \equiv B_A - B_B$, one can write

$$\begin{aligned}
 \mathcal{K}^{AB}(x, y; t) &= \frac{1}{(4\pi t)^{d/2}} e^{-\frac{i}{2} g B^{AB} (x_1 + y_1)(x_2 - y_2) - t m_{AB}^2} \frac{g B^{AB} t}{\sinh(g B^{AB} t)} \\
 &\times \exp \left[\frac{1}{4t} (x_\mu - y_\mu) \Sigma^{\mu\nu} (g B^{AB} t) (x_\nu - y_\nu) \right].
 \end{aligned}
 \tag{5.26}$$

In eq. (5.26), we have introduced the tensor

$$\Sigma_{\mu\nu}(g B^{AB} t) = \frac{g B^{AB} t}{\tanh(g B^{AB} t)} \eta_{\mu\nu}^\parallel + \eta_{\mu\nu}^\perp,
 \tag{5.27}$$

where the projectors $\eta_{\parallel}^{\mu\nu}$ and $\eta_{\perp}^{\mu\nu}$ identify components parallel and perpendicular to the background field, and are given by

$$\eta_{\parallel}^{\mu\nu} = f^{\mu\rho} f_{\rho}{}^\nu = \delta_1^\mu \delta_1^\nu + \delta_2^\mu \delta_2^\nu, \quad \eta_{\perp}^{\mu\nu} = \eta^{\mu\nu} - \eta_{\parallel}^{\mu\nu}.
 \tag{5.28}$$

The propagator $G^{AB}(x, y)$ in eq. (5.25) satisfies

$$(D_\mu^{(x)} D_\mu^\mu + m_{AB}^2) G^{AB}(x, y) = -i \delta^d(x - y), \quad (5.29)$$

where we noted explicitly the variable on which the derivatives act. In fact, covariant derivatives act on a propagator with color indices (AB) as

$$\begin{aligned} D_\mu^{(x)} G^{AB}(x, y) &\equiv \left[\frac{\partial}{\partial x^\mu} + i g A_\mu^{AB}(x) \right] G^{AB}(x, y), \\ D_\mu^{(y)} G^{AB}(x, y) &\equiv \left[\frac{\partial}{\partial y^\mu} - i g A_\mu^{AB}(y) \right] G^{AB}(x, y). \end{aligned} \quad (5.30)$$

For real scalar fields, or vanishing backgrounds, one recovers the well-known expression for the scalar propagator as a Schwinger parameter integral,

$$G_0^{AB}(x, y) \equiv \lim_{B^{AB} \rightarrow 0} G^{AB}(x, y) = \int_0^\infty dt \frac{e^{-t m_{AB}^2}}{(4\pi t)^{d/2}} \exp \left[\frac{(x - y)^2}{4t} \right]. \quad (5.31)$$

Ghosts fields are scalars, and they share the same propagator. For gluons, on the other hand, the background field strength $F_{\mu\rho}$ enters the kinetic term, given in the first line of eq. (5.11). The propagator must then satisfy

$$[\eta_{\mu\rho} (D_\sigma^{(x)} D_\sigma^\sigma + m_{AB}^2) + 2i g F_{\mu\rho}^{AB}] G^{AB, \rho\nu}(x, y) = i \delta_\mu^\nu \delta^d(x - y). \quad (5.32)$$

To diagonalize this equation, one can introduce the projection operators

$$(P_\pm)_{\rho\sigma} = \frac{\eta_{\rho\sigma} \pm f_{\rho\sigma}}{2}, \quad (P_\perp)_{\rho\sigma} = \eta_{\rho\sigma}^\perp, \quad (5.33)$$

satisfying

$$(P_+ + P_- + P_\perp)_{\mu\nu} = \eta_{\mu\nu} \quad (P_+ - P_-)_{\mu\nu} = f_{\mu\nu}. \quad (5.34)$$

It is then easy to show that the function

$$G^{AB, \sigma\alpha}(x, y) = -\eta_\perp^{\sigma\alpha} G^{AB}(x, y) - P_+^{\sigma\alpha} G_+^{AB}(x, y) - P_-^{\sigma\alpha} G_-^{AB}(x, y) \quad (5.35)$$

satisfies eq. (5.32), provided the functions $G_\pm^{AB}(x, y)$ satisfy

$$[D_\mu^{(x)} D_\mu^\mu + m_{AB}^2 \pm 2i g B^{AB}] G_\pm^{AB}(x, y) = -i \delta^d(x - y). \quad (5.36)$$

Eq. (5.36) simply gives a scalar propagator with a mass shifted by the appropriate background field. It's easy therefore to write the solution for the complete gluon propagator explicitly as

$$G_{\mu\nu}^{AB}(x, y) = - \int_0^\infty dt [\eta_{\mu\nu}^\perp + \eta_{\mu\nu}^\parallel \cosh(2gB^{AB}t) + f_{\mu\nu} \sinh(2gB^{AB}t)] \mathcal{K}^{AB}(x, y; t). \quad (5.37)$$

Note that this can be written also in the more compact and elegant form

$$G_{\mu\nu}^{AB}(x, y) = - \int_0^\infty dt [e^{-gt F_{\alpha\beta}^{AB} S_1^{\alpha\beta}}]_{\mu\nu} \mathcal{K}^{AB}(x, y; t), \quad (5.38)$$

where $S_1^{\alpha\beta}$ are the Lorentz generators in the spin one representation appropriate for gauge bosons,

$$[S_1^{\alpha\beta}]_{\mu\nu} = -i(\delta^\alpha_\mu \delta^\beta_\nu - \delta^\alpha_\nu \delta^\beta_\mu). \quad (5.39)$$

The propagator in eq. (5.38) naturally generalizes to other representations of the Lorentz group, simply changing the form of the generators. The spin one-half case, where $S_{1/2}^{\alpha\beta} = i[\gamma^\alpha, \gamma^\beta]/4$, will be useful for example when studying the gluino contribution to the effective action in the supersymmetric case.

5.3 Selected two-loop vacuum diagrams

We will now illustrate the structure of the field theory calculation of the effective action by outlining the calculation of a selection of the relevant two-loop diagrams. A complete list of the result for all 1PI diagrams depicted in figure 1 is given in appendix C.

We begin by considering the ghost-gluon diagram given by the sum of eq. (C.7) and eq. (C.8), which we denote by $H_b(B_{AB}, m_{AB})$. The relevant interaction vertex, involving ghost, antighost and gluon fields, arises from the sixth line in eq. (5.11), and may be written explicitly in component language using eq. (5.13). Upon integrating by parts, it can be rewritten as

$$\begin{aligned} \mathcal{L}_{\bar{c}cQ} = & \frac{ig}{\sqrt{2}} [(\delta_{BC}\delta_{DE}\delta_{FA} - \delta_{BE}\delta_{FC}\delta_{DA}) D_\mu \bar{c}^{AB} Q^{\mu,CD} c^{EF} \\ & - \gamma(\delta_{BC}\delta_{DE}\delta_{FA} + \delta_{BE}\delta_{FC}\delta_{DA}) \bar{c}^{AB} Q^{\mu,CD} D_\mu c^{EF}]. \end{aligned} \quad (5.40)$$

Sewing two copies of this vertex together to obtain the desired diagram, one first of all observes that terms linear in the gauge parameter γ , which involve double derivatives of scalar propagators, cancel out upon contracting color indices. Next, one notices that some of the color contractions lead to a non-planar configuration, which would correspond to an open string diagram with only one boundary. We are not interested in these contributions, since the corresponding diagram is built of propagators which are neutral with respect to the background field, and does not contribute to the effective action. Furthermore, we do not expect to obtain this diagram from our string configuration, since we start with a planar worldsheet. Discarding non-planar contributions, one finds that the remaining planar terms can be written as

$$\begin{aligned} H_b(B_{AB}, m_{AB}) = & -g^2 \frac{1 + \gamma^2}{4} \int d^d x d^d y [D_\mu^{(x)} G^{AB}(x, y) D_\nu^{(y)} G^{BC}(x, y) G^{\mu\nu, CA}(x, y) \\ & + (ABC) \leftrightarrow (CBA)]. \end{aligned} \quad (5.41)$$

Inserting the expressions for the scalar and gluon propagators given by eq. (5.25) and eq. (5.38), one can immediately rewrite eq. (5.41) in terms of covariant derivatives of the heat kernels \mathcal{K} . These, in turn, can be written as

$$\begin{aligned} D_\mu^{(x)} \mathcal{K}_{AB}(x, y; t) &= \frac{\Sigma_{\mu\rho}(gB^{AB}t) + it F_{\mu\rho}^{AB}}{2t} (x^\rho - y^\rho) \mathcal{K}_{AB}(x, y; t), \\ D_\nu^{(y)} \mathcal{K}_{BC}(x, y; t) &= -\frac{\Sigma_{\nu\sigma}(gB^{BC}t) - it F_{\nu\sigma}^{BC}}{2t} (x^\sigma - y^\sigma) \mathcal{K}_{BC}(x, y; t), \end{aligned} \quad (5.42)$$

where $\Sigma(gBt)$ is defined in eq. (5.27). The integrand in eq. (5.41) is then proportional to the product of three heat kernels, which we write as

$$\prod_{i=1}^3 \mathcal{K}_i(x, y; t_i) = \exp \left[\frac{1}{4} (x^\mu - y^\mu) \bar{\Sigma}_{\mu\nu} (x^\nu - y^\nu) \right] \prod_{i=1}^3 \frac{e^{-t_i m_i^2}}{(4\pi t_i)^{\frac{d}{2}}} \frac{g B_i t_i}{\sinh(g B_i t_i)}. \quad (5.43)$$

In eq. (5.43) we have simplified the notation by using a single index $i = 1, 2, 3$ in place of the pairs of color indices $(AB), (BC), (CA)$, respectively. Furthermore, we have defined $\bar{\Sigma}_{\mu\nu} = \sum_{i=1}^3 \Sigma_{\mu\nu}(gB^i t_i)/t_i$, and we have taken advantage of the fact that the complex phases in each $\mathcal{K}_i(x, y; t_i)$ cancel due to the fact that $\sum_{i=1}^3 B_i = 0$. At this point one sees that the integrand in eq. (5.41) is translationally invariant, depending only on the combination $z = x - y$. We can then, for example, replace the integral over x with an integral over z while the integral over y gives a factor of the volume of spacetime, which we will not write explicitly. One needs finally to evaluate the gaussian integral

$$\int d^d z z^\rho z^\sigma \exp \left[\frac{1}{4} z^\mu \bar{\Sigma}_{\mu\nu} z^\nu \right] = -2 (\bar{\Sigma}^{-1})^{\rho\sigma} \int d^d z \exp \left[\frac{1}{4} z^\mu \bar{\Sigma}_{\mu\nu} z^\nu \right]. \quad (5.44)$$

Note that taking the inverse of $\bar{\Sigma}_{\mu\nu}$ is trivial because it is a diagonal matrix, which can be written as

$$\bar{\Sigma}_{\mu\nu} = \Delta_0 \eta_{\mu\nu}^\perp \prod_{i=1}^3 \frac{1}{t_i} + \Delta_B \eta_{\mu\nu}^\parallel \prod_{i=1}^3 \frac{g B_i}{\sinh(g B_i t_i)}, \quad (5.45)$$

where Δ_0 and Δ_B were defined in eq. (4.29) and eq. (4.31) respectively, while $\eta_{\mu\nu}^\perp$ and $\eta_{\mu\nu}^\parallel$ are given in eq. (5.28). One finds then

$$\int d^d z \exp \left[\frac{1}{4} z^\mu \bar{\Sigma}_{\mu\nu} z^\nu \right] = -i (4\pi)^{d/2} \Delta_0^{1-d/2} \Delta_B^{-1} \prod_{i=1}^3 \frac{\sinh(g B_i t_i)}{g B_i t_i} t_i^{d/2}. \quad (5.46)$$

Putting together all these ingredients, one may evaluate eq. (5.41). Using the symmetry of the Schwinger parameter integrand under the exchange $t_1 \leftrightarrow t_2$ one can write

$$H_b(B_i, m_i) = -i \frac{g^2}{(4\pi)^d} \frac{1 + \gamma^2}{2} \int_0^\infty \prod_{i=1}^3 dt_i \frac{e^{-t_1 m_1^2 - t_2 m_2^2 - t_3 m_3^2}}{\Delta_0^{d/2-1} \Delta_B} \left[\frac{d-2}{\Delta_0} t_3 + \frac{2}{\Delta_B} \frac{\sinh(g B_3 t_3)}{g B_3} \cosh(2g B_3 t_3 - g B_1 t_1 - g B_2 t_2) \right], \quad (5.47)$$

which can be directly matched to the string theory result.

We conclude this section by briefly describing the calculation of two further Feynman diagrams, which arise in our theory because of the pattern of symmetry breaking and dimensional reduction. First of all, there are diagrams, like eq. (C.12), with the same topology as eq. (C.8), but with an odd number of scalar propagators, and vertices proportional to the scalar vacuum expectation values m_{ij} , characteristic of the broken symmetry phase. The relevant vertex can be found by expanding $\mathcal{L}_{\Phi Q^2}$ from eq. (5.11) in terms

of the component fields defined in the eq. (5.13). Upon relabeling the indices and using $m_I^{CB} + m_I^{BA} + m_I^{AC} = 0$, it reads

$$\mathcal{L}_{Q^2\phi} = \frac{g}{\sqrt{2}} [(1 + \gamma)m_I^{CB} - (1 - \gamma)m_I^{AC}] \phi^{AB} Q_\mu^{BC} Q^{\mu,CA}. \quad (5.48)$$

Labeling this diagram as $H_d(B_{AB}, m_{AB})$, we find for it the coordinate space expression

$$H_d(B_{AB}, m_{AB}) = \frac{g^2}{4} [(1 - \gamma)m_I^{CB} - (1 + \gamma)m_I^{AC}] [(1 - \gamma)m_I^{AC} - (1 + \gamma)m_I^{CB}] \\ \times \int d^d x d^d y G^{AB}(x, y) G_{\mu\nu}^{BC}(x, y) G^{\mu\nu,CA}(x, y), \quad (5.49)$$

where we neglected non-planar contributions, and we used $m_I^{BC} = -m_I^{CB}$. Manipulations similar to those leading to eq. (5.47), simplified by the absence of derivative interactions, yield the result

$$H_d(B_i, m_i) = -\frac{i}{(4\pi)^d} \frac{g^2}{2} [(1 + \gamma^2) m_3^2 - 2(m_1^2 + m_2^2)] \\ \times \int_0^\infty \prod_{i=1}^3 dt_i \frac{e^{-t_1 m_1^2 - t_2 m_2^2 - t_3 m_3^2}}{\Delta_0^{d/2-1} \Delta_B} [d - 2 + 2 \cosh(2gB_1 t_1 - 2gB_2 t_2)], \quad (5.50)$$

where we relabeled double indices as was done for eq. (5.47).

Finally, we briefly consider a diagram with a quartic vertex: the figure-of-eight scalar self-interaction shown in eq. (C.20), which we label $E_i(B_k, m_k)$. The relevant interaction term in the Lagrangian comes from \mathcal{L}_{Φ^4} in eq. (5.11) and can be written as

$$\mathcal{L}_{\Phi^4} = \frac{g^2}{4} [\delta_{KI} \delta_{LJ} - (1 - \gamma^2) \delta_{IL} \delta_{JK}] \phi_K^{AB} \phi_L^{BC} \phi_I^{CD} \phi_J^{DA}, \quad (5.51)$$

which immediately gives

$$E_i(B_k, m_k) = i \frac{g^2}{4} [\delta_{KI} \delta_{LJ} - (1 - \gamma^2) \delta_{IL} \delta_{JK}] \int d^d x [G^{DA}(x, x) G^{BC}(x, x) \delta_{AC} \delta^{IJ} \delta^{LK} \\ + G^{CD}(x, x) G^{DA}(x, x) \delta_{DB} \delta^{LI} \delta^{JK}]. \quad (5.52)$$

Contracting flavor indices we get, as expected, the product of two one-loop integrals,

$$E_i(B_k, m_k) = i \frac{g^2}{(4\pi)^d} \left[1 - \frac{1 - \gamma^2}{2} (1 + n_s) \right] n_s \int_0^\infty \prod_{i=1}^2 \left[\frac{dt_i}{t_i^{d/2-1}} \frac{g B_i e^{-t_i m_i^2}}{\sinh(g B_i t_i)} \right]. \quad (5.53)$$

The diagrams in eqs. (5.1)–(C.19) can be calculated similarly. One easily sees that all these results, and those for the remaining diagrams, given in appendix C, are directly comparable with the ones obtained from the field theory limit of the string effective action.

6 Discussion of results

6.1 Comparison between QFT and string theory

We have now assembled all the results that we need to establish and verify a precise mapping between the degeneration limits of the string world-sheet and the 1PI Feynman diagram topologies in the field theory limit. Furthermore, as announced, we can trace the contributions of individual string states propagating in each degenerate surface, and these can be unambiguously mapped to space-time states propagating in the field theory diagrams. This diagram-by-diagram mapping allows us in particular to confirm that covariantly quantized superstring theory⁶ naturally selects a specific gauge in the field theory limit, and the gauge condition is given here in eq. (5.3).

More precisely, our string theory results for the symmetric degeneration are given in eq. (4.42) and eq. (4.43). A careful inspection shows that these results reproduce all the Feynman diagrams in the first two lines of figure 1, which are listed in eqs. (C.3) through (C.14) in appendix C, with the choice $\gamma^2 = 1$. Similarly, our string theory results for the incomplete degeneration are given in eq. (4.54) and eq. (4.55), and one may verify that one recovers all Feynman diagrams in the last two lines of figure 1, given in eqs. (C.15) through (C.20). It is easy to identify each term in eq. (4.42) with a particular Feynman diagram: for example, the term \mathbf{f}_\perp^{111} in eq. (4.43) matches the diagram resulting in eq. (C.3), in which all three lines correspond to gluons that are polarized in directions perpendicular to the external magnetic field; on the other hand, the term $\mathbf{f}_\parallel^{001}\mathbf{f}_\perp^{110}$, plus its cyclic permutations, matches the result of eq. (C.4), in which one line carries a gluon polarized in the plane parallel to the magnetic field, while the other two gluons are polarized in the directions perpendicular to the magnetic fields. One may easily continue through the list, identifying the other available combinations of gluons, ghosts and scalars. In a similar vein, one can associate individual Feynman graphs to each term in eq. (4.54): for example, $\mathbf{f}_\parallel^{11}$ corresponds to eq. (C.15), \mathbf{f}_\perp^{11} to eq. (C.17), while $\mathbf{f}_{\text{scal}}^{11}$ gives the diagram with two scalar propagators given in eq. (C.20). Note also that diagrams with a quartic vertex where the two propagators come from different sectors, such as for example eqs. (5.1), (C.18) and (C.19), all vanish for $\gamma^2 = 1$, so it comes as no surprise that no contribution of this kind arises on the string theory side.

We finally note that we can also characterize the contributions to all 1PI Feynman diagrams according to the Schottky multiplier they originate from. As an example, consider the infinite product over the Schottky group which arises from the determinant of the non-zero modes of the Laplacian, appearing in eq. (3.11). Tracing the gluon contributions to different Feynman diagrams back to that product, one may verify that all terms appearing in 1PI diagrams originate from at most one value of the index α in the product. More precisely, gluon contributions in eq. (4.42) come from $\mathbf{T}_\alpha = \{\mathbf{S}_1, \mathbf{S}_2, \mathbf{S}_1^{-1}\mathbf{S}_2\}$, and if, say, a factor of $k_1^{1/2} = \sqrt{p_1}\sqrt{p_3}$ comes from the infinite product, then the necessary factor of $\sqrt{p_2}$ must come from elsewhere in the amplitude. On the other hand, all terms in eq. (4.54)

⁶On the other hand, it has been shown in refs. [72, 73] that light-cone quantization of string theory results in quantum field theory amplitudes computed in a light-cone gauge.

come from $\mathbf{T}_\alpha = \mathbf{S}_1\mathbf{S}_2$. This is not surprising from a world-sheet point of view: in fact, one may recall from figure 5 that $\mathbf{S}_1\mathbf{S}_2$ corresponds to a homology cycle which passes around both handles with a self-intersection between them, and furthermore this is the only Schottky group element with this property which survives in the field theory limit. We see that this homological property is directly related to the graphical structure of the resulting Feynman diagram.

6.2 Comparison with bosonic string theory

It is interesting to compare our results with the field theory limit of the bosonic string effective action which was studied in refs. [15, 35, 67]. This comparison was discussed also in [11], but we are now in a position to make a more detailed analysis.

Bosonic strings are clearly a simpler framework, since the world-sheet is an ordinary two-dimensional manifold, and not a super-manifold: one can then use the techniques applying to ordinary Riemann surfaces, and specifically the (purely bosonic) Schottky parametrization discussed in detail for example in ref. [11]. At two loops, one can use the $\mathrm{SL}(2, \mathbf{R})$ invariance of the amplitude to choose the fixed points of the two Schottky group generators as

$$\eta_1 = 0, \quad \xi_1 = \infty, \quad \eta_2 \equiv u, \quad \xi_2 = 1. \quad (6.1)$$

The two-loop partition function can then be written as

$$Z_2(\vec{\epsilon}, \vec{d}) = \int \frac{dk_1 dk_2 du}{k_1^2 k_2^2 (1-u)^2} F_{\mathrm{gh}}(\mu) F_{\parallel}^{(\vec{\epsilon})}(\mu) F_{\perp}(\mu) F_{\mathrm{scal}}^{(\vec{d})}(\mu), \quad (6.2)$$

where μ denotes the set of bosonic moduli, $\mu = \{k_1, k_2, u\}$, and one may compare with the corresponding two-loop superstring expression, given in eq. (3.18). Note that the integration variable u is equal to the gauge-fixed value of a projective-invariant cross ratio of fixed points, $u = \frac{\eta_1 - \eta_2}{\eta_1 - \xi_2} \frac{\xi_1 - \xi_2}{\xi_1 - \eta_2}$. The various factors in eq. (6.2), already discussed in [11, 15], are given by

$$\begin{aligned} F_{\mathrm{gh}}(k_i, u) &= (1 - k_1)^2 (1 - k_2)^2 \prod'_{\alpha} \prod_{n=2}^{\infty} (1 - k_{\alpha}^n)^2, \\ F_{\parallel}^{(\vec{\epsilon})}(k_i, u) &= e^{-i\pi\vec{\epsilon}\cdot\tau\cdot\vec{\epsilon}} [\det(\mathrm{Im} \tau_{\vec{\epsilon}})]^{-1} \prod'_{\alpha} \prod_{n=1}^{\infty} (1 - e^{2\pi i\vec{\epsilon}\cdot\tau\cdot\vec{N}_{\alpha}} k_{\alpha}^n)^{-1} (1 - e^{-2\pi i\vec{\epsilon}\cdot\tau\cdot\vec{N}_{\alpha}} k_{\alpha}^n)^{-1}, \\ F_{\perp}(k_i, u) &= [\det(\mathrm{Im} \tau)]^{-(d-2)/2} \prod'_{\alpha} \prod_{n=1}^{\infty} (1 - k_{\alpha}^n)^{-d+2}, \\ F_{\mathrm{scal}}^{(\vec{d})}(k_i, u) &= \prod_{I=1}^{n_s} e^{\vec{d}_I \cdot \tau \cdot \vec{d}_I / (2\pi i \alpha')} \prod'_{\alpha} \prod_{n=1}^{\infty} (1 - k_{\alpha}^n)^{-n_s}. \end{aligned} \quad (6.3)$$

Here τ is the period matrix of the Riemann surface, whose expression in the Schottky parametrization can be found, for instance, in eq. (A.14) of [31]. Similarly, $\tau_{\vec{\epsilon}}$ is the twisted period matrix, the bosonic equivalent of $\tau_{\vec{\epsilon}}$, computed here in appendix B.

The most obvious difference between the measures in eq. (3.18) and eq. (6.2) is the occurrence of half-integer powers of the multipliers in the former. In the bosonic string,

the mass level of states propagating in the i -th loop increases with the power of k_i , whereas in the superstring it increases with the power of $k_i^{1/2}$. Necessarily, the propagation of a massless state must correspond to terms of the form $dk_i/k_i = d \log k_i$ in the integrand, so tachyons propagating in loops correspond to terms of the form dk_i/k_i^2 in the bosonic theory and $dk_i/k_i^{3/2}$ in the superstring, as seen explicitly in eq. (6.2) and in eq. (3.18), respectively. These tachyonic states must be removed by hand in the bosonic theory, whereas they are automatically eliminated from the spectrum of the superstring upon integrating over the odd moduli and carrying out the GSO projection.

The identification of the symmetric degeneration proceeds in the same way for the two theories: in particular, the symmetry of figure 6a leads to the choice of the parameters p_i , defined by eq. (4.12). The cross-ratio u can then be written as

$$u = \frac{(1 + p_1)(1 + p_2) p_3}{(1 + p_3)(1 + p_1 p_2 p_3)}, \tag{6.4}$$

and the integration measure takes the symmetric form

$$\frac{dk_1}{k_1^2} \frac{dk_2}{k_2^2} \frac{du}{(1-u)^2} (1-k_1)^2 (1-k_2)^2 = \frac{dp_1}{p_1^2} \frac{dp_2}{p_2^2} \frac{dp_3}{p_3^2} (1-p_2 p_3)(1-p_1 p_3)(1-p_1 p_2). \tag{6.5}$$

It is interesting to note that in the field theory limit a number of contributions arise in slightly different ways in the two approaches. As an example, let us consider the twisted determinant of the period matrix for the bosonic string. To lowest order in k_i , it is given by a combination of hypergeometric functions with argument u , in a manner similar to what happens for its supersymmetric counterpart. In the neighborhood of the symmetric degeneration, the hypergeometric functions can be expanded in powers of p_3 , and the bosonic string determinant reduces to

$$\det(\text{Im } \tau_{\vec{\epsilon}}) = \frac{1}{4\pi^2(\alpha')^2} \left[\Delta_B - 2\alpha' p_3 \cosh(g(2B_3 t_3 - B_1 t_1 - B_2 t_2)) \frac{\sinh(gB_3 t_3)}{gB_3} + \mathcal{O}(p_1, p_2, p_3^2; (\alpha')^2) \right], \tag{6.6}$$

where Δ_B is defined in eq. (4.31). We note that the term proportional to p_3 in eq. (6.6) receives a contribution from the series expansion of the hypergeometric functions, and contributes to Feynman diagrams with a gluon polarized parallel to the magnetic field propagating in the leg parametrized by t_3 .

For the superstring, the situation changes: one needs to keep terms only up to order q_i , which implies that all the hypergeometric functions appearing in the expression for the supersymmetric twisted determinant can be replaced by unity. Since the first-order term in the expansion of the hypergeometric functions is crucial in order to get the correct coefficient of p_3 in eq. (6.6), and in turn to match the field theory diagrams, it is necessary that terms proportional to q_3 arise from the nilpotent contributions to $\det(\text{Im } \tau_{\vec{\epsilon}})$. This is indeed what happens: expanding the supersymmetric twisted determinant in powers of q_i

one finds

$$\det(\text{Im } \tau_{\vec{\epsilon}}) = \frac{1}{4\pi^2(\alpha')^2} \left[\Delta_B - 2\alpha' q_3 \hat{\theta}_{12} \hat{\phi}_{12} \cosh(g(2B_3 t_3 - B_1 t_1 - B_2 t_2)) \frac{\sinh(gB_3 t_3)}{gB_3} + \mathcal{O}(q_1, q_2, q_3^2; (\alpha')^2) \right]. \quad (6.7)$$

To be precise, we note that terms proportional to p_3 and $q_3 \hat{\theta}_{12} \hat{\phi}_{12}$ in $\det(\text{Im } \tau_{\vec{\epsilon}})$ and $\det(\text{Im } \tau_{\vec{\epsilon}})$, respectively, also receive contributions from sources other than the ones we have discussed, specifically from factors of the form $u^{n_i \epsilon_i/2}$, with n_i integers. It is easy to see, however, that these contribute in the same way in the two cases, since in the bosonic case we have

$$u^{n_i \epsilon_i/2} = p_3^{n_i \epsilon_i/2} \left(1 + \frac{n_i \epsilon_i}{2} p_3 \right) + \mathcal{O}(p_1, p_2, p_3^2), \quad (6.8)$$

while in the superstring case we get

$$u^{n_i \epsilon_i/2} = p_3^{n_i \epsilon_i/2} \left(1 + \frac{n_i \epsilon_i}{2} q_3 \hat{\theta}_{12} \hat{\phi}_{12} \right) + \mathcal{O}(q_1, q_2, q_3^2). \quad (6.9)$$

As a consequence, and as required, when all of the other factors are inserted, the coefficient of $p_1 p_2 p_3$ in the bosonic string measure is the same as the coefficient of $q_1 q_2 q_3 \hat{\theta}_{12} \hat{\phi}_{12}$ in the superstring measure, and the same field theory amplitude is obtained for the massless sectors of the bosonic and supersymmetric theories.

The terms computed in section 4.5, which correspond to field theory diagrams with the topology of the diagrams in the bottom two rows of figure 1, as well as 1PR graphs, also appear in the bosonic theory. In fact, one gets once more an expression of the form of eq. (4.47) in the field theory limit, but the integrals I_1 , I_2 and I_3 get replaced by

$$\tilde{I}_1 = \int_0^1 \frac{du}{(1-u)^2}, \quad \tilde{I}_2 = \int_0^1 du, \quad \tilde{I}_3 = \int_0^1 \frac{du}{u^2}. \quad (6.10)$$

When using the bosonic string, the integral \tilde{I}_3 has to be discarded by hand, either by arguing that it corresponds to tachyon propagation, or by explicitly matching to the field theory result. In the case of the superstring, on the other hand, the correct result emerges automatically, provided a consistent integration procedure in super-moduli space is followed. The complete answer for the four-point vertex diagrams emerges in both cases from the terms proportional to $I_2 = \tilde{I}_2 = 1$. As in the superstring case, the contribution \tilde{I}_1 is related to the separating degeneration.

Acknowledgments

We would like to thank Paolo Di Vecchia for discussions. The work of LM was partially funded by MIUR (Italy), under contract 2010YJ2NYW_006, and by the University of Torino and the Compagnia di San Paolo under contract ORTO11TPXK. The work of SP was partially supported by a Science and Technology Facilities Council (STFC) studentship and partially supported by the Compagnia di San Paolo contract ‘‘MAST: Modern Applications of String Theory’’ TO-Call3-2012-0088. The work of RR was partially supported

by the STFC Consolidated Grant ST/L000415/1 “String theory, gauge theory & duality”. We made use of the Mathematica package `grassmann.m` [74] in our computations.

A Super Schottky groups

In this appendix we discuss the super-Schottky parametrization of super moduli space in the Neveu-Schwarz sector, and we compute some relevant geometric quantities in this parametrization. Bosonic Schottky groups are discussed, for example, in section 2 of ref. [11]: here we focus only on the supersymmetric case.

A.1 Super-projective transformations

Super-projective transformations are automorphisms of the super-Riemann sphere $\mathbf{CP}^{1|1}$, which is defined in terms of homogeneous coordinates in $\mathbf{C}^{2|1}$ by the equivalence relation $(z_1, z_2|\theta) \sim (\lambda z_1, \lambda z_2|\lambda\theta)$ for non-zero complex λ , where the bosonic coordinates z_1 and z_2 are not allowed to vanish simultaneously. To fix the superconformal structure, we introduce a skew-symmetric quadratic form, using a bra-ket notation $\langle \mathbf{u}|\mathbf{v} \rangle$ defined by⁷

$$\langle \mathbf{u} | = (u_2, -u_1, \theta), \quad | \mathbf{u} \rangle = (u_1, u_2|\theta)^t, \quad (\text{A.1})$$

satisfying $\langle \mathbf{u}|\mathbf{v} \rangle = -\langle \mathbf{v}|\mathbf{u} \rangle$. This bracket is related to the super-difference between two points, $\mathbf{z} - \mathbf{w}$, defined in eq. (3.5), as follows: if $|\mathbf{z} \rangle = (\lambda_1 z, \lambda_1, \lambda_1 \psi)^t$, and $|\mathbf{w} \rangle = (\lambda_2 w, \lambda_2, \lambda_2 \theta)^t$, for $\lambda_1, \lambda_2 \neq 0$, then

$$\langle \mathbf{w}|\mathbf{z} \rangle = \lambda_1 \lambda_2 (\mathbf{z} - \mathbf{w}) = \lambda_1 \lambda_2 (z - w - \psi\theta). \quad (\text{A.2})$$

The group of transformations which preserves the skew-symmetric quadratic form is the group $\text{OSp}(1|2)$, which can be realised by $\text{GL}(2|1)$ matrices of the form

$$\mathbf{S} = \left(\begin{array}{cc|c} a & b & \alpha \\ c & d & \beta \\ \hline \gamma & \delta & e \end{array} \right), \quad (\text{A.3})$$

where the five even and four odd variables are subject to the two odd and two even constraints,

$$\begin{pmatrix} \alpha \\ \beta \end{pmatrix} = \begin{pmatrix} a & b \\ c & d \end{pmatrix} \begin{pmatrix} -\delta \\ \gamma \end{pmatrix}, \quad ad - bc - \alpha\beta = 1, \quad e = 1 - \alpha\beta, \quad (\text{A.4})$$

so that the group has dimension $3|2$.

We can define a map from homogeneous coordinates to superconformal coordinates by

$$\mathbf{f} : \{(z_1, z_2|\theta)^t \mid z_2 \neq 0\} \rightarrow \mathbf{C}^{1|1}, \quad (z_1, z_2|\theta)^t \mapsto \mathbf{f}((z_1, z_2|\theta)^t) \equiv (z_1/z_2|\theta/z_2). \quad (\text{A.5})$$

⁷Notice that $\langle \mathbf{u}|\mathbf{v} \rangle = -\langle \mathbf{u}, \mathbf{v} \rangle$ where $\langle \mathbf{u}, \mathbf{v} \rangle$ is the skew-symmetric quadratic form introduced in eq. (5.54) of ref. [21].

Then, any other map of the form $f \circ \mathbf{S}$, with \mathbf{S} an $\text{OSp}(1|2)$ matrix, also defines superconformal coordinates. Recall [75] that two $\mathbf{CP}^{1|1}$ charts $(z|\theta)$ and $(\hat{z}|\hat{\theta})$ belong to the same superconformal class whenever $D_\theta \hat{z} = \hat{\theta} D_\theta \hat{\theta}$, where

$$D_\theta \equiv \partial_\theta + \theta \partial_z \quad (\text{A.6})$$

is the super derivative which satisfies $D_\theta^2 = \partial_z$. In particular, we can cover $\mathbf{CP}^{1|1}$ with two superconformal charts $\mathbf{z}_1 = f((z_1, z_2|\theta)^t)$ and $\mathbf{z}_2 = (f \circ \mathbf{I})((z_1, z_2|\theta)^t)$, where \mathbf{I} is the $\text{OSp}(1|2)$ matrix

$$\mathbf{I} = \left(\begin{array}{cc|c} 0 & -1 & 0 \\ 1 & 0 & 0 \\ 0 & 0 & 1 \end{array} \right). \quad (\text{A.7})$$

In general, one can find an $\text{OSp}(1|2)$ matrix taking two given points $|\mathbf{u}\rangle = (u_1, u_2|\theta)^t$ and $|\mathbf{v}\rangle = (v_1, v_2|\phi)^t$ to $|\mathbf{0}\rangle \equiv (0, 1|0)^t$ and $|\infty\rangle \equiv (1, 0|0)^t \sim \mathbf{I}|\mathbf{0}\rangle$ respectively; one such matrix is

$$\Gamma_{\mathbf{uv}} = \frac{1}{\sqrt{\langle \mathbf{v}|\mathbf{u}\rangle}} \left(\begin{array}{cc|c} u_2 & -u_1 & \theta \\ v_2 & -v_1 & \phi \\ \frac{u_2\phi - v_2\theta}{\sqrt{\langle \mathbf{v}|\mathbf{u}\rangle}} & \frac{v_1\theta - u_1\phi}{\sqrt{\langle \mathbf{v}|\mathbf{u}\rangle}} & \sqrt{\langle \mathbf{v}|\mathbf{u}\rangle} - \frac{\theta\phi}{\sqrt{\langle \mathbf{v}|\mathbf{u}\rangle}} \end{array} \right). \quad (\text{A.8})$$

We can further stipulate that a point $|\mathbf{w}\rangle = (w_1, w_2|\omega)^t$ be mapped to a point equivalent to $(1, 1|\Theta_{\mathbf{uvw}})^t$, where now there is no freedom in choosing the fermionic co-ordinate, which is therefore a super-projective invariant built out of the triple $\{|\mathbf{u}\rangle, |\mathbf{v}\rangle, |\mathbf{w}\rangle\}$. The image of $|\mathbf{w}\rangle$ under $\Gamma_{\mathbf{uv}}$ is then

$$\Gamma_{\mathbf{uv}}|\mathbf{w}\rangle = \frac{1}{\sqrt{\langle \mathbf{v}|\mathbf{u}\rangle}} \left(\langle \mathbf{u}|\mathbf{w}\rangle, \langle \mathbf{v}|\mathbf{w}\rangle \left| \frac{\theta\langle \mathbf{w}|\mathbf{v}\rangle + \phi\langle \mathbf{u}|\mathbf{w}\rangle + \omega\langle \mathbf{v}|\mathbf{u}\rangle + \omega\theta\phi}{\sqrt{\langle \mathbf{v}|\mathbf{u}\rangle}} \right. \right)^t. \quad (\text{A.9})$$

A general dilatation of the superconformal coordinates corresponds to the $\text{OSp}(1|2)$ matrix⁸

$$\mathbf{P}(\varepsilon) = \left(\begin{array}{cc|c} \varepsilon & 0 & 0 \\ 0 & \varepsilon^{-1} & 0 \\ 0 & 0 & 1 \end{array} \right), \quad (\text{A.10})$$

which has $|\mathbf{0}\rangle$ and $|\infty\rangle$ as fixed points. Note that for $|\varepsilon| < 1$, $|\mathbf{0}\rangle$ is an attractive fixed point and $|\infty\rangle$ is a repulsive fixed point.

We may use such a dilatation to scale the bosonic coordinates of $\Gamma_{\mathbf{uv}}|\mathbf{w}\rangle$ as desired, obtaining for example

$$\mathbf{P} \left(\frac{\sqrt{\langle \mathbf{v}|\mathbf{w}\rangle}}{\sqrt{\langle \mathbf{u}|\mathbf{w}\rangle}} \right) \Gamma_{\mathbf{uv}}|\mathbf{w}\rangle \sim \left(1, 1 \left| \frac{\theta\langle \mathbf{v}|\mathbf{w}\rangle + \omega\langle \mathbf{u}|\mathbf{v}\rangle + \phi\langle \mathbf{w}|\mathbf{u}\rangle + \theta\omega\phi}{\sqrt{\langle \mathbf{u}|\mathbf{v}\rangle\langle \mathbf{w}|\mathbf{u}\rangle\langle \mathbf{v}|\mathbf{w}\rangle}} \right. \right)^t, \quad (\text{A.11})$$

which gives us an explicit expression for the odd super-projective invariant $\Theta_{\mathbf{z}_1\mathbf{z}_2\mathbf{z}_3}$, as

$$\Theta_{\mathbf{z}_1\mathbf{z}_2\mathbf{z}_3} = \frac{\zeta_1\langle \mathbf{z}_3|\mathbf{z}_2\rangle + \zeta_2\langle \mathbf{z}_1|\mathbf{z}_3\rangle + \zeta_3\langle \mathbf{z}_2|\mathbf{z}_1\rangle + \zeta_1\zeta_2\zeta_3}{\sqrt{\langle \mathbf{z}_2|\mathbf{z}_1\rangle\langle \mathbf{z}_3|\mathbf{z}_2\rangle\langle \mathbf{z}_1|\mathbf{z}_3\rangle}}, \quad (\text{A.12})$$

where $\mathbf{z}_i = (z_i|\zeta_i)$, as in eq. (3.4) of [64] and eq. (3.222) of [20].

⁸Note that the same symbol \mathbf{P} was used in eq. (4.10) of ref. [11] for a square root of this definition.

As with projective transformations, super-projective transformations preserve cross-ratios of the form

$$(\mathbf{z}_1, \mathbf{z}_2, \mathbf{z}_3, \mathbf{z}_4) \equiv \frac{\langle \mathbf{z}_1 | \mathbf{z}_2 \rangle \langle \mathbf{z}_3 | \mathbf{z}_4 \rangle}{\langle \mathbf{z}_1 | \mathbf{z}_4 \rangle \langle \mathbf{z}_3 | \mathbf{z}_2 \rangle} = \frac{(\mathbf{z}_1 - \mathbf{z}_2)(\mathbf{z}_3 - \mathbf{z}_4)}{(\mathbf{z}_1 - \mathbf{z}_4)(\mathbf{z}_3 - \mathbf{z}_2)}; \quad (\text{A.13})$$

one must keep in mind, however, that the simple relations between the three possible cross ratios that can be constructed with four points are modified by nilpotent terms. For example, one finds that

$$(\mathbf{z}_1, \mathbf{z}_2, \mathbf{z}_3, \mathbf{z}_4) + (\mathbf{z}_1, \mathbf{z}_3, \mathbf{z}_2, \mathbf{z}_4) - (\mathbf{z}_1, \mathbf{z}_3, \mathbf{z}_2, \mathbf{z}_4)^{1/2} \Theta_{\mathbf{z}_1 \mathbf{z}_3 \mathbf{z}_2} \Theta_{\mathbf{z}_1 \mathbf{z}_4 \mathbf{z}_2} = 1, \quad (\text{A.14})$$

which can be checked quickly by noting that the left-hand side is $\text{OSp}(1|2)$ -invariant, so that one can fix 3|2 parameters, for example by choosing $|\mathbf{z}_1\rangle = |\mathbf{0}\rangle$, $|\mathbf{z}_2\rangle = |\infty\rangle$, and $|\mathbf{z}_4\rangle = (1, 1|\phi)^t$.

With these ingredients, it is now easy to construct a super-projective transformation with chosen fixed points and multiplier: using $\Gamma_{\mathbf{uv}}$ to map a pair of points $|\mathbf{u}\rangle$ and $|\mathbf{v}\rangle$ to $|\mathbf{0}\rangle$ and $|\infty\rangle$ respectively, one easily verifies that the transformation

$$\mathbf{S} = \Gamma_{\mathbf{uv}}^{-1} \mathbf{P}(-e^{i\pi\varsigma} k^{1/2}) \Gamma_{\mathbf{uv}} \quad (\text{A.15})$$

has $|\mathbf{u}\rangle$ as an attractive fixed point and $|\mathbf{v}\rangle$ as a repulsive fixed point. Here k , for which we take $|k| < 1$, is called the multiplier⁹ of the super-projective transformation \mathbf{S} .

The bracket notation has the benefit of allowing us to write \mathbf{S} as

$$\mathbf{S} = \mathbb{1} + \frac{1}{\langle \mathbf{v} | \mathbf{u} \rangle} \left[(1 + e^{i\pi\varsigma} k^{\frac{1}{2}}) |\mathbf{v}\rangle \langle \mathbf{u}| - (1 + e^{-i\pi\varsigma} k^{-\frac{1}{2}}) |\mathbf{u}\rangle \langle \mathbf{v}| \right], \quad (\text{A.16})$$

which satisfies

$$\frac{\langle \mathbf{S}(\mathbf{z}) | \mathbf{u} \rangle}{\langle \mathbf{S}(\mathbf{z}) | \mathbf{v} \rangle} = k \frac{\langle \mathbf{z} | \mathbf{u} \rangle}{\langle \mathbf{z} | \mathbf{v} \rangle}. \quad (\text{A.17})$$

A.2 The super Schottky group

Taking the quotient of $\mathbf{CP}^{1|1}$ by the action of \mathbf{S} , defined in eq. (A.16), is equivalent to the insertion of a pair of NS punctures at $|\mathbf{u}\rangle$ and $|\mathbf{v}\rangle$, which are then sewn with a sewing parameter related to k . To see this, recall that sewing of NS punctures at P_1 and P_2 is defined by taking two sets of superconformal coordinates, say $(x|\theta)$ and $(y|\psi)$, which vanish respectively at the two points, $(x|\theta)(P_1) = (0|0) = (y|\psi)(P_2)$, and then imposing the conditions [9]

$$xy = -\varepsilon^2, \quad y\theta = \varepsilon\psi, \quad x\psi = -\varepsilon\theta, \quad \theta\psi = 0. \quad (\text{A.18})$$

Now, let $|\mathbf{x}\rangle$ and $|\mathbf{y}\rangle$ be homogeneous coordinates satisfying $\mathfrak{f}|\mathbf{x}\rangle = (x|\theta)$ and $\mathfrak{f}|\mathbf{y}\rangle = (y|\psi)$, where \mathfrak{f} is the map defined in eq. (A.5). If we make the identification

$$|\mathbf{x}\rangle \sim (\mathbf{P}(\varepsilon) \circ \mathbf{I}) |\mathbf{y}\rangle, \quad (\text{A.19})$$

⁹The sign $e^{i\pi\varsigma}$ is related to the spin structure: see the discussion between eq. (3.7) and eq. (3.8) for the conventions.

where \mathbf{P} and \mathbf{I} are defined in eq. (A.10) and eq. (A.7), respectively. Then, by acting on both sides with \mathfrak{f} , we get $(x|\theta) \sim (-\varepsilon^2/y | \varepsilon\psi/y)$, which can easily be found to satisfy eq. (A.18).

Let us take $(z|\zeta)$ to be a superconformal coordinate on $\mathbf{CP}^{1|1}$, with $(z|\zeta)(P_1) = \mathfrak{f}|\mathbf{u}\rangle$ and $(z|\zeta)(P_2) = \mathfrak{f}|\mathbf{v}\rangle$. Recall that the super-projective transformation $\Gamma_{\mathbf{uv}}$ defined in eq. (A.8) simultaneously maps $|\mathbf{u}\rangle$ and $|\mathbf{v}\rangle$ to $|\mathbf{0}\rangle$ and $|\infty\rangle$, respectively. Then if $|\mathbf{x}\rangle = \Gamma_{\mathbf{uv}} \circ \mathfrak{f}^{-1} \circ (z|\zeta)$ and $|\mathbf{y}\rangle = \mathbf{I}^{-1} \circ \Gamma_{\mathbf{uv}} \circ \mathfrak{f}^{-1} \circ (z|\zeta)$, we have that $(x|\theta) = \mathfrak{f}|\mathbf{x}\rangle$ and $(y|\psi) = \mathfrak{f}|\mathbf{y}\rangle$ are local superconformal coordinates which vanish at P_1 and P_2 respectively, since $\mathbf{I}^{-1}|\infty\rangle = |\mathbf{0}\rangle$ and $\mathfrak{f}|\mathbf{0}\rangle = (0|0)$. As a consequence, we can perform a NS sewing by making the identification in eq. (A.19) using these expressions for $|\mathbf{x}\rangle$ and $|\mathbf{y}\rangle$, and we find that we need to impose an equivalence relation on $(z|\zeta)$: we have $\Gamma_{\mathbf{uv}} \circ \mathfrak{f}^{-1} \circ (z|\zeta) \sim \mathbf{P}(\varepsilon) \circ \mathbf{I} \circ \mathbf{I}^{-1} \circ \Gamma_{\mathbf{uv}} \circ \mathfrak{f}^{-1} \circ (z|\zeta)$, or to put it differently,

$$(z|\zeta) \sim \mathfrak{f} \mathbf{S} \mathfrak{f}^{-1} (z|\zeta), \quad \mathbf{S} \equiv \Gamma_{\mathbf{uv}}^{-1} \circ \mathbf{P}(\varepsilon) \circ \Gamma_{\mathbf{uv}}. \tag{A.20}$$

This is what we wanted to show, with \mathbf{S} matching the definition in eq. (A.16), as long as we identify $\varepsilon = -e^{i\pi\varsigma} k^{1/2}$, so the NS sewing parameter is directly related to the Schottky group multiplier. Topologically, this sewing has the same effect (at least on the reduced space \mathbf{CP}^1) as cutting out discs around \mathbf{u} and \mathbf{v} and identifying their boundaries, so this quotient adds a handle to the surface, increasing the genus by one.

To build a genus- h SRS, we may repeat this sewing procedure h times, choosing h pairs of attractive and repulsive fixed points $\mathbf{u}_i = (u_i|\theta_i)$, $\mathbf{v}_i = (v_i|\phi_i)$, and h multipliers k_i , for $i = 1, \dots, h$. The super-Schottky group $\overline{\mathcal{S}}_h$ is the group freely generated by

$$\mathbf{S}_i = \Gamma_{\mathbf{u}_i\mathbf{v}_i}^{-1} \mathbf{P}(-e^{i\pi\varsigma_i} k_i^{1/2}) \Gamma_{\mathbf{u}_i\mathbf{v}_i}, \quad i = 1, \dots, h. \tag{A.21}$$

We then subtract the limit set Λ (the set of accumulation points of the orbits of $\overline{\mathcal{S}}_h$) from $\mathbf{CP}^{1|1}$, and we quotient by the action of the super Schottky group. This leads to the definition

$$\Sigma_h = (\mathbf{CP}^{1|1} - \Lambda) / \overline{\mathcal{S}}_h. \tag{A.22}$$

Note that the fixed points must be sufficiently far from each other, and the multipliers sufficiently small, to allow for the existence of a fundamental domain with the topology of $\mathbf{CP}^{1|1}$ with $2h$ discs cut out. The fixed points \mathbf{u}_i , \mathbf{v}_i and the multipliers k_i are moduli for the surface, but for $h \geq 2$ we can use the $\text{OSp}(1|2)$ symmetry to fix $3|2$ of these: in our conventions, we take $|\mathbf{u}_1\rangle = |\mathbf{0}\rangle$, $|\mathbf{v}_1\rangle = |\infty\rangle$, $|\mathbf{v}_2\rangle = |1, 1|_{\Theta_{\mathbf{u}_1\mathbf{v}_2\mathbf{v}_1}}\rangle$, so the super-moduli space $\widehat{\mathfrak{M}}_h$ has complex dimension $3h - 3|2h - 2$.

To build multi-loop open superstring world-sheets in a similar way, we should start with the super-disc $\mathbf{D}^{1|1}$ which can be obtained by quotienting $\mathbf{CP}^{1|1}$ by the involution $(z|\theta) \mapsto (z^*|\theta)$, so that $\mathbf{RP}^{1|1}$ becomes the boundary of the disk. A super-projective map will be an automorphism of $\mathbf{D}^{1|1}$ if it preserves $\mathbf{RP}^{1|1}$, so we should build the super Schottky group from super-projective transformations whose fixed points \mathbf{u}_i , \mathbf{v}_i are in $\mathbf{R}^{1|1}$ and whose multipliers k_i are real. If we quotient $\mathbf{D}^{1|1} - \Lambda$ by h of these, then we will get a SRS with $(h + 1)$ borders and no handles. The moduli space $\widehat{\mathfrak{M}}_h^{\text{open}}$ of such SRSs has real dimension $3h - 3|2h - 2$. In the case of $h = 2$ surfaces, we use the $\text{OSp}(1|2)$ symmetry to write the fixed points as in eq. (3.16).

A.2.1 Multipliers

Every element \mathbf{S}_α of a super Schottky group is similar to a matrix of the form

$$\mathbf{P}\left(-e^{i\pi\vec{\zeta}\cdot\vec{N}_\alpha} k_\alpha^{1/2}\right), \tag{A.23}$$

as in eq. (A.10), for some $k_\alpha^{1/2}$. We can find $k_\alpha^{1/2}$ by setting the spin structure around the b -cycles to zero, $\vec{\zeta} = \vec{0}$, then using the cyclic property of the supertrace.¹⁰ This leads to a quadratic equation, with roots

$$k_\alpha^{1/2} = -\frac{1 + \text{sTr}(\mathbf{S}_\alpha) \pm \sqrt{(\text{sTr}(\mathbf{S}_\alpha) + 1)^2 - 4}}{2}, \tag{A.24}$$

one root being the inverse of the other. We then pick $k_\alpha^{1/2}$ to be the root whose absolute value satisfies $|k_\alpha^{1/2}| < 1$. With this choice, we can expand the $k_\alpha^{1/2}$ in powers of $k_i^{1/2}$: for $h = 2$, using the fixed points in eq. (3.16), we find

$$\begin{aligned} k^{1/2}(\mathbf{S}_1\mathbf{S}_2) &= -y k_1^{1/2} k_2^{1/2} + \mathcal{O}(k_i) = -(\mathbf{u}_1, \mathbf{v}_1, \mathbf{u}_2, \mathbf{v}_2) k_1^{1/2} k_2^{1/2} + \mathcal{O}(k_i) \\ k^{1/2}(\mathbf{S}_1^{-1}\mathbf{S}_2) &= \frac{y}{u} k_1^{1/2} k_2^{1/2} + \mathcal{O}(k_i) = -(\mathbf{v}_1, \mathbf{u}_1, \mathbf{u}_2, \mathbf{v}_2) k_1^{1/2} k_2^{1/2} + \mathcal{O}(k_i), \end{aligned} \tag{A.25}$$

where y was defined in eq. (3.19). Note that $k^{1/2}(\mathbf{S}_1^{-1}\mathbf{S}_2)$ can be obtained from $k^{1/2}(\mathbf{S}_1\mathbf{S}_2)$ by swapping the attractive and repulsive fixed points of \mathbf{S}_1 in the cross-ratio, as might be expected.

A.2.2 The super period matrix

The super abelian differentials are an h -dimensional space of holomorphic volume forms, i.e. sections of the Berezinian bundle, defined on a genus- h SRS. They are spanned by Ω_i , $i = 1, \dots, h$, which can be normalized by their integrals around the a -cycles, according to

$$\frac{1}{2\pi i} \oint_{a_i} \Omega_j = \delta_{ij}, \tag{A.26}$$

while their integrals around the b -cycles define the *super period matrix*

$$\frac{1}{2\pi i} \oint_{b_i} \Omega_j \equiv \tau_{ij}. \tag{A.27}$$

Here a_i and b_i are closed cycles on the SRS which are projected to the usual homology cycles on the reduced space. The Ω_i 's can be expressed in terms of the super Schottky parametrization as in eq. (21) of ref. [30]. In our current notation

$$\begin{aligned} \Omega_i(z|\psi) &= dz \sum_\alpha^{(i)} D_\psi \log \frac{\langle \mathbf{z} | \mathbf{T}_\alpha | \mathbf{u}_i \rangle}{\langle \mathbf{z} | \mathbf{T}_\alpha | \mathbf{v}_i \rangle} \\ &= dz \sum_\alpha^{(i)} \left[\frac{\langle \mathbf{z} | \Phi \mathbf{T}_\alpha | \mathbf{u}_i \rangle}{\langle \mathbf{z} | \mathbf{T}_\alpha | \mathbf{u}_i \rangle} - \frac{\langle \mathbf{z} | \Phi \mathbf{T}_\alpha | \mathbf{v}_i \rangle}{\langle \mathbf{z} | \mathbf{T}_\alpha | \mathbf{v}_i \rangle} \right], \end{aligned} \tag{A.28}$$

¹⁰Recall that the supertrace of a $\text{GL}(2|1)$ matrix $M = (M_i^j)$ is given by $\text{sTr}(M) = M_1^1 + M_2^2 - M_3^3$.

where $d\mathbf{z} = (dz | d\psi)$, the sum $\sum_{\alpha}^{(i)}$ is over all elements of the super-Schottky group which do not have $\mathbf{S}_i^{\pm 1}$ as their right-most factor, D_{ψ} is the superconformal derivative $D_{\psi} = \partial_{\psi} + \psi \partial_z$, and finally Φ is the matrix

$$\Phi = \begin{pmatrix} 0 & 0 & | & 1 \\ 0 & 0 & | & 0 \\ 0 & -1 & | & 0 \end{pmatrix}. \tag{A.29}$$

The matrix Φ has the property that, if $\mathfrak{f}|\mathbf{z}\rangle = (z|\psi)$, then

$$D_{\psi}\langle\mathbf{z}| = \langle\mathbf{z}|\Phi, \tag{A.30}$$

and furthermore for $|\mathbf{w}\rangle = (w, 1|\omega)^t$ and $|\mathbf{z}\rangle = (z, 1|\psi)^t$ the map $(z|\psi) \mapsto (\langle\mathbf{w}|\mathbf{z}\rangle|\langle\mathbf{w}|\Phi|\mathbf{z}\rangle)$ is superconformal. The super period matrix can be computed as

$$\tau_{ij} = \frac{1}{2\pi i} \left[\delta_{ij} \log k_i - {}^{(j)}\sum_{\alpha}^{(i)} \log \frac{\langle\mathbf{u}_j|\mathbf{T}_{\alpha}|\mathbf{v}_i\rangle\langle\mathbf{v}_j|\mathbf{T}_{\alpha}|\mathbf{u}_i\rangle}{\langle\mathbf{u}_j|\mathbf{T}_{\alpha}|\mathbf{u}_i\rangle\langle\mathbf{v}_j|\mathbf{T}_{\alpha}|\mathbf{v}_i\rangle} \right]. \tag{A.31}$$

The sum is over all elements of the super Schottky group which do not have $\mathbf{S}_j^{\pm 1}$ as their left-most element or $\mathbf{S}_i^{\pm 1}$ as their right-most element. It is not difficult to compute the leading terms of the super period matrix in the small- k_i expansion. For $h = 2$, using the fixed points in eq. (3.16), we find

$$2\pi i \boldsymbol{\tau} = \begin{pmatrix} \log k_1 - 2\theta\phi \frac{y}{u} e^{i\pi\varsigma_2} k_2^{1/2} & \log u \\ \log u & \log k_2 - 2\theta\phi \frac{y}{u} e^{i\pi\varsigma_1} k_1^{1/2} \end{pmatrix} + \mathcal{O}(k_i) \tag{A.32}$$

so that

$$4\pi^2 \det(\text{Im } \boldsymbol{\tau}) = \log(k_1) \log(k_2) - \log(u)^2 - 2\theta\phi \frac{y}{u} (e^{i\pi\varsigma_2} k_2^{1/2} \log k_1 + e^{i\pi\varsigma_1} k_1^{1/2} \log k_2) + \mathcal{O}(k_i). \tag{A.33}$$

This completes our review of the super Schottky parametrization. Our next task is to introduce twisted boundary conditions corresponding to external background gauge fields.

B Twisted determinants

B.1 The twisted determinant on a Riemann surface

The world-sheet theory of strings becomes ‘twisted’ in a number of contexts: for example, on orbifolds [76], in electromagnetic fields [13, 14, 77] or when an open string is stretched between a pair of D-branes which have a velocity [78] or are at an angle [79] with respect to each other. If we appropriately pair up the string space-time coordinate fields X^{μ} as complex coordinates (for example, in our case, by setting $Z^{\pm} = (X^1 \pm iX^2)/\sqrt{2}$), then, in these backgrounds, the world-sheet fields ∂Z^{\pm} are described by non-integer mode expansions on the upper-half plane, as in eq. (2.5). This means that, on the double of the world-sheet,¹¹ $\partial Z^{\pm}(z, \bar{z})$ is no longer a single-valued field but rather has a monodromy, changing by a factor of $e^{\pm 2\pi i \epsilon}$ as it is transported counter-clockwise around $z = 0$.

¹¹The double of the upper-half plane is the complex plane, see figure 7.

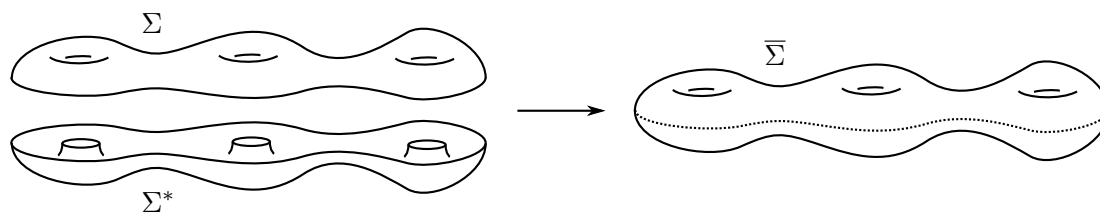


Figure 7. Recall that the double of a Riemann surface Σ is defined by taking two copies of Σ , replacing the charts on one copy with their complex conjugates, and identifying corresponding points on the boundaries of the two copies [24].

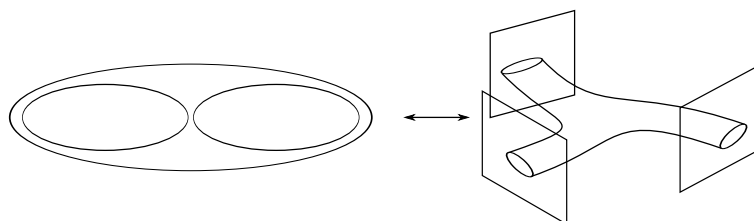


Figure 8. The same string diagram can be computed as an open string vacuum multi-loop diagram, or, in a T-dual setup, as a tree-level interaction between closed strings emitted from D-branes at angles.

Computing multi-loop amplitudes in these backgrounds is complicated, because it is not easy to use the sewing procedure when states propagating along plumbing fixture belong to a twisted sector. We must use, instead, the approach of [67]. This takes advantage of the fact that, although the ∂Z^\pm fields have non-trivial monodromies along the a -cycles of the double world-sheet, the monodromies along the b -cycles are trivial. Therefore, the idea is to build the double world-sheet by sewing along the b cycles, and then to perform the modular transformation swapping the a and b cycles with each other, in order to obtain the partition function expressed in terms of the Schottky moduli which are appropriate for the world-sheet degeneration we are interested in.

From a more physical point of view, we are using the fact that, in a different region of moduli space, the string diagram can be described as a tree-level interaction between three closed strings being emitted or absorbed by the D-branes (see figure 8). In terms of closed string moduli, the string partition function is given by [67]

$$Z(F_i) = \left[\prod_{i=0}^h \sqrt{\det(1 - G^{-1} \mathcal{F}_i)} \right] \int [dZ]_h^{\text{cl}} \mathcal{R}_h(q_i, \vec{\epsilon}). \tag{B.1}$$

The pre-factor is just the Born-Infeld lagrangian for the background fields on the D-branes, divided by \sqrt{G} because all of the background-field independent factors are included in the measure $[dZ]_h^{\text{cl}}$.

The factor $\mathcal{R}_h(q_i, \vec{\epsilon})$, which is dependent on both the world-sheet moduli and the background field strengths, has a simple form, so long as it is expressed in terms of the closed string Schottky moduli; in particular, these include the multipliers of a Schottky group whose $2h$ Schottky circles are homotopic to the b cycles of the world-sheet, instead of the a cycles which we have been using so far. Denoting the multiplier of element T_α of

this Schottky group as q_α , we have

$$\mathcal{R}_h(q_i, \vec{\epsilon}) = \frac{\prod'_\alpha \prod_{n=1}^\infty (1 - q_\alpha^n)^2}{\prod'_\alpha \prod_{n=1}^\infty (1 - e^{-2\pi i \vec{N}_\alpha \cdot \vec{\epsilon}} q_\alpha^n) (1 - e^{2\pi i \vec{N}_\alpha \cdot \vec{\epsilon}} q_\alpha^n)}, \quad (\text{B.2})$$

where the notation \prod'_α was defined after eq. (3.7).

The modular transformation that swaps the a and b cycles, necessary to switch between the open string and the closed string channels, acts non-analytically on the Schottky group multipliers.¹² We need to rewrite eq. (B.2) in terms of the open string moduli, so the following strategy is used: $\mathcal{R}_h(q_i, \vec{\epsilon})$ is re-expressed in terms of functions which transform in simple ways under modular transformations, the modular transformations are carried out, and finally the results are re-expressed in terms of the open string Schottky moduli, allowing us to investigate the field theory limit. This analysis was performed in [33, 35] and the results are summarized in section 2 of [15]. Assuming without loss of generality that $\epsilon_h \neq 0$, the result is that

$$\mathcal{R}_h(q_\alpha, \vec{\epsilon}) = \mathcal{R}_h(k_\alpha, \vec{\epsilon} \cdot \tau) e^{-i\pi \vec{\epsilon} \cdot \tau \cdot \vec{\epsilon}} \frac{\det(\text{Im } \tau)}{\det(\text{Im } \tau_\vec{\epsilon})}, \quad (\text{B.3})$$

where τ is the period matrix computed in the open string channel, while $\tau_\vec{\epsilon}$ is the *twisted period matrix*, defined by eq. (3.24) of [67] as

$$(\tau_\vec{\epsilon})_{ji} = \begin{cases} \frac{1}{2\pi i} \int_w^{S_j(w)} \Omega_i^{\vec{\epsilon}, \tau}(z) e^{\frac{2\pi i}{h-1} \vec{\epsilon} \cdot \vec{\Delta}(z)} & j \neq h \neq i \\ \frac{\mathcal{S}_h^{\vec{\epsilon}, \tau} - 1}{\mathcal{S}_h^{\vec{\epsilon}} - 1} & j = i = h, \\ 0 & \text{otherwise,} \end{cases} \quad (\text{B.4})$$

where

$$\mathcal{S}_i^{\vec{\epsilon}} \equiv e^{2\pi i \epsilon_i}. \quad (\text{B.5})$$

The Prym differentials $\Omega_i^{\vec{\epsilon}}$ appearing in the integrand in the first line of eq. (B.4) are $(h-1)$ one-forms with trivial monodromies along the a cycles and twists along the b cycles. More precisely, they obey

$$\Omega_i^{\vec{\epsilon}}(S_j(z)) = \mathcal{S}_j^{\vec{\epsilon}} \Omega_i^{\vec{\epsilon}}(z), \quad (\text{B.6})$$

and they are regular everywhere. Assuming again that $\epsilon_h \neq 0$, they can be expressed as in eq. (3.11) of [67],

$$\Omega_j^{\vec{\epsilon}}(z) = \zeta_j^{\vec{\epsilon}}(z) - \frac{1 - \mathcal{S}_j^{\vec{\epsilon}}}{1 - \mathcal{S}_h^{\vec{\epsilon}}} \zeta_h^{\vec{\epsilon}}(z) \quad j = 1, \dots, h-1. \quad (\text{B.7})$$

In eq. (B.7), the $\zeta_i^{\vec{\epsilon}}$ are a basis of one-forms which are holomorphic everywhere, except at some arbitrarily chosen base point z_0 . They can be computed in the Schottky parametriza-

¹²This is easy to see in the $h = 1$ case, where the open string multiplier k is related to the annulus period τ via $k = e^{2\pi i \tau}$, and similarly the multiplier in the closed string channel, q , is related to the torus period τ^{cl} via $q = e^{2\pi i \tau^{\text{cl}}}$. The two periods, in turn, are related by $\tau^{\text{cl}} = -1/\tau$, so that $(\log q)(\log k) = 4\pi^2$.

tion as in eq. (3.15) of [67],

$$\zeta_i^{\vec{\epsilon}}(z) = \left[\mathcal{S}_i^{\vec{\epsilon}} \sum_{\alpha}^{(i)} e^{2\pi i \vec{\epsilon} \cdot \vec{N}_{\alpha}} \left(\frac{1}{z - T_{\alpha}(\eta_i)} - \frac{1}{z - T_{\alpha}(\xi_i)} \right) + (1 - \mathcal{S}_i^{\vec{\epsilon}}) \sum_{\alpha} e^{2\pi i \vec{\epsilon} \cdot \vec{N}_{\alpha}} \left(\frac{1}{z - T_{\alpha}(z_0)} - \frac{1}{z - T_{\alpha}(a_i^{\alpha})} \right) \right] dz, \tag{B.8}$$

where the first sum is over all Schottky group elements which do not have S_i as their right-most factor, and the second sum is over all Schottky group elements. η_i and ξ_i are the attractive and repulsive fixed points of the generator S_i , respectively; note that the dependence on z_0 cancels out when the $\zeta_i^{\vec{\epsilon}}$ are combined as in eq. (B.7); furthermore, we defined

$$a_i^{\alpha} = \begin{cases} \eta_i & \text{if } T_{\alpha} = T_{\beta} S_i^{\ell} \quad \text{with } \ell \geq 1 \\ \xi_i & \text{otherwise.} \end{cases} \tag{B.9}$$

The other object appearing in the integrand in the first line of eq. (B.4) is the vector of Riemann constants, or Riemann class; it can be expressed in the Schottky parametrization as in eq. (A.21) of [31],

$$\Delta_i(z) = \frac{1}{2\pi i} \left[-\frac{1}{2} \log k_i + i\pi + \sum_{j=1}^h {}^{(j)}\sum_{\alpha}^{(i)} \log \frac{\xi_j - T_{\alpha}(\eta_i)}{\xi_j - T_{\alpha}(\xi_i)} \frac{z - T_{\alpha}(\xi_i)}{z - T_{\alpha}(\eta_i)} \right], \tag{B.10}$$

where the second sum, ${}^{(j)}\sum_{\alpha}^{(i)}$, is over all elements of the Schottky group which have neither $S_j^{\pm 1}$ as their left-most factor nor $S_i^{\pm 1}$ as their right-most factor. Owing to the transformation properties of $\Delta_i(z)$, one finds that

$$\Delta_i(z) = \Delta_i(z_0) - \frac{h-1}{2\pi i} \int_{z_0}^z \omega_i, \tag{B.11}$$

where ω_i are the abelian differentials, defined for example in eq. (A.10) of [31]. It is easy to check that the integrand of the first line of eq. (B.4) has twists along the a cycles and trivial monodromies along the b cycles, so that it does not depend on the choice of the integration limit w .

For simplicity, from now on we focus only on the case $h = 2$, which yields

$$\det[\text{Im } \tau_{\vec{\epsilon}}] = \frac{1}{2\pi i} \frac{\mathcal{S}_2^{\vec{\epsilon}\tau} - 1}{\mathcal{S}_2^{\vec{\epsilon}} - 1} \int_w^{S_1(w)} \Omega^{\vec{\epsilon}\tau}(z) e^{2\pi i \vec{\epsilon} \cdot \vec{\Delta}(z)}, \tag{B.12}$$

where $\Omega^{\vec{\epsilon}}$ is the sole component of the Prym form for $h = 2$. Instead of explicitly evaluating the integral over z in eq. (B.12), it is possible to find an alternative expression for $\det(\text{Im } \tau_{\vec{\epsilon}})$ in the following way. We begin by constructing a set of matrices $\mathbf{D}_{ij}(\vec{\epsilon})$, defined in eq. (3.14) of [67] as integrals of Prym differentials. For each $i, j = 1, \dots, h-1$, $\mathbf{D}_{ij}(\vec{\epsilon})$ is a space-time rotation matrix, while the i, j indices refer to world-sheet homology cycles. Using the complex space-time coordinates in which the background fields are diagonal, the matrix $\mathbf{D}_{ij}(\vec{\epsilon})$ is also diagonal, with two non-trivial entries $D_{ij}(\pm\vec{\epsilon})$. In particular, for $h = 2$, since

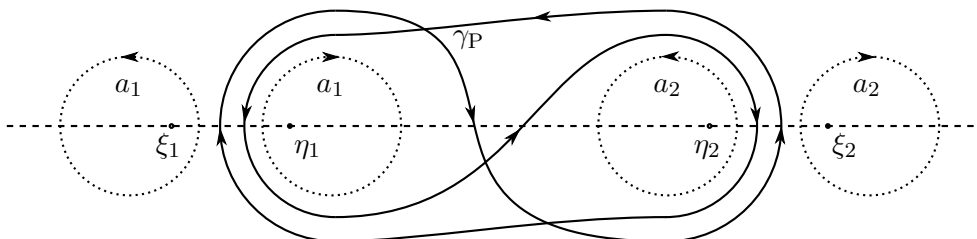


Figure 9. The Pochhammer contour $\gamma_P = a_2 a_1 a_2^{-1} a_1^{-1}$.

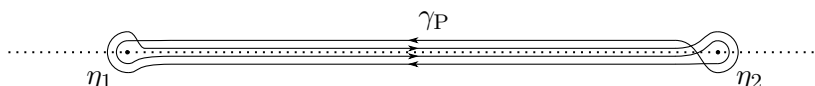


Figure 10. Our Pochhammer contour (figure 9) can be deformed arbitrarily close to four copies of the line interval $[\eta_1, \eta_2] \subseteq \mathbf{R}$, with each copy on a different branch of the Prym form $\tilde{\Omega}^{\vec{\epsilon}}$.

there is only one independent Prym differential, one also has only one independent matrix $D(\pm\vec{\epsilon})$. It is given by

$$D(\vec{\epsilon}) \equiv \frac{1}{2\pi i} \frac{(\mathcal{S}_1^{\vec{\epsilon}})^{-1}}{1 - \mathcal{S}_2^{\vec{\epsilon}}} \int_{\gamma_P} \tilde{\Omega}^{\vec{\epsilon}}, \quad (\text{B.13})$$

where $\gamma_P \equiv a_2 a_1 a_2^{-1} a_1^{-1}$ is the Pochhammer contour shown in figure 9, and $\tilde{\Omega}^{\vec{\epsilon}}$ is the Prym differential which has trivial monodromies around the b cycles and monodromies $\mathcal{S}_i^{\vec{\epsilon}}$ around the a cycles. $\tilde{\Omega}^{\vec{\epsilon}}$ can be expressed in the Schottky representation thanks to a relation derived in [67], given by eq. (3.28) of that reference. In the case $h = 2$, it becomes simply

$$\tilde{\Omega}^{\vec{\epsilon}}(z) = \frac{e^{2\pi i \vec{\epsilon} \cdot \vec{\Delta}(z)} \Omega^{\vec{\epsilon} \cdot \tau}(z)}{(\tau_{\vec{\epsilon}})_{11}} = \frac{1 - \mathcal{S}_2^{\vec{\epsilon} \cdot \tau} e^{2\pi i \vec{\epsilon} \cdot \vec{\Delta}(z)} \Omega^{\vec{\epsilon} \cdot \tau}(z)}{1 - \mathcal{S}_2^{\vec{\epsilon}} \det(\text{Im } \tau_{\vec{\epsilon}})} \quad (\text{B.14})$$

where the second equality is obtained by writing $(\tau_{\vec{\epsilon}})_{11}$ in terms of $\det(\text{Im } \tau_{\vec{\epsilon}})$, using eq. (B.4). Note that γ_P crosses each boundary of the worldsheet once in each direction, so it starts and ends on the same branch of $\tilde{\Omega}^{\vec{\epsilon}}$, and the integral in eq. (B.13) is well-defined.

Now we can use eq. (B.7), eq. (B.8) and eq. (B.10) to get an expression for $\tilde{\Omega}^{\vec{\epsilon}}(z)$, via eq. (B.14). To this end, we can expand $\tilde{\Omega}^{\vec{\epsilon}}(z)$ as a power series in k_i , and verify that, to first order, it has poles only at the Schottky fixed points. At this order, we are then free to deform the Pochhammer contour through the Schottky circles and arbitrarily close to the line interval $[\eta_1, \eta_2]$, as in figure 10. The integral can now be written as

$$\int_{\gamma_P} \tilde{\Omega}^{\vec{\epsilon}} = (1 - \mathcal{S}_1^{\vec{\epsilon}})(1 - \mathcal{S}_2^{\vec{\epsilon}}) \int_{\eta_1}^{\eta_2} \tilde{\Omega}^{\vec{\epsilon}} + \mathcal{O}(k_i^2). \quad (\text{B.15})$$

Inserting eq. (B.15) and eq. (B.14) into eq. (B.13), we now find a relation between the quantity $D(\vec{\epsilon})$ and $\det(\text{Im } \tau_{\vec{\epsilon}})$, as reported in eqs. (4.13)–(4.15) of [67],

$$D(\vec{\epsilon}) = -\frac{1}{2\pi i} \frac{1 - (\mathcal{S}_1^{\vec{\epsilon}})^{-1}}{1 - \mathcal{S}_2^{\vec{\epsilon}}} \frac{1 - \mathcal{S}_2^{\vec{\epsilon} \cdot \tau}}{\det(\text{Im } \tau_{\vec{\epsilon}})} \int_0^u e^{2\pi i \vec{\epsilon} \cdot \vec{\Delta}(z)} \Omega^{\vec{\epsilon} \cdot \tau}(z) + \mathcal{O}(k_i^2). \quad (\text{B.16})$$

Next, we can exploit the relationship between $D(\vec{\epsilon})$ and $D(-\vec{\epsilon})$ given by eq. (3.21) of [67]; for $h = 2$ it can be stated as¹³

$$D(\vec{\epsilon}) - D(-\vec{\epsilon}) = -2i \frac{\sin(\pi\epsilon_1) \sin(\pi\epsilon_1 + \pi\epsilon_2)}{\sin(\pi\epsilon_2)}. \quad (\text{B.17})$$

This simple expression for the antisymmetric part of the function D can be found [36] by cutting between the Schottky circles to get a simply-connected fundamental domain for $\bar{\Sigma}_h$, then using Stokes' theorem to integrate $\tilde{\Omega}^{\vec{\epsilon}} \wedge \tilde{\Omega}^{-\vec{\epsilon}}$, which vanishes since it is a $(2, 0)$ form. Inserting eq. (B.16) in eq. (B.17), we can finally use the fact that $\det(\text{Im } \tau_{\vec{\epsilon}})$ is even under the substitution $\vec{\epsilon} \mapsto -\vec{\epsilon}$, as follows from eq. (B.3). We can then solve for the determinant, to find

$$\det(\text{Im } \tau_{\vec{\epsilon}}) = \frac{1}{4\pi} \frac{e^{-i\pi(\epsilon_1+\epsilon_2)}(1-\mathcal{S}_2^{\vec{\epsilon}\tau})}{\sin(\pi(\epsilon_1+\epsilon_2))} \int_0^u e^{2\pi i \vec{\epsilon} \cdot \vec{\Delta}(z)} \Omega^{\vec{\epsilon}\tau}(z) + (\vec{\epsilon} \rightarrow -\vec{\epsilon}) + \mathcal{O}(k_i^2), \quad (\text{B.18})$$

which provides a simple route to the calculation of the twisted determinant to first order in the multipliers.

B.2 The twisted determinant on a super Riemann surface

We now turn to the supersymmetric generalization of eq. (B.18), which will be needed to compute the superstring partition function in our chosen background. As a starting point, we backtrack slightly, and write down an expression for the bosonic twisted determinant of the period matrix, which can be obtained by the same procedure leading to eq. (B.16), but without using eq. (B.15) to deform the integration cycle. We write

$$\det(\text{Im } \tau_{\vec{\epsilon}}) = \frac{1}{4\pi} \frac{e^{-i\pi(\epsilon_1+\epsilon_2)}(1-\mathcal{S}_2^{\vec{\epsilon}\tau})}{\sin(\pi(\epsilon_1+\epsilon_2))(1-\mathcal{S}_1^{\vec{\epsilon}})(1-\mathcal{S}_2^{\vec{\epsilon}})} \int_{\gamma_{\mathcal{P}}} e^{2\pi i \vec{\epsilon} \cdot \vec{\Delta}(z)} \Omega^{\vec{\epsilon}\tau}(z) + (\vec{\epsilon} \rightarrow -\vec{\epsilon}). \quad (\text{B.19})$$

To proceed, we must replace $\Delta_i(z)$ and $\Omega^{\vec{\epsilon}}$ with their supersymmetric counterparts, $\mathbf{\Delta}_i(\mathbf{z})$ and $\mathbf{\Omega}^{\vec{\epsilon}}$ respectively. Furthermore, we must replace the period matrix τ with the super-period matrix $\boldsymbol{\tau}$ in the phases $e^{2\pi i(\vec{\epsilon}\tau)_i}$, and we must carry out the integration over a Pochhammer contour $\gamma_{\mathcal{P}} = \mathbf{a}_2 \mathbf{a}_1 \mathbf{a}_2^{-1} \mathbf{a}_1^{-1}$ on the super Riemann surface. The result is the same as in eq. (B.19), where the individual ingredients have been supersymmetrized.

The integrand will now be locally of the form $d\mathbf{z} f(z|\psi)$. One can, as usual, carry out the $d\psi$ integral, simply by picking out the coefficient of ψ in the integrand. The integral is then reduced to an ordinary line integral over a Pochhammer contour $\gamma_{\mathcal{P}}$ in the reduced space of the SRS. As in section B.1, we are free at this point to expand the integrand as a power series in k_i , and deform $\gamma_{\mathcal{P}}$ as in eq. (B.15). This yields

$$\det(\text{Im } \boldsymbol{\tau}_{\vec{\epsilon}}) = \frac{1}{4\pi} \frac{e^{-i\pi(\epsilon_1+\epsilon_2)}(1-\mathcal{S}_2^{\vec{\epsilon}\boldsymbol{\tau}})}{\sin(\pi(\epsilon_1+\epsilon_2))} \int_0^u \partial_{\psi} [e^{2\pi i \vec{\epsilon} \cdot \vec{\Delta}(z|\psi)} \mathbf{\Omega}^{\vec{\epsilon}\boldsymbol{\tau}}(z|\psi)] + (\vec{\epsilon} \rightarrow -\vec{\epsilon}) + \mathcal{O}(k_i). \quad (\text{B.20})$$

¹³To get this from eq. (3.21) of [67], we have to put $\epsilon_h = -\epsilon_2$; the relative sign occurs because our a_2 and b_2 homology cycles have opposite orientation.

Now we need to define the objects appearing in eq. (B.20). The Prym differentials $\Omega_i^{\vec{\epsilon}}$ we used to compute $\det(\text{Im } \tau_{\vec{\epsilon}})$ are holomorphic one-forms; the natural analogues on SRSs are holomorphic volume forms: sections of the Berezinian bundle. Just as holomorphic differentials can be written locally as $dz \partial_z f(z)$, sections of the Berezinian bundle can be written locally as $d\mathbf{z} D_\psi f(z|\psi)$, which is a combination invariant under changes of superconformal coordinates [21]. More specifically, we can write eq. (B.8) for $\zeta_i^{\vec{\epsilon}}$ as

$$\zeta_i^{\vec{\epsilon}}(z) = dz \frac{\partial}{\partial z} \left\{ \mathcal{S}_i^{\vec{\epsilon}} \sum_{\alpha}^{(i)} e^{2\pi i \vec{\epsilon} \cdot \vec{N}_\alpha} \log \left[\frac{z - T_\alpha(\eta_i)}{z - T_\alpha(\xi_i)} \right] + (1 - \mathcal{S}_i^{\vec{\epsilon}}) \sum_{\alpha} e^{2\pi i \vec{\epsilon} \cdot \vec{N}_\alpha} \log \left[\frac{z - T_\alpha(z_0)}{z - T_\alpha(a_i^\alpha)} \right] \right\}. \quad (\text{B.21})$$

To find the corresponding volume forms, we replace the expressions inside the logarithms with their natural superconformal analogues, and replace $dz \partial_z \mapsto d\mathbf{z} D_\psi$. This yields

$$\begin{aligned} \zeta_i^{\vec{\epsilon}}(z|\psi) &= d\mathbf{z} D_\psi \left\{ \mathcal{S}_i^{\vec{\epsilon}} \sum_{\alpha}^{(i)} e^{2\pi i \vec{\epsilon} \cdot \vec{N}_\alpha} \log \left[\frac{\langle \mathbf{z} | \mathbf{T}_\alpha | \mathbf{u}_i \rangle}{\langle \mathbf{z} | \mathbf{T}_\alpha | \mathbf{v}_i \rangle} \right] \right. \\ &\quad \left. + (1 - \mathcal{S}_i^{\vec{\epsilon}}) \sum_{\alpha} e^{2\pi i \vec{\epsilon} \cdot \vec{N}_\alpha} \log \left[\frac{\langle \mathbf{z} | \mathbf{T}_\alpha | \mathbf{z}_0 \rangle}{\langle \mathbf{z} | \mathbf{T}_\alpha | \mathbf{a}_i \rangle} \right] \right\} \\ &= d\mathbf{z} \left\{ \mathcal{S}_i^{\vec{\epsilon}} \sum_{\alpha}^{(i)} e^{2\pi i \vec{\epsilon} \cdot \vec{N}_\alpha} \left[\frac{\langle \mathbf{z} | \Phi \mathbf{T}_\alpha | \mathbf{u}_i \rangle}{\langle \mathbf{z} | \mathbf{T}_\alpha | \mathbf{u}_i \rangle} - \frac{\langle \mathbf{z} | \Phi \mathbf{T}_\alpha | \mathbf{v}_i \rangle}{\langle \mathbf{z} | \mathbf{T}_\alpha | \mathbf{v}_i \rangle} \right] \right. \\ &\quad \left. + (1 - \mathcal{S}_i^{\vec{\epsilon}}) \sum_{\alpha} e^{2\pi i \vec{\epsilon} \cdot \vec{N}_\alpha} \left[\frac{\langle \mathbf{z} | \Phi \mathbf{T}_\alpha | \mathbf{z}_0 \rangle}{\langle \mathbf{z} | \mathbf{T}_\alpha | \mathbf{z}_0 \rangle} - \frac{\langle \mathbf{z} | \Phi \mathbf{T}_\alpha | \mathbf{a}_i \rangle}{\langle \mathbf{z} | \mathbf{T}_\alpha | \mathbf{a}_i \rangle} \right] \right\}, \end{aligned} \quad (\text{B.22})$$

where we used Φ defined in eq. (A.29), $|\mathbf{z}_0\rangle$ is an arbitrary base point, and

$$|\mathbf{a}_i^\alpha\rangle = \begin{cases} |\mathbf{u}_i\rangle & \text{if } \mathbf{T}_\alpha = \mathbf{T}_\beta \mathbf{S}_i^\ell \text{ with } \ell \geq 1, \\ |\mathbf{v}_i\rangle & \text{otherwise.} \end{cases} \quad (\text{B.23})$$

It is now possible to write down a basis of $(h-1)$ holomorphic volume forms $\Omega_j^{\vec{\epsilon}}(z)$, with the expected monodromies, using the analogue of eq. (B.7), and noting that the dependence on the base point $|\mathbf{z}_0\rangle$ cancels out. They are given by

$$\Omega_j^{\vec{\epsilon}}(z|\psi) = \zeta_j^{\vec{\epsilon}}(z|\psi) - \frac{1 - \mathcal{S}_j^{\vec{\epsilon}}}{1 - \mathcal{S}_h^{\vec{\epsilon}}} \zeta_h^{\vec{\epsilon}}(z|\psi), \quad j = 1, \dots, h-1. \quad (\text{B.24})$$

We can calculate $\Omega_j^{\vec{\epsilon}}(z|\psi)$ as a series expansion in powers of $k_i^{1/2}$; then, as usual, truncating to finite order, we only need to include finitely many terms in the sum in eq. (B.22). In particular, restricting ourselves to $h=2$, and since we only need terms of order $k_i^{1/2}$, the required super Schottky group elements are

$$\mathbf{T}_\alpha \in \{\text{Id}, \mathbf{S}_1^{\pm 1}, \mathbf{S}_2^{\pm 1}, (\mathbf{S}_1 \mathbf{S}_2)^{\pm 1}, (\mathbf{S}_1^{-1} \mathbf{S}_2)^{\pm 1}, (\mathbf{S}_1 \mathbf{S}_2^{-1})^{\pm 1}, (\mathbf{S}_2 \mathbf{S}_1)^{\pm 1}\}. \quad (\text{B.25})$$

Using the fixed points given in eq. (3.16), we can compute $\Omega^{\vec{e}}(\mathbf{z}) \equiv \Omega_1^{\vec{e}}(\mathbf{z})$ to the required accuracy, obtaining

$$\begin{aligned}
 \Omega^{\vec{e}}(z|\psi) = dz \left\{ & -\frac{(1-\mathcal{S}_1^{\vec{e}})\mathcal{S}_2^{\vec{e}}\theta}{(1-\mathcal{S}_2^{\vec{e}})(u-z)} + \frac{(1-\mathcal{S}_1^{\vec{e}})\phi}{(1-\mathcal{S}_2^{\vec{e}})(1-z)} \right. \\
 & + \frac{[\mathcal{S}_1^{\vec{e}}(1-\mathcal{S}_2^{\vec{e}})u - (\mathcal{S}_1^{\vec{e}}-\mathcal{S}_2^{\vec{e}}-\mathcal{S}_1^{\vec{e}}\mathcal{S}_2^{\vec{e}}u+u)z + z^2(1-\mathcal{S}_2^{\vec{e}})]\psi}{(1-\mathcal{S}_2^{\vec{e}})(u-z)z(1-z)} \\
 & + e^{i\pi\varsigma_1} k_1^{1/2} \left[-\frac{(1-\mathcal{S}_1^{\vec{e}})\mathcal{S}_1^{\vec{e}}(\mathcal{S}_2^{\vec{e}}\theta-\phi)}{(1-\mathcal{S}_2^{\vec{e}})z} + \frac{(1-\mathcal{S}_1^{\vec{e}})(\mathcal{S}_2^{\vec{e}}\theta-u\phi)}{\mathcal{S}_1^{\vec{e}}(1-\mathcal{S}_2^{\vec{e}})u} \right] \\
 & + e^{i\pi\varsigma_2} k_2^{1/2} \left[-\frac{\mathcal{S}_2^{\vec{e}}(1-\mathcal{S}_1^{\vec{e}})\theta}{u-z} + \frac{\mathcal{S}_2^{\vec{e}}(1-\mathcal{S}_1^{\vec{e}}u)\phi}{u-z} - \frac{(\mathcal{S}_1^{\vec{e}}-u)\theta}{\mathcal{S}_2^{\vec{e}}u(1-z)} \right. \\
 & \quad \left. - \frac{\mathcal{S}_2^{\vec{e}}(1-\mathcal{S}_1^{\vec{e}}u)\theta\phi\psi}{(u-z)^2} - \frac{(\mathcal{S}_1^{\vec{e}}-u)\theta\phi\psi}{\mathcal{S}_2^{\vec{e}}u(1-z)^2} - \frac{(1-\mathcal{S}_1^{\vec{e}})\phi}{\mathcal{S}_2^{\vec{e}}(1-z)} \right] \\
 & + e^{i\pi(\varsigma_1+\varsigma_2)} k_1^{1/2} k_2^{1/2} \left[\frac{\mathcal{S}_1^{\vec{e}}\mathcal{S}_2^{\vec{e}}[\phi-\mathcal{S}_1^{\vec{e}}u\phi-(1-\mathcal{S}_1^{\vec{e}})\theta]}{z} \right. \\
 & \quad + \frac{\mathcal{S}_2^{\vec{e}}[(1-\mathcal{S}_1^{\vec{e}})\theta-\phi+\mathcal{S}_1^{\vec{e}}u\phi]}{\mathcal{S}_1^{\vec{e}}u} - \frac{(u-\mathcal{S}_1^{\vec{e}})\theta-(1-\mathcal{S}_1^{\vec{e}})u\phi}{\mathcal{S}_1^{\vec{e}}\mathcal{S}_2^{\vec{e}}u} \\
 & \quad + \frac{\mathcal{S}_1^{\vec{e}}[u\theta-\mathcal{S}_1^{\vec{e}}\theta-u\phi(1-\mathcal{S}_1^{\vec{e}})]}{\mathcal{S}_2^{\vec{e}}uz} + \frac{(1-\mathcal{S}_1^{\vec{e}})\mathcal{S}_1^{\vec{e}}(1-u)\theta}{(1-\mathcal{S}_2^{\vec{e}})u(1-z)} \\
 & \quad - \frac{(1-\mathcal{S}_1^{\vec{e}})\mathcal{S}_1^{\vec{e}}(1-u)\phi}{(1-\mathcal{S}_2^{\vec{e}})\mathcal{S}_2^{\vec{e}}u(1-z)} - \frac{(1-\mathcal{S}_1^{\vec{e}})\mathcal{S}_1^{\vec{e}}\mathcal{S}_2^{\vec{e}}(1-u)(\mathcal{S}_2^{\vec{e}}\theta-\phi)}{(1-\mathcal{S}_2^{\vec{e}})(u-z)} \\
 & \quad - \frac{(1-\mathcal{S}_1^{\vec{e}})\mathcal{S}_1^{\vec{e}}\mathcal{S}_2^{\vec{e}}(1-u)\theta\phi\psi}{(1-\mathcal{S}_2^{\vec{e}})(u-z)^2} - \frac{(1-\mathcal{S}_1^{\vec{e}})^2(1+\mathcal{S}_1^{\vec{e}})(1-u)\theta\phi\psi}{\mathcal{S}_1^{\vec{e}}(1-\mathcal{S}_2^{\vec{e}})u(1-z)^2} \\
 & \quad + \frac{(1-\mathcal{S}_1^{\vec{e}})(1-u)(u\phi-\mathcal{S}_2^{\vec{e}}\theta)}{\mathcal{S}_1^{\vec{e}}(1-\mathcal{S}_2^{\vec{e}})\mathcal{S}_2^{\vec{e}}(1-z)u} + \frac{(1-\mathcal{S}_1^{\vec{e}})(\mathcal{S}_2^{\vec{e}})^2(1-u)\theta}{\mathcal{S}_1^{\vec{e}}(1-\mathcal{S}_2^{\vec{e}})u(u-z)} \\
 & \quad \left. + \frac{(1-\mathcal{S}_1^{\vec{e}})\mathcal{S}_2^{\vec{e}}(1-u)\theta\phi\psi}{\mathcal{S}_1^{\vec{e}}(1-\mathcal{S}_2^{\vec{e}})(u-z)^2} - \frac{(1-\mathcal{S}_1^{\vec{e}})\mathcal{S}_2^{\vec{e}}(1-u)\phi}{\mathcal{S}_1^{\vec{e}}(1-\mathcal{S}_2^{\vec{e}})(u-z)} \right] + \mathcal{O}(k_i) \left. \right\},
 \end{aligned} \tag{B.26}$$

where $\mathcal{S}_i^{\vec{e}}$ is defined in eq. (B.5).

In our calculation of the twisted super period matrix, the Prym differential appears not with monodromies \vec{e} , but $(\vec{e}\cdot\boldsymbol{\tau})$; therefore to compute $\Omega^{\vec{e}\cdot\boldsymbol{\tau}}(\mathbf{z})$ we need to replace $\mathcal{S}_i^{\vec{e}}$ in eq. (B.26) with $\mathcal{S}_i^{\vec{e}\cdot\boldsymbol{\tau}}$. Using $\boldsymbol{\tau}$ from eq. (A.32), we find

$$\begin{aligned}
 \mathcal{S}_1^{\vec{e}\cdot\boldsymbol{\tau}} &= e^{2\pi i(\vec{e}\cdot\boldsymbol{\tau})_1} = k_1^{\epsilon_1} u^{\epsilon_2} \left(1 - 2\epsilon_1 e^{i\pi\varsigma_2} k_2^{1/2} \frac{y}{u} \theta\phi \right) + \mathcal{O}(k_i), \\
 \mathcal{S}_2^{\vec{e}\cdot\boldsymbol{\tau}} &= e^{2\pi i(\vec{e}\cdot\boldsymbol{\tau})_2} = k_2^{\epsilon_2} u^{\epsilon_1} \left(1 - 2\epsilon_2 e^{i\pi\varsigma_1} k_1^{1/2} \frac{y}{u} \theta\phi \right) + \mathcal{O}(k_i).
 \end{aligned} \tag{B.27}$$

To supersymmetrize the Riemann class $\Delta_i(z)$, we need to replace the cross-ratios in eq. (B.10) with super-projective invariant cross-ratios, the Schottky fixed points η_i, ξ_i with the super fixed points $\mathbf{u}_i = (u_i|\theta_i)$, $\mathbf{v}_i = (v_i|\phi_i)$, and finally the base point z with $\mathbf{z} = (z|\psi)$.

We find then

$$\Delta_i(\mathbf{z}) = \frac{1}{2\pi i} \left\{ -\frac{1}{2} \log k_i + i\pi + \sum_{j=1}^h \binom{j}{j} \sum_{\alpha} \binom{i}{\alpha} \log \frac{\langle \mathbf{v}_j | \mathbf{T}_\alpha | \mathbf{u}_i \rangle \langle \mathbf{z} | \mathbf{T}_\alpha | \mathbf{v}_i \rangle}{\langle \mathbf{v}_j | \mathbf{T}_\alpha | \mathbf{v}_i \rangle \langle \mathbf{z} | \mathbf{T}_\alpha | \mathbf{u}_i \rangle} \right\}. \quad (\text{B.28})$$

Setting $h = 2$ and using the fixed points given in eq. (3.16), at order $\mathcal{O}(k_i^{1/2})$ we find

$$\begin{aligned} \Delta_1(\mathbf{z}) &= \frac{1}{2\pi i} \left\{ -\frac{1}{2} \log k_1 + i\pi - \log z + e^{i\pi\varsigma_2} k_2^{1/2} (1-u) \left[\frac{\psi\theta + \theta\phi}{u(1-z)} + \frac{\theta\phi - \psi\phi}{u-z} \right] \right. \\ &\quad \left. - e^{i\pi(\varsigma_1+\varsigma_2)} k_1^{1/2} k_2^{1/2} \frac{1-u}{uz} [(1-z)\theta\psi + (u-z)\psi\phi] \right\} + \mathcal{O}(k_i), \\ \Delta_2(\mathbf{z}) &= \frac{1}{2\pi i} \left\{ -\frac{1}{2} \log k_2 + i\pi + \log \frac{1-z}{u-z} + \frac{1}{u-z} \theta\psi + \frac{1}{1-z} \psi\phi \right. \\ &\quad \left. + e^{i\pi\varsigma_1} k_1^{1/2} \frac{1}{uz} [(u-z)\theta\psi + z(1-u)\theta\phi + u(1-z)\psi\phi] \right. \\ &\quad \left. - e^{i\pi(\varsigma_1+\varsigma_2)} k_1^{1/2} k_2^{1/2} \frac{(1-u)^2}{u} \left(\frac{1}{u-z} \theta\psi + \frac{1}{1-z} \psi\phi \right) \right\} + \mathcal{O}(k_i). \end{aligned} \quad (\text{B.29})$$

Using these expressions, it is easy to compute the phase $\exp(2\pi i \vec{\epsilon} \cdot \Delta(\mathbf{z}))$ to the desired order. We have thus assembled all the ingredients needed to compute the twisted determinant $\det(\text{Im } \tau_{\vec{\epsilon}})$: we take $\Omega_1^{\vec{\epsilon}; \tau}(z|\psi)$ from eq. (B.26), the phases $\mathcal{S}_i^{\vec{\epsilon}; \tau}$ from eq. (B.27), we compute $e^{2\pi i \vec{\epsilon} \cdot \Delta(z|\psi)}$ from eq. (B.29), and finally we insert the results into eq. (B.20). The final expression is a linear combination of integrals of the form

$$\frac{\pi}{\sin(\pi(\epsilon_1 + \epsilon_2))} \int_0^u dz \frac{z^{n_1 - \epsilon_1} (1-z)^{n_2 + \epsilon_2}}{(u-z)^{-n_3 + \epsilon_2}} \equiv \frac{u^{1+n_1+n_3-\epsilon_1-\epsilon_3}}{(-1)^{1+n_1+n_3}} \mathcal{J}(n_1, n_2, n_3), \quad (\text{B.30})$$

with integer values of n_i . The relevant integrals can be expressed in terms of standard hypergeometric functions by changing the integration variable according to $z = tu$, giving

$$\begin{aligned} \mathcal{J}(n_1, n_2, n_3) &= \Gamma(1+n_1-\epsilon_1) \Gamma(1+n_3-\epsilon_2) \Gamma(-1-n_1-n_3+\epsilon_1+\epsilon_2) \\ &\quad \times {}_2F_1(-n_2-\epsilon_2, 1+n_1-\epsilon_1; 2+n_1+n_3-\epsilon_1-\epsilon_2; u), \end{aligned} \quad (\text{B.31})$$

and the identity $\Gamma(x)\Gamma(1-x)\sin(\pi x) \equiv \pi$ was used. We can finally write the determinant as

$$\begin{aligned} \det(\text{Im } \tau_{\vec{\epsilon}}) &= \frac{1}{4\pi^2} \sum_{p,q,r=-2}^2 \sum_{i,j,n=0}^1 \mathcal{A}_{ijn;pqr} (e^{i\pi\varsigma_1} k_1^{1/2})^i (e^{i\pi\varsigma_2} k_2^{1/2})^j (\theta\phi)^n \mathcal{J}(p, q, r) \\ &\quad + (\vec{\epsilon} \leftrightarrow -\vec{\epsilon}) + \mathcal{O}(k_i). \end{aligned} \quad (\text{B.32})$$

The necessary coefficients, $\mathcal{A}_{ijn;pqr} = \mathcal{A}_{ijn;pqr}(k_l, \epsilon_m, u)$, for i, j, n ranging from 0 to 1, are listed in a Mathematica notebook which we have included as supplemental material.¹⁴ As

¹⁴Twisted_determinant_coefficients.nb.

an example, at lowest order in k_i , we find

$$\begin{aligned}
 4\pi^2 \det(\text{Im } \boldsymbol{\tau}_{\vec{\epsilon}}) &= k_1^{\epsilon_1/2} k_2^{-\epsilon_2/2} u^{-\epsilon_1} (k_2^{\epsilon_2} u^{\epsilon_1} - 1) \mathcal{J}(-1, -1, -1) \\
 &+ k_1^{-\epsilon_1/2} k_2^{-\epsilon_2/2} u^{\epsilon_3+1} (k_2^{\epsilon_2} u^{\epsilon_1} - 1) \mathcal{J}(1, -1, -1) \\
 &+ k_1^{-\epsilon_1/2} k_2^{-\epsilon_2/2} u^{\epsilon_3} [k_2^{\epsilon_2} u^{\epsilon_1} - k_1^{\epsilon_1} u^{\epsilon_2} + u((k_1 u)^{\epsilon_1} (k_2 u)^{\epsilon_2} - 1)] \mathcal{J}(0, -1, -1) \\
 &- \theta\phi \epsilon_2 u^{\epsilon_3} k_1^{-\epsilon_1/2} k_2^{-\epsilon_2/2} (k_1^{\epsilon_1} u^{\epsilon_2} - 1)(k_2^{\epsilon_2} u^{\epsilon_1} - 1) \mathcal{J}(0, -1, -1) \\
 &+ (\vec{\epsilon} \leftrightarrow -\vec{\epsilon}) + \mathcal{O}(k_i^{1/2});
 \end{aligned}
 \tag{B.33}$$

where, as before, $\epsilon_3 = -\epsilon_1 - \epsilon_2$. We note that, when rewriting $\det(\text{Im } \boldsymbol{\tau})$ in the parametrization in eq. (4.12), appropriate for the symmetric degeneration depicted in figure 6a, all hypergeometric functions can be replaced by unity to the relevant accuracy.

C Feynman diagrams

We list here all the two-loop one-particle-irreducible planar Feynman diagrams obtained from the vertices in eq. (5.11). To compare easily with the string theory results, we will order the results by their color indices. In other words, we will list all diagrams whose propagators have three chosen color indices A , B and C ; all such diagrams come from the field theory limit of the world-sheet whose boundaries are on the D-branes labelled by the indices A , B and C . One should then sum the diagrams, weighted appropriately, over $A \leq B \leq C$, where we write

$$\begin{aligned}
 B_{BA} &= B_1, & B_{AC} &= B_2, & B_{CB} &= B_3, \\
 m_{AB}^2 &= m_1^2, & m_{CA}^2 &= m_2^2, & m_{BC}^2 &= m_3^2.
 \end{aligned}
 \tag{C.1}$$

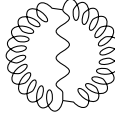
We draw the Feynman diagrams with the following conventions for the propagators

$$\begin{aligned}
 \text{|||||} &= \text{gluon modes polarized parallel to the background field,} \\
 \text{~~~~~} &= \text{gluon modes polarized perpendicular to the background field,} \\
 \text{.....} &= \text{Faddeev-Popov ghosts,} \\
 \text{———} &= \text{scalars.}
 \end{aligned}
 \tag{C.2}$$

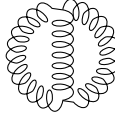
The relevant Feynman diagrams then give the following results.

$$\text{[Diagram: Star-shaped loop with wavy lines]} = -(3 - \gamma^2) \frac{(d-2)(d-3)}{2} \frac{g^2}{(4\pi)^d} \int_0^\infty \frac{\prod_{i=1}^3 dt_i e^{-t_i m_i^2}}{\Delta_0^{d/2-1} \Delta_B} \frac{t_1 + t_2 + t_3}{\Delta_0},
 \tag{C.3}$$


$$\begin{aligned}
 \text{[Diagram: Star-shaped loop with wavy lines and a vertical wavy line]} &= -(d-2) \frac{g^2}{(4\pi)^d} \int_0^\infty \frac{\prod_{i=1}^3 dt_i e^{-t_i m_i^2}}{\Delta_0^{d/2-1} \Delta_B} \frac{1}{\Delta_B} \left\{ \frac{\sinh(gB_3 t_3)}{gB_3} \right. \\
 &\times \left. [(1 - \gamma^2) \cosh(gB_2 t_2 - gB_1 t_1) + 2 \cosh(2gB_3 t_3 - gB_2 t_2 - gB_1 t_1)] + \text{cycl. perm.} \right\},
 \end{aligned}
 \tag{C.4}$$



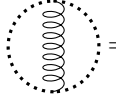
$$= -(d-2) \frac{g^2}{(4\pi)^d} \int_0^\infty \frac{\prod_{i=1}^3 dt_i e^{-t_i m_i^2}}{\Delta_0^{d/2-1} \Delta_B} \frac{1}{\Delta_0} \left\{ \left[2t_3 + \frac{1-\gamma^2}{2} (t_1 + t_2) \right] \right. \\ \left. \times \cosh(2gB_1 t_1 - 2gB_2 t_2) + \text{cycl. perm.} \right\}, \quad (\text{C.5})$$




$$= -\frac{g^2}{(4\pi)^d} \int_0^\infty \frac{\prod_{i=1}^3 dt_i e^{-t_i m_i^2}}{\Delta_0^{d/2-1} \Delta_B} \frac{1}{\Delta_B} \left\{ \frac{\sinh(gB_3 t_3)}{gB_3} \right. \\ \left. \times [2 + (1-\gamma^2) \cosh(2gB_1 t_1 - 2gB_2 t_2)] \cosh(2gB_3 t_3 - gB_2 t_2 - gB_1 t_1) + \text{cycl. perm.} \right\}, \quad (\text{C.6})$$



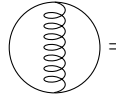
$$= (1+\gamma^2) \frac{d-2}{2} \frac{g^2}{(4\pi)^d} \int_0^\infty \frac{\prod_{i=1}^3 dt_i e^{-t_i m_i^2}}{\Delta_0^{d/2-1} \Delta_B} \frac{t_1 + t_2 + t_3}{\Delta_0}, \quad (\text{C.7})$$



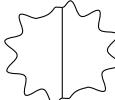
$$= (1+\gamma^2) \frac{g^2}{(4\pi)^d} \int_0^\infty \frac{\prod_{i=1}^3 dt_i e^{-t_i m_i^2}}{\Delta_0^{d/2-1} \Delta_B} \frac{1}{\Delta_B} \left\{ \frac{\sinh(gB_3 t_3)}{gB_3} \right. \\ \left. \times \cosh(2gB_3 t_3 - gB_1 t_1 - gB_2 t_2) + \text{cycl. perm.} \right\}, \quad (\text{C.8})$$



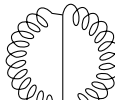
$$= -(d-2) n_s \frac{g^2}{(4\pi)^d} \int_0^\infty \frac{\prod_{i=1}^3 dt_i e^{-t_i m_i^2}}{\Delta_0^{d/2-1} \Delta_B} \frac{1}{\Delta_0} \left\{ \left[t_3 + \frac{1-\gamma^2}{4} (t_1 + t_2) \right] + \text{cycl. perm.} \right\}, \quad (\text{C.9})$$



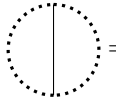
$$= -2 n_s \frac{g^2}{(4\pi)^d} \int_0^\infty \frac{\prod_{i=1}^3 dt_i e^{-t_i m_i^2}}{\Delta_0^{d/2-1} \Delta_B} \frac{1}{\Delta_B} \left\{ \frac{\sinh(gB_3 t_3)}{gB_3} \right. \\ \times \cosh(2gB_3 t_3 - gB_1 t_1 - gB_2 t_2) \\ \left. + \frac{1-\gamma^2}{4} \left(\frac{\sinh(gB_1 t_1)}{gB_1} \cosh(gB_3 t_3 - gB_2 t_2) + (1 \leftrightarrow 2) \right) + \text{cycl. perm.} \right\}, \quad (\text{C.10})$$



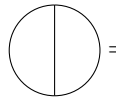
$$= \frac{g^2}{(4\pi)^d} \int_0^\infty \frac{\prod_{i=1}^3 dt_i e^{-t_i m_i^2}}{\Delta_0^{d/2-1} \Delta_B} \left\{ \frac{d-2}{2} [(1+\gamma^2) m_3^2 - 2(m_1^2 + m_2^2)] + \text{cycl. perm.} \right\}, \quad (\text{C.11})$$



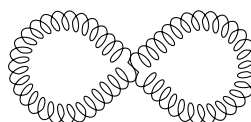
$$= \frac{g^2}{(4\pi)^d} \int_0^\infty \frac{\prod_{i=1}^3 dt_i e^{-t_i m_i^2}}{\Delta_0^{d/2-1} \Delta_B} \left\{ [(1+\gamma^2) m_3^2 - 2(m_1^2 + m_2^2)] \right. \\ \left. \times \cosh(2gB_1 t_1 - 2gB_2 t_2) + \text{cycl. perm.} \right\}, \quad (\text{C.12})$$



$$= \frac{g^2}{(4\pi)^d} \int_0^\infty \frac{\prod_{i=1}^3 dt_i e^{-t_i m_i^2}}{\Delta_0^{d/2-1} \Delta_B} (m_1^2 + m_2^2 + m_3^2), \quad (\text{C.13})$$

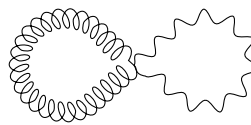


$$= (1-n_s) \frac{3-\gamma^2}{2} \frac{g^2}{(4\pi)^d} \int_0^\infty \frac{\prod_{i=1}^3 dt_i e^{-t_i m_i^2}}{\Delta_0^{d/2-1} \Delta_B} (m_1^2 + m_2^2 + m_3^2), \quad (\text{C.14})$$



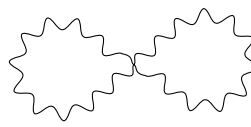
$$= -\frac{g^2}{(4\pi)^d} \int_0^\infty \left[\prod_{i=1}^2 \frac{dt_i e^{-t_i m_i^2} g B_i}{t_i^{d/2-1} \sinh(g B_i t_i)} \right. \tag{C.15}$$

$$\times \left\{ 2 \cosh(2g B_1 t_1 + 2g B_2 t_2) - \frac{1-\gamma^2}{2} [2 \cosh(2g B_1 t_1 - 2g B_2 t_2) + 4 \cosh(2g B_1 t_1) \cosh(2g B_2 t_2)] \right\} + \text{cycl. perm.},$$



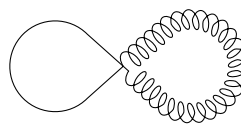
$$= 2(1-\gamma^2)(d-2) \frac{g^2}{(4\pi)^d} \int_0^\infty \left[\prod_{i=1}^2 \frac{dt_i e^{-t_i m_i^2} g B_i}{t_i^{d/2-1} \sinh(g B_i t_i)} \right. \tag{C.16}$$

$$\left. \times \cosh(2g B_1 t_1) + \text{cycl. perm.} \right],$$

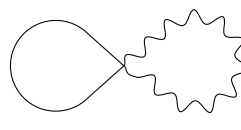


$$= -\left\{ (d-2) - \frac{1-\gamma^2}{2} [d-2 + (d-2)^2] \right\} \tag{C.17}$$

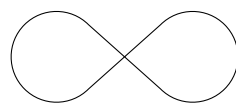
$$\times \frac{g^2}{(4\pi)^d} \int_0^\infty \left[\prod_{i=1}^2 \frac{dt_i e^{-t_i m_i^2} g B_i}{t_i^{d/2-1} \sinh(g B_i t_i)} + \text{cycl. perm.} \right],$$



$$= 2n_s(1-\gamma^2) \frac{g^2}{(4\pi)^d} \int_0^\infty \left[\prod_{i=1}^2 \frac{dt_i e^{-t_i m_i^2} g B_i}{t_i^{d/2-1} \sinh(g B_i t_i)} \cosh(2g B_2 t_2) + \text{cycl. perm.} \right], \tag{C.18}$$



$$= n_s(1-\gamma^2)(d-2) \frac{g^2}{(4\pi)^d} \int_0^\infty \left[\prod_{i=1}^2 \frac{dt_i e^{-t_i m_i^2} g B_i}{t_i^{d/2-1} \sinh(g B_i t_i)} + \text{cycl. perm.} \right], \tag{C.19}$$



$$= -n_s \left[1 - \frac{1-\gamma^2}{2} (1+n_s) \right] \tag{C.20}$$

$$\times \frac{g^2}{(4\pi)^d} \int_0^\infty \left[\prod_{i=1}^2 \frac{dt_i e^{-t_i m_i^2} g B_i}{t_i^{d/2-1} \sinh(g B_i t_i)} + \text{cycl. perm.} \right].$$

In all cases, adding cyclic permutations means summing two additional copies of the integrand with the replacements $(B_1, B_2, B_3; m_1^2, m_2^2, m_3^2) \mapsto (B_2, B_3, B_1; m_2^2, m_3^2, m_1^2)$ and $(B_3, B_1, B_2; m_3^2, m_1^2, m_2^2)$. Note that the gauge choice $\gamma^2 = 1$ greatly simplifies many of these diagrams: for example, the second lines of eq. (C.4) and eq. (C.6), the third line of eq. (C.10) and the third and fourth lines of the eq. (C.15) all vanish in this gauge. In fact, the last example is a special case of the fact that both propagators in the diagrams with quartic vertices must have the same polarization, precisely when $\gamma^2 = 1$, which corresponds to the fact that $k_1^{1/2}$ and $k_2^{1/2}$ must be taken from the same CFT sector in string theory.

Open Access. This article is distributed under the terms of the Creative Commons Attribution License ([CC-BY 4.0](https://creativecommons.org/licenses/by/4.0/)), which permits any use, distribution and reproduction in any medium, provided the original author(s) and source are credited.

References

- [1] E. Witten, *The super period matrix with Ramond punctures*, *J. Geom. Phys.* **92** (2015) 210 [[arXiv:1501.02499](#)] [[INSPIRE](#)].
- [2] E. D'Hoker and D.H. Phong, *The super period matrix with Ramond punctures in the supergravity formulation*, [arXiv:1501.02675](#) [[INSPIRE](#)].
- [3] R. Pius, A. Rudra and A. Sen, *Mass renormalization in string theory: general states*, *JHEP* **07** (2014) 062 [[arXiv:1401.7014](#)] [[INSPIRE](#)].
- [4] R. Pius, A. Rudra and A. Sen, *String perturbation theory around dynamically shifted vacuum*, *JHEP* **10** (2014) 070 [[arXiv:1404.6254](#)] [[INSPIRE](#)].
- [5] A. Sen, *Off-shell amplitudes in superstring theory*, *Fortschr. Phys.* **63** (2015) 149 [[arXiv:1408.0571](#)] [[INSPIRE](#)].
- [6] E. D'Hoker and M.B. Green, *Zhang-Kawazumi invariants and superstring amplitudes*, [arXiv:1308.4597](#) [[INSPIRE](#)].
- [7] E. D'Hoker, M.B. Green, B. Pioline and R. Russo, *Matching the D^6R^4 interaction at two-loops*, *JHEP* **01** (2015) 031 [[arXiv:1405.6226](#)] [[INSPIRE](#)].
- [8] P. Tourkine, *Tropical amplitudes*, [arXiv:1309.3551](#) [[INSPIRE](#)].
- [9] E. Witten, *Superstring perturbation theory revisited*, [arXiv:1209.5461](#) [[INSPIRE](#)].
- [10] E. D'Hoker, *Topics in two-loop superstring perturbation theory*, [arXiv:1403.5494](#) [[INSPIRE](#)].
- [11] L. Magnea, S. Playle, R. Russo and S. Sciuto, *Multi-loop open string amplitudes and their field theory limit*, *JHEP* **09** (2013) 081 [[arXiv:1305.6631](#)] [[INSPIRE](#)].
- [12] E.S. Fradkin and A.A. Tseytlin, *Nonlinear electrodynamics from quantized strings*, *Phys. Lett. B* **163** (1985) 123 [[INSPIRE](#)].
- [13] A. Abouelsaood, C.G. Callan Jr., C.R. Nappi and S.A. Yost, *Open strings in background gauge fields*, *Nucl. Phys. B* **280** (1987) 599 [[INSPIRE](#)].
- [14] C. Bachas and M. Porrati, *Pair creation of open strings in an electric field*, *Phys. Lett. B* **296** (1992) 77 [[hep-th/9209032](#)] [[INSPIRE](#)].
- [15] L. Magnea, R. Russo and S. Sciuto, *Two-loop Euler-Heisenberg effective actions from charged open strings*, *Int. J. Mod. Phys. A* **21** (2006) 533 [[hep-th/0412087](#)] [[INSPIRE](#)].
- [16] J.-L. Gervais and A. Neveu, *Feynman rules for massive gauge fields with dual diagram topology*, *Nucl. Phys. B* **46** (1972) 381 [[INSPIRE](#)].
- [17] L. Crane and J.M. Rabin, *Super Riemann surfaces: uniformization and Teichmüller theory*, *Commun. Math. Phys.* **113** (1988) 601 [[INSPIRE](#)].
- [18] E.J. Martinec, *Conformal field theory on a (super-)Riemann surface*, *Nucl. Phys. B* **281** (1987) 157 [[INSPIRE](#)].
- [19] S.B. Giddings and P.C. Nelson, *The geometry of super Riemann surfaces*, *Commun. Math. Phys.* **116** (1988) 607 [[INSPIRE](#)].
- [20] E. D'Hoker and D.H. Phong, *The geometry of string perturbation theory*, *Rev. Mod. Phys.* **60** (1988) 917 [[INSPIRE](#)].
- [21] E. Witten, *Notes on super Riemann surfaces and their moduli*, [arXiv:1209.2459](#) [[INSPIRE](#)].
- [22] C. Lovelace, *M-loop generalized Veneziano formula*, *Phys. Lett. B* **32** (1970) 703 [[INSPIRE](#)].

- [23] M. Kaku and L. Yu, *The general multi-loop Veneziano amplitude*, *Phys. Lett.* **B 33** (1970) 166 [INSPIRE].
- [24] V. Alessandrini, *A general approach to dual multiloop diagrams*, *Nuovo Cim.* **A 2** (1971) 321 [INSPIRE].
- [25] D.I. Olive, *Operator vertices and propagators in dual theories*, *Nuovo Cim.* **A 3** (1971) 399 [INSPIRE].
- [26] V. Alessandrini and D. Amati, *Properties of dual multiloop amplitudes*, *Nuovo Cim.* **A 4** (1971) 793 [INSPIRE].
- [27] C. Montonen, *Multiloop amplitudes in additive dual-resonance models*, *Nuovo Cim.* **A 19** (1974) 69 [INSPIRE].
- [28] P. Di Vecchia, R. Nakayama, J.L. Petersen, J. Sidenius and S. Sciuto, *BRST invariant N -reggeon vertex*, *Phys. Lett.* **B 182** (1986) 164 [INSPIRE].
- [29] P. Di Vecchia, M. Frau, A. Lerda and S. Sciuto, *A simple expression for the multiloop amplitude in the bosonic string*, *Phys. Lett.* **B 199** (1987) 49 [INSPIRE].
- [30] P. Di Vecchia, K. Hornfeck, M. Frau, A. Lerda and S. Sciuto, *N -string, g -loop vertex for the fermionic string*, *Phys. Lett.* **B 211** (1988) 301 [INSPIRE].
- [31] P. Di Vecchia et al., *N -point g -loop vertex for a free bosonic theory with vacuum charge Q* , *Nucl. Phys.* **B 322** (1989) 317 [INSPIRE].
- [32] P. Di Vecchia et al., *N -point g -loop vertex for a free fermionic theory with arbitrary spin*, *Nucl. Phys.* **B 333** (1990) 635 [INSPIRE].
- [33] R. Russo and S. Sciuto, *Twisted determinants on higher genus Riemann surfaces*, *Nucl. Phys.* **B 669** (2003) 207 [hep-th/0306129] [INSPIRE].
- [34] K. Aoki, E. D'Hoker and D.H. Phong, *Two loop superstrings on orbifold compactifications*, *Nucl. Phys.* **B 688** (2004) 3 [hep-th/0312181] [INSPIRE].
- [35] R. Russo and S. Sciuto, *Twisted determinants and bosonic open strings in an electromagnetic field*, *Fortschr. Phys.* **52** (2004) 678 [hep-th/0312205] [INSPIRE].
- [36] I. Antoniadis, K.S. Narain and T.R. Taylor, *Open string topological amplitudes and gaugino masses*, *Nucl. Phys.* **B 729** (2005) 235 [hep-th/0507244] [INSPIRE].
- [37] J. Scherk, *Zero-slope limit of the dual resonance model*, *Nucl. Phys.* **B 31** (1971) 222 [INSPIRE].
- [38] M.B. Green, J.H. Schwarz and L. Brink, *$N = 4$ Yang-Mills and $N = 8$ supergravity as limits of string theories*, *Nucl. Phys.* **B 198** (1982) 474 [INSPIRE].
- [39] M.L. Mangano, S.J. Parke and Z. Xu, *Duality and multi-gluon scattering*, *Nucl. Phys.* **B 298** (1988) 653 [INSPIRE].
- [40] M.L. Mangano and S.J. Parke, *Multiparton amplitudes in gauge theories*, *Phys. Rept.* **200** (1991) 301 [hep-th/0509223] [INSPIRE].
- [41] Z. Bern and D.A. Kosower, *A new approach to one loop calculations in gauge theories*, *Phys. Rev.* **D 38** (1988) 1888 [INSPIRE].
- [42] Z. Bern and D.A. Kosower, *Efficient calculation of one loop QCD amplitudes*, *Phys. Rev. Lett.* **66** (1991) 1669 [INSPIRE].

- [43] Z. Bern and D.A. Kosower, *Color decomposition of one loop amplitudes in gauge theories*, *Nucl. Phys. B* **362** (1991) 389 [INSPIRE].
- [44] Z. Bern and D.A. Kosower, *The computation of loop amplitudes in gauge theories*, *Nucl. Phys. B* **379** (1992) 451 [INSPIRE].
- [45] Z. Bern and D.C. Dunbar, *A mapping between Feynman and string motivated one loop rules in gauge theories*, *Nucl. Phys. B* **379** (1992) 562 [INSPIRE].
- [46] Z. Bern, *A compact representation of the one loop N -gluon amplitude*, *Phys. Lett. B* **296** (1992) 85 [INSPIRE].
- [47] Z. Bern, L.J. Dixon and D.A. Kosower, *One loop corrections to five gluon amplitudes*, *Phys. Rev. Lett.* **70** (1993) 2677 [hep-ph/9302280] [INSPIRE].
- [48] M.J. Strassler, *Field theory without Feynman diagrams: one loop effective actions*, *Nucl. Phys. B* **385** (1992) 145 [hep-ph/9205205] [INSPIRE].
- [49] M.G. Schmidt and C. Schubert, *On the calculation of effective actions by string methods*, *Phys. Lett. B* **318** (1993) 438 [hep-th/9309055] [INSPIRE].
- [50] M.G. Schmidt and C. Schubert, *The worldline path integral approach to Feynman graphs*, [hep-ph/9412358](#) [INSPIRE].
- [51] C. Schubert, *Perturbative quantum field theory in the string inspired formalism*, *Phys. Rept.* **355** (2001) 73 [hep-th/0101036] [INSPIRE].
- [52] P. Dai and W. Siegel, *Worldline Green functions for arbitrary Feynman diagrams*, *Nucl. Phys. B* **770** (2007) 107 [hep-th/0608062] [INSPIRE].
- [53] F. Bastianelli, O. Corradini and E. Latini, *Higher spin fields from a worldline perspective*, *JHEP* **02** (2007) 072 [hep-th/0701055] [INSPIRE].
- [54] P. Di Vecchia, L. Magnea, A. Lerda, R. Russo and R. Marotta, *Renormalization constants from string theory*, [hep-th/9602055](#) [INSPIRE].
- [55] A. Frizzo, L. Magnea and R. Russo, *Systematics of one loop Yang-Mills diagrams from bosonic string amplitudes*, *Nucl. Phys. B* **604** (2001) 92 [hep-ph/0012129] [INSPIRE].
- [56] P. Di Vecchia, L. Magnea, A. Lerda, R. Marotta and R. Russo, *Two loop scalar diagrams from string theory*, *Phys. Lett. B* **388** (1996) 65 [hep-th/9607141] [INSPIRE].
- [57] A. Frizzo, L. Magnea and R. Russo, *Scalar field theory limits of bosonic string amplitudes*, *Nucl. Phys. B* **579** (2000) 379 [hep-th/9912183] [INSPIRE].
- [58] R. Marotta and F. Pezzella, *Two loop ϕ^4 diagrams from string theory*, *Phys. Rev. D* **61** (2000) 106006 [hep-th/9912158] [INSPIRE].
- [59] L. Magnea and R. Russo, *String derivation of two loop Feynman diagrams*, *AIP Conf. Proc.* **415** (1997) 347 [hep-ph/9708471] [INSPIRE].
- [60] L. Magnea and R. Russo, *Two loop gluon diagrams from string theory*, *AIP Conf. Proc.* **407** (1997) 913 [hep-ph/9706396] [INSPIRE].
- [61] B. K ors and M.G. Schmidt, *Two loop Feynman diagrams in Yang-Mills theory from bosonic string amplitudes*, [hep-th/0003171](#) [INSPIRE].
- [62] J. Polchinski, *String theory. Vol. 1: An introduction to the bosonic string*, Cambridge University Press, Cambridge U.K. (1998) [INSPIRE].

- [63] R.R. Metsaev and A.A. Tseytlin, *On loop corrections to string theory effective actions*, *Nucl. Phys. B* **298** (1988) 109 [INSPIRE].
- [64] K. Hornfeck, *Three-reggeon light-cone vertex of the Neveu-Schwarz string*, *Nucl. Phys. B* **293** (1987) 189 [INSPIRE].
- [65] L. Álvarez-Gaumé, G.W. Moore and C. Vafa, *Theta functions, modular invariance and strings*, *Commun. Math. Phys.* **106** (1986) 1 [INSPIRE].
- [66] M. Frau, I. Pesando, S. Sciuto, A. Lerda and R. Russo, *Scattering of closed strings from many D-branes*, *Phys. Lett. B* **400** (1997) 52 [hep-th/9702037] [INSPIRE].
- [67] R. Russo and S. Sciuto, *The twisted open string partition function and Yukawa couplings*, *JHEP* **04** (2007) 030 [hep-th/0701292] [INSPIRE].
- [68] P. Di Vecchia, L. Magnea, A. Lerda, R. Russo and R. Marotta, *String techniques for the calculation of renormalization constants in field theory*, *Nucl. Phys. B* **469** (1996) 235 [hep-th/9601143] [INSPIRE].
- [69] P. Vanhove, *The physics and the mixed Hodge structure of Feynman integrals*, *Proc. Symp. Pure Math.* **88** (2014) 161 [arXiv:1401.6438] [INSPIRE].
- [70] P. Di Vecchia and A. Liccardo, *D branes in string theory, II*, hep-th/9912275 [INSPIRE].
- [71] E. Witten, *Notes on supermanifolds and integration*, arXiv:1209.2199 [INSPIRE].
- [72] P. Goddard, J. Goldstone, C. Rebbi and C.B. Thorn, *Quantum dynamics of a massless relativistic string*, *Nucl. Phys. B* **56** (1973) 109 [INSPIRE].
- [73] C.B. Thorn, *A world sheet description of planar Yang-Mills theory*, *Nucl. Phys. B* **637** (2002) 272 [hep-th/0203167] [INSPIRE].
- [74] M. Headrick, *grassmann.m: a package that teaches Mathematica how to manipulate Grassmann variables* (2015), <http://web.archive.org/web/20150317172836/http://people.brandeis.edu/~headrick/Mathematica/grassmann.m>.
- [75] D. Friedan, *Notes on string theory and two dimensional conformal field theory*, in M.B. Green et al. eds., *Unified string theories*, World Scientific (1986), pp. 162–213.
- [76] L.J. Dixon, D. Friedan, E.J. Martinec and S.H. Shenker, *The conformal field theory of orbifolds*, *Nucl. Phys. B* **282** (1987) 13 [INSPIRE].
- [77] A.A. Tseytlin, *Open superstring partition function in constant gauge field background at finite temperature*, *Nucl. Phys. B* **524** (1998) 41 [hep-th/9802133] [INSPIRE].
- [78] C. Bachas, *D-brane dynamics*, *Phys. Lett. B* **374** (1996) 37 [hep-th/9511043] [INSPIRE].
- [79] M. Berkooz, M.R. Douglas and R.G. Leigh, *Branes intersecting at angles*, *Nucl. Phys. B* **480** (1996) 265 [hep-th/9606139] [INSPIRE].